University of Ottawa

Measurement and statistical analysis of the passive viscoelastic properties of the human knee joint during flexion and extension motion

by

Steven R. McFaull

School of Human Kinetics

Submitted in partial fulfilment

of the degree of Master of Science

ISBN 0-315-82503-0

TABLE OF CONTENTS

Page

ACKNOWLEDGEMENTS

I would like to thank my wife, Lori, for her support, both moral and financial, throughout this project. Also, I would like to thank my parents for their financial assistance. I would also like to acknowledge my advisor, Dr. Mario Lamontagne, for his patience over the past few years.

Thanks are also due to Gordon Evans for his technical support and to Yves Fortin, who served as a pilot subject and who also offered many helpful suggestions. Also, I thank Dr. Gordon Robertson for his software assistance.

This study was partly funded by the Natural Sciences and Engineering Research Council of Canada and the Research Committee of the University of Ottawa.

LIST OF FIGURES

LIST OF TABLES

ABSTRACT

The purpose of the present investigation was to determine the net passive elastic joint moment and the angular damping coefficient of the human knee joint in full range flexion-extension. A secondary purpose was to develop regression equations to predict the measured passive properties from anthropometric data. Seventeen male subjects (22-31 years) participated in the study. The passive elastic moments were determined using a specially constructed apparatus: a horizontal knee arthrograph (HKA). The subject's leg was rotated through the full range of voluntary motion and forced slowly into the extremes of flexion and extension. Transducers mounted on the HKA measured the resistive moment as a function of the knee angle. The damping coefficient was determined using the small oscillation technique. This technique is a linearization method that allows determination of the angular damping coefficient as a function of knee angle through a simple analysis of the underdamped response curve. The viscous moments may be obtained by multiplying the damping coefficient by the angular velocity (in $rad \cdot s^{-1}$). Measurements were made at 10°, 45°, 90°, 110°, and 130° of flexion (0° is full extension). All measurements were made with the subject's muscles in the passive state. This state was ensured by monitoring the surface EMG activity of five major muscles crossing the knee joint. The hip joint was fixed at 90° and the ankle was set at 0° (neutral). The passive elastic moments increased exponentially as the limits of either flexion or extension were approached. The midrange of joint motion was a low moment (<5 N·m), low stiffness region. Considerable variability in the magnitudes of the passive elastic moments existed across subjects. At 140° of flexion, between about 5 N·m and 86 N·m was measured while the range at full extension (0°) was about 6 N·m to 22 N·m. The angular damping coefficient was a nonlinear function (approximately quadratic) of the knee joint angle. The variability was not quite as high compared to the elastic component. Robust multiple linear regression techniques showed that, depending on the knee angle, between 50% and 98% of the variation in the passive elastic moments could be accounted for by up to three anthropometric parameters. For the damping coefficients, the range was slightly lower: 43% to 96%. Application of the data to the late swing phase of walking indicated that, for some subjects, the passive moments may contribute (or oppose) significantly to the net joint moment. In conclusion, it appears that the resistance offered by the passive tissues spanning the knee joint varies considerably across subjects (in the age range of 22-31 years). Researchers may consider including such sources in their biomechanical models to enhance their fidelity.

Keywords: Passive moments, elasticity, viscosity, damping, musculoskeletal models, human knee joint.

CHAPTER I

INTRODUCTION

Due to ethical and technical considerations biomechanics relies heavily on modelling to understand the mechanics of the human body in various external loading environments. The evolution of biomechanical models has paralleled the progress in related fields of study such as anatomy, physiology, electromyography, signal processing, and anthropometry.

Early models of the human system (e.g., Bresler and Frankel, 1950; McHenry, 1963) treated the body as a set of interconnected rigid links. The links, or segments, were imparted properties such as mass, location of the centre of mass, and the principal mass moments of inertia. These properties were obtained from the early works of Braune and Fischer (1889), Dempster (1955), and others. For model simplicity and due to the lack of experimental data the articulations that connected these segments were represented simplistically - as resistance free, one degree of freedom, kinematically constrained hinge joints. Modellers of the human system (e.g., Hatze, 1976) realized the importance of detailed articular properties to the fidelity of a biomechanical model. As a result, articular mechanics has become the focus of more investigations recently (e.g., Berme, Engin, and Correia da Silva, 1985; Mow, Ratcliffe, and Woo, 1990).

Investigations dealing with articular mechanics will generally fall into one of two categories: articular kinematics or articular kinetics. Studies focussing on the kinematic aspects of an articulation (e.g., Blacharski, Somerset, and Murray, 1975;

Huiskes, Van Dijk, de Lange, Woltring, and Van Rens, 1985) deal with describing the two- or three-dimensional translations and rotations of the segments and supporting structures which define the joint using the principles of rigid body mechanics. Articular kinetics is concerned with determining the forces and moments acting within and about a joint. By its nature, this area of research is quite broad. Significant research efforts are aimed at determining the forces that exist at the articular interface such as joint contact forces and contact areas (Fukubayashi and Kurosawa, 1980; Morrison, 1970; Seireg and Arvikar, 1975) and lubrication and viscosity (Renaudeaux, 1985).

The orthopaedic literature is especially rich in research (mostly cadaveric) which attempts to identify the load bearing functions and kinematic effects of specific joint structures such as ligaments, menisci, cartilage, and the joint capsule (Brantigan and Voshell, 1941; Butler, Noyes, and Grood, 1980; France, Daniels, Golbe, and Dunn, 1983; Kennedy, Hawkins, Willis, and Danylchuk, 1976; Piziali, Rastegar, Nagel, and Schurman, 1980). The limitations and biases of cadaver data have led to the emergence of *in vivo* experimental testing (Crowninshield, Pope, Johnson, and Miller, 1976; Mills and Hull, 1991a, 1991b; Pope, Crowninshield, Miller, and Johnson, 1976; Quinn, Mote, and Skinner, 1991). The experimental protocol usually involves vibrating or otherwise rotating or translating the distal segment of the joint (proximal segment is fixed) and measuring the mechanical response (laxity, stiffness, or impedance) which is due to the lumped effect of all of the strained tissue structures and fluids surrounding the joint. The joint can be either active or passive, that is, the muscles crossing the joint can be contracting at some specified level (%MVC) or can be inactive. The responses measured experimentally are often used to develop a theoretical mechanical model of the joint. Although this area has been quite thoroughly researched for the knee joint, most studies measure the response of the joint in the most clinically relevant motions: varus-valgus (V-V), internal-external rotation (I-E), and anterior-posterior drawer (A-P). Studies of the passive mechanical response of the knee in full range flexion-extension (F-E) are limited (e.g., Engin, 1985; Heerkins et al., 1985). Some modellers, however, (e.g., Dowling, 1987; Hatze, 1976; Luo and Goldsmith, 1991) require passive F-E data of major human joints as input into their musculoskeletal models.

Passive F-E properties have not attracted much interest since many investigators feel that these properties have a negligible influence on the joint mechanics (Pierrynowski, 1982; Vrahas, Brand, Brown, and Andrews, 1990). This may be a suitable first approximation for slower movements in the midrange of joint motion, however, for more rapid movements and motions approaching the mechanical limits of the joint (e.g., sprinting, impacts, late swing phase of walking) this approximation is questionable. As the mechanical limits of the joint are approached the increase in periarticular tissue strain coupled with the decrease in the potential for active muscle force generation (force-length relation) results in the passive kinetics playing a relatively more dominant role in the behaviour of the joint (An, Kaufman, and Chao, 1989; Davy and Audu, 1987; Weiss, Kearney, and Hunter, 1986).

Two major areas of biomechanical modelling in which the passive mechanical response of human articulations is required are crash simulation models with associated validation studies (Fleck, Butler, and Vogel, 1975; Padgaonkar, Krieger, and King, 1977) and individual muscle force prediction models (Davy and Audu, 1987).

Crash simulation models attempt to predict the kinematic response (relative and/or absolute) of the multi-segmented human body (occupant or pedestrian) in a vehicle impact environment. Most models incorporate a short time response which is the initial response of the body during the time period over which no muscle activity is present (i.e., less than human reaction time). Thus, the passive mechanical properties of all major articulations along with segmental parameters and environmental constraints (seat belt, steering column, hood, windshield, etc.) will completely determine the short time response of the system and also set up the initial conditions for the subsequent long time response. While these models are verified with live humans for low acceleration dosages, a full high acceleration impact must be validated using either anesthetized animals, cadavers, physical models, or anthropometric test dummies (e.g., Cichowski, 1968; Foster, Kortge, and Wolanin, 1977; Viano et al., 1978).

One of the earliest simulation models was that of McHenry (1963). This model was a two-dimensional vehicle-occupant simulation model. The joint properties were based on estimates of resistive torques about the articulations and were represented mechanically by torsional springs and dampers. The model underwent a number of modifications including revision of joint stops (Segal and McHenry, 1967; Segal, 1971).

The Calspan Corporation introduced a number of more sophisticated three dimensional models (e.g., Bartz, 1972; Fleck et al., 1975). The model by Fleck et al., (1975) was the final revised version; the passive resistive moments were represented by elastic, viscous, and Coulomb friction elements which were either linear, quadratic, or cubic in nature. The joint stop properties were adapted from biostereometric work done by Herron, Cuzzi, Goulet, and Hugg (1974).

Muscle force prediction models (Davy and Audu, 1987; Herzog, 1985) attempt to determine the force contribution (magnitudes and temporally) of individual muscles to the net joint moment across a given joint for a particular movement pattern. To realize a movement pattern the muscles spanning a joint must produce a specific moment profile. Production of this profile requires that the muscles interact with four types of stiffness: gravitational, inertial, elastic and viscous. Inertia and viscosity will always oppose the movement; however, elasticity and gravity, due to their position dependence can either contribute to or oppose the movement. Thus, not including the passive moments in a model may lead to over or underestimates of the muscle forces. These discrepancies will be propagated into calculations of bone-on-bone forces and individual muscle work and power. Dowling (1988) found that the mechanical power of the passive tissues crossing the elbow joint caused overestimates of the metabolic cost approaching 20% in slow flexion-extension movements.

Due to the nature of biological materials (Fung, 1981) spanning and surrounding a joint, the passive joint properties will be mostly of a viscoelastic character; however, friction, Coulomb friction, and plasticity have also been identified. It is possible to separate viscosity and elasticity and measure each component separately.

Passive elasticity in F-E can be represented by the net passive elastic joint moment (NPEJM) which is a function of the knee joint angle (tissue deformation) and, to a lesser degree, of the hip and ankle joint angles (the biarticular muscle effect). Various investigators (e.g., Hatze, 1975a; Heerkins et al., 1985; Such, Unsworth, Wright, and Dowson, 1975) have attempted to determine the passive moments about the knee. Most of these investigations differed in purpose and protocol. As a result, much of the current database remains incomplete. Regardless of the lack of data, it is clear that the resistive moments rise sharply as the mechanical limits of the joint are approached.

Smith (1957) investigated the passive resistance of the knee as it related to the limiting mechanism of postural control. The experiments were carried out on three subjects under anesthesia prior to unrelated surgery. Due to the intent of the study only the extension phase was studied. The maximum moment attained was 8.16 N·m at -10°. Otahal (1971) determined the passive moment function of the knee of 26 subjects from full extension to 120° of flexion. For a typical subject 11 N·m of resistive moment was measured at 0° while 13 N·m was reached at 120°. Hatze (1975a) used a technique similar to Otahal (1971) to determine the passive moments about the knee of one male subject for a slightly larger range of motion. However, significantly larger moments were obtained: 35 N·m at full extension and 31 N·m at 130°. Engin (1985) made a significant contribution to the database by studying all major human articulations in three-dimensions over the full range of voluntary motion and beyond using a sophisticated mechanical apparatus called a global force applicator. The sample consisted of three males. For the knee joint large moments were observed at the extremes of joint motion: at full extension 66 N·m was recorded while at 160° of flexion 88 N·m was measured. Mansour and Audu (1986) studied a rather limited range of motion (0° to 100°) on four male subjects. The maximum moment attained was 60 N·m at full extension.

A number of investigators have used a sinusoidal oscillation technique to measure the passive moments. Such et al., (1975) obtained data from 49 males and 21 females. The test was performed only at one knee joint angle (90°; average moment=4 N·m). Anthropometric parameters were correlated with the measured data. Thompson, Wright, and Dowson (1978) attempted to improve the design of the vertical apparatus of Such et al., (1975) by employing a horizontal configuration. The knee joints of six males and six females were tested. Apparatus constraints and anatomical considerations permitted only the midrange (50° to 120°) of joint motion to be studied and hence the measured moments were low (< 5 N·m). Heerkins et al., (1985) used the same technique as Such et al., (1975), however, a full correlation analysis was employed with anthropometric parameters as the independent variables. Twenty-nine males and 20 females were tested. The knee joint was studied from 5° (11 N·m for a typical male subject) to 110°of flexion (9 N·m).

From the above brief review it is clear that two of the main weaknesses in the current literature are small samples and a limited range of motion. The variability in the passive mechanics of the knee needs to be addressed statistically and data for the terminal phases of joint motion (especially in flexion) must be obtained since these positions are most important to modellers, given that it is at these positions where the passive moments can become substantial in magnitude and rate of change.

Passive viscosity in F-E can be represented by the net passive viscous joint moment (NPVJM) which is a function of both the knee joint angle (and the ankle and hip joint angles to a lesser degree) and the segmental angular velocity. The velocity dependence makes this function more difficult to measure. As such, limited data are available in the literature. The main technique which has been used is the small oscillation technique (Engin, 1984; Hatze, 1975a, 1975b). This technique is a linearization method which is based on the theory of underdamped free vibrations of a linear mechanical system about an equilibrium position and allows for the determination of the angular damping coefficient of the knee joint as a function of joint angle.

Hatze (1975a, 1975b) appears to be the only investigator to use the technique on the knee joint. The technique was employed over the whole range of knee joint motion. However, only one male subject was studied. Much more data needs to be compiled on the viscous properties of the knee joint, especially large sample statistical studies.

STATEMENT OF THE PROBLEM

Given the lack of a large normative database on the passive mechanical properties of the knee joint *in vivo* over the whole range of motion in flexion-extension, the objective of this study was to measure the net passive elastic joint moment as a function of joint angle and the angular damping coefficient (which leads to the NPVJM) of the knee joint of live human subjects over the full range of flexion-extension of a reasonably sized subject sample. Also, in an attempt to account for some of the observed variance and to predict the passive moments, a multiple linear regression analysis with anthropometric parameters as independent variables was performed.

RESEARCH HYPOTHESIS

The net passive elastic joint moment and the angular damping coefficient of the knee joint will be nonlinear functions of the knee joint angle, θ. These functions will take on substantial magnitudes and rates of change as the mechanical limits of the joint are approached.

Some of the observed variance of the NPEJM and the damping coefficient can be accounted for, and the passive properties predicted by, the specific anthropometry of the subject such as knee breadth, knee depth, knee circumference, and thigh circumference, as well as a flexibility parameter. It is also expected that predictability will vary over the range of knee joint motion.

DEFINITIONS

The following are definitions of some basic concepts and terms which will be used repeatedly throughout this document.

Elasticity

That property of a material which allows it to return to its original size or shape after being deformed. The restoring force can be either linearly (Hookean) or nonlinearly (non-Hookean) related to the deformation.

Viscosity

That property of a fluid which introduces tangential forces between layers of fluid in relative motion and results in dissipation of mechanical energy. There exist linear (Newtonian) and nonlinear (non-Newtonian) cases.

Viscoelasticity

A collective term which characterizes a material which displays the phenomena of hysteresis, stress relaxation, and creep.

Net passive elastic joint moment (NPEJM, $M_e\ (\theta)$)

The average net moment produced, at a given joint angle, by the elastic deformation of all passive tissues (tendons, fascia, ligaments, joint capsule, skin, cartilage, menisci, and relaxed muscles) crossing a joint.

Net passive viscous joint moment (NPVJM, $M_v(\theta,\dot{\theta})$)

The net moment produced, at a given joint angle and segmental angular velocity, by the viscosity of all passive tissues (interstitial fluid, protoplasm, synovia, relaxed muscles, and the ground substance of the tendons, fascia, ligaments, joint capsule, and skin) crossing a joint.

Net passive joint moment (NPJM, $M_p(\theta,\dot{\theta})$)

The average net moment produced, at a given joint angle and segmental angular velocity, by the average elastic deformation and the viscosity of all passive tissues (tendons, ligaments, fascia, joint capsule, skin, synovia, cartilage, menisci, interstitial fluids, and relaxed muscles) spanning a joint. This moment is a linear combination of the elastic and viscous components (NPEJM + NPVJM).

Tangential angular elastic stiffness (TAES, $K_e(\theta)$)

The rate of change of the NPEJM with respect to the knee joint angle, θ.

Knee joint angle (θ)

The angle between the distal extension of the femur and the tibia. Zero degrees is full extension and negative values indicate hyperextension.

Hip joint angle (θ_H)

The angle between the proximal extension of the femur and the trunk. Zero degrees is full extension (anatomical position) while negative values indicate hyperextension.

Ankle joint angle (θ_A)

The angle between the plantar surface of the foot and the neutral position. The neutral position (0°) is defined as the foot being perpendicular to the tibia. Plantar flexion is positive and dorsiflexion is negative.

Soft joint stops (θ_{SE} and θ_{SF})

The knee joint angles (one in extension, θ_{SE} , and one in flexion, θ_{SF}) at which the net passive elastic joint moment begins to increase significantly. The positions of the soft joint stops are criterion dependent.

Equilibrium angle (θ_e)

The knee joint angle at which the NPEJM=0.

LIMITATIONS AND DELIMITATIONS

The NPEJM which was measured was a net resistive moment. At any given knee angle some of the passive tissues may have been contributing to the measured moment while other structures may have been opposing it. Hence, the NPEJM represents the differential, lumped effect of the periarticular tissues. The NPEJM represents the moment which was measured with the right knee joint in an unloaded state in the neutral position (i.e., no initial I-E or V-V) and the hip and ankle angles set at 90° and 0° (neutral), respectively. Since the kinematics of the knee in F-E is dependent on the length of the biarticular muscles and the level of loading and is coupled to the degree of I-E and/or V-V, the NPEJM function was actually a single member of a family of functions. Hysteresis and stress relaxation effects were not considered (quantified) in this investigation.

The small oscillation technique, being a linearization method, will contain inherent approximation errors. Although the objective was to measure the damping in the sagittal (F-E) plane, in practice this is a very difficult task. Thus, some out-of-plane motion was expected. As with the elastic component, the measured damping coefficient represented the differential effect of the tissues surrounding the joint and the measured function was actually a member of a family of curves each representing a specific kinematic state of the knee joint. The present research effort was delimited to measuring the damping properties of the unloaded right neutral knee at joint angles of 10°, 45°, 90°, 110°, and 130° of flexion with the hip joint fixed at 90° (130° for $\theta = 130°$) and the ankle joint set at 0° (neutral).

CHAPTER II

REVIEW OF THE LITERATURE

The following review consists of a preliminary discussion of knee joint anatomy and kinematics followed by a discussion of some general aspects of viscoelasticity. The mechanical properties of biological tissues are then considered. Next, a brief review of the frictional properties of human synovial joints and the physiological factors affecting joint stiffness are reported. Finally, a detailed review and discussion of the various studies dealing with the determination of the viscoelastic properties of the knee joint is presented.

FUNCTIONAL ANATOMY OF THE KNEE JOINT

The basic anatomy of the knee joint, including a discussion of soft tissue structures and muscles, is reviewed in this section.

The basic joint

The knee joint is typically classified as a modified diarthrodial hinge joint (Welsh, 1980) consisting of three separate articulations: 1) lateral tibiofemoral; 2) medial tibiofemoral; and 3) Patellofemoral.

The tibiofemoral joints are formed by the mating of the femoral condyles with the tibial plateau through intervening articular cartilage. Depressions in the tibial plateau are deepened by the medial and lateral menisci which also increase the articular surface area by 50% and joint lubrication by 20%.

Unlike the hip and ankle joints, the knee joint is inherently unstable and requires ligamentous and muscular restraints for stability (Nordin and Frankel, 1989).

Articular capsule

The knee joint is surrounded by the articular capsule which, unlike in other joints, does not form a complete envelope around the joint. The few true capsular ligaments which do connect the bones are assisted by the tendinous tissues of the associated knee joint muscles and other ligamentous structures (Grabiner, 1989). These structures include the patellar, the oblique popliteal, the arcuate popliteal, the medial and lateral collateral, and the anterior and posterior cruciate ligaments. All of these structures serve to stabilize the knee joint in specific planes of motion.

Major Ligaments

The four major ligaments of the knee joint include the lateral (fibular) collateral ligament (LCL), the medial (tibial) collateral ligament (MCL), the anterior cruciate ligament (ACL), and the posterior cruciate ligament (PCL). The ACL and PCL are referred to as intra-articular structures in that they lie within the capsule of the knee joint but not within the synovial membrane.

The collateral ligaments appear to behave similarly during passive F-E. Edwards, Lafferty, and Lange (1970) and France et al., (1983) have found that both the MCL and LCL become maximally elongated at full extension and decrease to minimum values at approximately 130° of flexion.

The ACL is a complex structure which has been classified as an isometric ligament due to the reciprocal functions of various fibre bands (France et al., 1983; O'Connor and Zavatsky, 1990). Recent cadaver work (Markolf, Gorek, Kabo, Shapiro, and Finerman, 1990) showed a very sharp increase in actual ACL force from

10° of passive (unloaded) flexion to -5°. Force was minimal beyond 10° of flexion.

The PCL appears to become tense as flexion progresses up to about 80° to 90° after which the tension decreases somewhat (Brantigan and Voshell, 1941; France et al., 1983).

Due to the unique structure of the knee, the tension patterns of all ligaments can be modulated by muscle forces.

More recently, ligaments have also been found to have a neurosensory role (De Avila, O'Connor, Visco, and Sisk, 1989; Johansson, 1991).

Muscles spanning the knee joint

The major muscles crossing the knee (which are responsible for flexion-extension) are separated into two categories (Spence, 1982). The anterior compartment (extensors) includes the quadriceps group: rectus femoris (RF), vastus lateralis (VL), vastus medialis (VM), vastus intermedius (VI), and sartorius (SR). All muscles of this group are innervated by the femoral nerve. The RF and the SR are biarticular muscles since they also cross the hip joint. The VI lies deep to the other muscles in the group. Muscles of the posterior compartment (flexors) include the hamstrings group which consists of the long and short heads of the biceps femoris, LBF and SBF, respectively, the semitendinosus (ST), and the semimembranosus (SM). All of the muscles in the posterior compartment are innervated by the sciatic nerve. The LBF, ST, and SM are biarticular since they also span the hip joint. The gastrocnemius (GA) is a biarticular muscle with two distinct heads (medial: MGA and lateral: LGA) which spans the ankle joint as well as the knee joint. While primarily a plantarflexor the GA also contributes to flexion of the leg about the knee. The GA is innervated by the tibial nerve. The popliteus (PO) is a small deep muscle which may play a role in early flexion (i.e., the unlocking mechanism). The PO is also innervated by the tibial nerve. Also, the gracilis muscle (GS), although mainly an adductor, also crosses the knee and can contribute to leg flexion. The GS is innervated by the obturator nerve.

THE KINEMATICS OF THE KNEE JOINT

The following paragraphs review the motion of the knee joint with respect to degrees of freedom, range of motion, mechanical stops, centre of rotation, and load dependence.

Degrees of freedom

Conceptually, the knee joint has six degrees of freedom: three translations (anterior-posterior, medial-lateral, compression-distraction) and three rotations (internal-external, varus-valgus, flexion-extension). Several of these are either suppressed or coupled due to ligamentous or bony constraints (Blankevoort, Huiskes, and de Lange, 1988). The two major degrees of freedom are considered to be F-E and I-E.

The range of motion and joint stops in F-E

Barter, Emanuel, and Truett (1957) undertook a statistical study of joint mobility of college aged males. Subjects were required to voluntarily flex their leg while standing. The mean flexion angle was found to be 113° (range: 92° to 134°). The knee was also forced into extreme flexion by having the subject kneel on the floor. In this position, the mean flexion angle attained was 159° (range: 144° to 174°). Thus, even within the same gender and age group considerable variation in joint mobility exists. Since no bony stops exist at the knee, many individuals can attain 5 to 10° of hyperextension depending on joint laxity. The voluntary range of motion of the knee joint reported in most sources (e.g., Nordin and Frankel, 1989) is 0° (full extension) to 140° of flexion.

Certain factors can affect the range of joint motion. Females were found to have greater joint mobility than males (Webb Associates, 1978). Body fat content was also observed to be predictive of joint motion (Laubach, 1969). Biarticular muscles also affect the voluntary range of motion of a joint; Laubach (1969) found that knee flexion was decreased by 34° when the hip was also flexed.

The passive mechanical limits (hard stops) of the knee joint are determined by the anatomy and the mechanical properties of the joint structures. In extension, the passive mechanical stop is determined by tension in the collateral ligaments, some aspects of the ACL, the posterior aspect of the joint capsule, the oblique popliteal ligament, meniscal restoring moments as well as passive musculotendinous tension in the posterior compartment (Brantigan and Voshell, 1941; Grabiner, 1989). As the extremes of flexion are passively approached the hard stop is controlled by tension in some aspects of the cruciate ligaments, the femoral attachment of the posterior joint capsule, close packing of the joint surfaces, passive musculotendinous tension in the anterior compartment, and apposition of the posterior calf and thigh (Brantigan and Voshell, 1941; Grabiner, 1989).

The instantaneous centre of rotation (ICOR) and surface joint motion

The instant centre technique (based on the Reuleaux method) as described in Nordin and Frankel (1989) was used by Webb Associates (1978) on the knee joint. For the knee joint, in the sagittal plane, progressing from flexion to extension the instant centre pathway followed a semicircular arc in the same direction. The approximate joint centre of rotation was defined as the midpoint of a line between the centres of the posterior convexities of the femoral condyles. The lateral femoral epicondyle is used as a palpable surface landmark (Nordin and Frankel, 1989). The error in measuring the leg segment length due to the variable ICOR was estimated to be $\pm$ 5%.

The results of the ICOR analysis allows one to study the surface joint motion (Nordin and Frankel, 1989). In a normal joint the femur glides on the tibia; however, in a pathological joint with an abnormal ICOR pathway the joint can compress or distract and change the kinematics (Frankel, Burstein, and Brooks, 1971).

Load dependence of knee joint kinematics

The knee joint is a unique and complex articulation which is inherently unstable. The stability and motion are controlled by soft tissues which, due to their nonlinear load-displacement behaviour, allow an envelope of motion pathways. Thus, the actual kinematic behaviour of the joint is a function of external loading conditions and muscle forces (Huiskes et al., 1985; Spoor, Van Leeuwen, Meskers, Titulaer, and Huson, 1990). The commonly described 'screw-home mechanism' (Nordin and Frankel, 1989) has been shown not to be an obligatory effect of the passive joint characteristics, but a direct result of external loads (Blankevoort et al., 1988).

GENERAL ASPECTS OF VISCOELASTIC THEORY

Before reviewing the viscoelastic properties of the passive tissues spanning the knee joint, a review of the basic concepts of viscoelastic theory (Fung, 1977, 1981; Nash, 1977) will be covered in this section.

Hooke's Law and the stress-strain relationship

It has been found that for most engineering materials subject to an infinitesimal strain in uniaxial loading, a relation of the form $\sigma = E\epsilon$ is valid within a certain range of stresses. The parameter σ is the stress in units of force per unit area, ϵ is the strain which is defined as the ratio of the stretched length of a material to its unstretched length. The parameter **E** is a constant for a particular material and is called Young's modulus of elasticity and represents the slope of the stress-strain relation. The above relation is called Hooke's law and a material obeying Hooke's law is said to be a Hookean elastic solid.

Non-Hookean materials also exist. These materials do not obey Hooke's law and the concept of a constant Young's modulus is not appropriate, instead the tangential modulus, which must be stated with respect to a deformation state, is defined (Fung, 1981).

Elasticity

Elasticity is that property of a material which allows it to return to its original undeformed state after the deforming load is removed. The restoring force (or moment) can be linearly or nonlinearly related to the deformation of the material. For a Hookean material the slope of the stress-strain curve represents the elastic stiffness of the material. The stiffness of a nonlinear material changes over the deformation range and can only be assumed constant over very small intervals.

Viscosity

The resistance to movement of one layer of fluid over an adjacent layer can be ascribed to the viscosity of the fluid. For viscous forces to manifest themselves movement is required (Massey, 1979). Viscosity is temperature dependent and is not related to density. As with elasticity, linear and nonlinear fluids exist. Linear fluids are called Newtonian fluids and they obey a relation of the form $\sigma_s = \mu\dot{\epsilon}$, where σ_s is the shear stress, $\dot{\epsilon}$ is the shearing rate, and μ is the coefficient of viscosity which is a scalar quantity characteristic of the fluid. For the majority of fluids the viscosity is independent of the shear rate and hence the graph of σ_s versus $\dot{\epsilon}$ is linear through the origin with slope μ. There exists, however, a fairly large category of fluids (which includes many biofluids) for which the viscosity is not independent of the shear rate (Massey, 1979) and these fluids are referred to as non-Newtonian or nonlinear fluids. Nonlinear fluids often display linear characteristics at low shear stresses (Nash, 1977).

Viscoelasticity

When a material is suddenly strained and then the strain is maintained constant for a period afterward, the corresponding stresses induced in the material decrease with time. This phenomenon is called stress relaxation. If the material is suddenly stressed and the stress is maintained constant afterward, the material continues to deform and the phenomenon is called creep. If the material is subject to cyclic loading, the stress-strain relationship of the loading process is usually different from that of the unloading process: a phenomenon known as hysteresis. The phenomena of stress relaxation, creep, and hysteresis are collectively called the features of viscoelasticity (Fung, 1981).

THE MECHANICAL PROPERTIES OF BIOLOGICAL TISSUES

Since the passive moments across a joint are due mainly to the viscoelastic nature of the periarticular tissues, a brief review of these viscoelastic properties will be discussed in this section.

Collagen and ground substance

Collagen, a family of fibrous proteins, is the main load carrying element in almost all tissues of the human body. The high tensile strength of collagen is due to intramolecular cross-linking (Stryer, 1981). Fresh collagen has a Young's modulus of 1×10^9 $N \cdot m^{-2}$ (essentially inextensible).

Most connective tissues consist of relatively few cells (fibroblasts) and an abundant extracellular matrix. About 70% of the matrix is water and 30% is solids. These solids are collagen, ground substance, reticulin and a small amount of elastin (Fung, 1981). The collagen content is generally over 75%.

The primary constituents of ground substance are water, mucopolysaccharides (GAGs and Proteoglycans), and tropocollagen molecules. Most of the water in ground substance is bonded to the mucopolysaccharides to form a thixotropic viscous gel

(Binkley, 1989; Jackson and Bently, 1968). Ground substance can vary in consistency from a fluid to a semisolid gel. The viscosity of the ground substance gel decreases, or thins, with agitation (which is the property of thixotropy or shear thinning). This change in viscosity is reversible with cessation of agitation. Thus, within a ligament, tendon, capsule, or skin, movement between collagen fibres produces a decrease in the viscosity of the intervening ground substance. Thixotropic fluids are shear rate dependent (non-Newtonian). Thus, ground substance is very important in determining the viscous properties of an articulation.

Tendons and ligaments

Depending on how cells are organized into a structure, the mechanical properties of the tissue will vary (Fung, 1981). The arrangement of collagen fibres in tendon and in ligaments differs somewhat and is suited to the function of the structure. Fibres composing tendons have an orderly parallel arrangement which is consistent with the uniaxial tensile loads to which the tendon is subjected. Ligaments generally sustain tensile loads in one predominant direction, however, they may also bear smaller tensile loads in other directions. Collagen fibres in ligaments, therefore, may not be completely parallel but are closely interlaced with one another.

The load-deformation relationship of tendons and ligaments *in vitro* has been studied extensively (Fung, 1981; Viidik, 1972, 1978) and a definite relationship has emerged. Load-deformation curves of tendons and ligaments always assume a basic triphasic pattern. The initial phase, which has been called the *toe region,* is characterized by an approximately exponential increase (concave upwards) in load as the specimen is stretched. In the second phase a relatively linear relationship is observed while the third phase becomes nonlinear and ends with rupture of the specimen.

The toe region is believed to be the result of a change in the wavy pattern of the relaxed collagen fibres which become straighter as loading progresses - the so called uncrimping effect (Elliot, 1965; Viidik, 1966). Some data suggest, however, that this elongation may be due to interfibrillar sliding and shear of the ground substance (Viidik, Danielsen, and Oxlund, 1982).

If the load-deformation curve is expressed in terms of stress (σ) and strain (ϵ) it is seen that the end of the toe region corresponds to strain in the range of 1.5% to 4.0% (Abrahams, 1967; Diamant, Keller, Baer, Litt, and Arridge, 1972; Haut and Littel, 1972; and Viidik, 1973). The upper limit for physiological strain in tendons and ligaments is from 2% to 5% (Fung, 1981; Kear and Smith, 1975; Viidik, 1980). Therefore, biomechanically, the toe region and the initial part of the linear region are very important since they represent the operating range of the passive tissues in most human movements.

Ligaments and tendons also show the viscoelastic properties of stress relaxation, creep, and hysteresis (Fung, 1981).

Unstimulated muscle

Since a portion of the passive moments is most likely attributable to the relaxed antagonistic muscles as the passive parallel and series elastic elements are stretched within the interstitial fluids, the properties of unstimulated muscle will be reviewed briefly.

It is known (Zajac, 1989) that the passive force of skeletal muscle is approximately an exponentially increasing function of muscle length. The x-intercept of the passive force-length (F-L) curve is at L_o. That is, at muscle lengths below L_o the passive force is zero. It is believed that the passive F-L relation is not altered by muscle activity.

Most studies dealing with the stretch properties of muscle study the response of a single *in vitro* fibre. Woittiez, Huijing, Boom, and Rozendal (1984) constructed a three-dimensional muscle model based on muscle architecture and geometry. The model was validated against experimental findings on rat muscle and reasonable agreement was reached. Model predictions indicated a passive F-L relationship which was approximately exponential. The passive force at fibre optimum length was approximately 6.5% of the maximal active twitch force. At 130% of fibre optimum length the passive force was predicted to be approximately 87% of the maximal active twitch force. One must be cautious, however, in interpreting these results since it is questionable whether 130% fibre optimal length could ever be achieved *in vivo*.

Heerkins, Woittiez, Huijing, Van Ingen Schenau, and Rozendal (1987) studied the passive resistance of the rat knee with respect to actual muscle length. The passive force was about 9% of the active force at L_o. Two parameters were defined: the dynamic elastic stiffness (DES) and the dynamic viscous stiffness (DVS). Both DES and DVS exhibited an exponential increase with muscle length, DES more so than DVS.

Fung (1967) tested resting muscle and other tissues in simple elongation and found that the tensile stress was nearly an exponential function of strain in the lower stress range. It was also noted that tissues cannot be represented by a constant Young's modulus since this modulus varies over a wide range; tangential modulus is a more appropriate parameter.

Kabo, Goldsmith, and Nystrom (1982) performed one of the few studies of the stretch properties of whole resting muscle. Human sternocleidomastoid (SCM) and extensor carpi radialis (ECR) muscles were tested in tension up to stretch ratios of 1.30. The two muscles behaved differently. The SCM exhibited a very nearly linear response up to the failure point while the ECR showed an exponential response.

Fascia

Yamada (1970) has done extensive experiments on resting skeletal muscle with and without their fasciae. Stress-strain curves were obtained for a variety of human and animal muscles devoid of their fasciae. These curves all had the same characteristic shape (approximately exponential) although the elongations corresponding to a specific stress varied over a wide range for different muscles. Yamada (1970) has also investigated the mechanical response of human and animal fasciae. It was found that fascia also exhibited an exponential response but was much stiffer than resting muscle. These findings led Hatze (1975a) to conclude that in the *in vivo* muscle the fascia is the dominating structure in the parallel elastic element.

Skin

Skin by far has the most complex structure of collagen fibres. Fung (1981) stated that the configuration of collagen in skin must be considered as a complex three-dimensional network of interwoven fibrils.

Manschot and Brakkee (1986a, 1986b) measured (*in vivo*) and modelled the mechanical properties of human calf skin. One purpose of the experiment was to test the skin in large deformations (up to 50%) and large stresses (up to 1 $MN \cdot m^{-2}$). The stress-strain relationship was highly nonlinear for low stresses but became almost linear for large stresses. It has been accepted that the stress-strain relation for skin at high stresses reflects the stretching of collagen fibrils.

Synovial fluid

Synovial fluid fills the cavities of synovial joints of mammals. According to Fung (1981) synovia is similar in constitution to blood plasma, but with less protein. It contains hyaluronic acid, a polysaccharide. Synovia is much more viscous than blood, and this seems to be due to the presence of the hyaluronic acid since enzymatic removal of this substance greatly reduces the viscosity.

King (1966) tested the synovia of bullock knee and ankle joints in a rheogoniometer. It was observed that synovial fluid is strongly shear thinning (thixotropic). The viscosity was high at low shear rates but decreased rapidly as the shear rate increased. This is the standard behaviour of a non-Newtonian fluid. However, at low shear rates, although the viscosity was high, it remained almost constant and thus exhibited Newtonian characteristics. This is also typical of many non-Newtonian fluids (Giles, 1977).

From the preceding review of the viscoelastic properties of biological tissues it appears that under the conditions of the present investigation the soft tissues are most likely operating in the toe region of the stress-strain curve, possibly entering the linear region at the extremes of joint motion. The toe region is approximately exponential while the load-deformation curve for passive muscle also appears to be exponential (starting at L_o). However, one must be cautious when attempting to apply uniaxial *in vitro* test results to an *in vivo* situation. The *in vivo* situation involves successive engagement, disengagement, and cancellation effects of various tissues to varying degrees over the range of motion. Hence, one may expect to observe a response curve which is a superimposition of exponential functions of the various tissues. Also, since the relations are expected to be nonlinear, the concept of a constant joint stiffness is inappropriate and a more feasible parameter would be the tangential or incremental joint stiffness.

It also appears that the viscous damping about a joint is due to muscle, tendon, ligament, and capsule (if they are being strained) viscosity as well as from the viscosity of the synovial fluid bathing the joint. The viscosity of the synovial fluid must not be confused with frictional forces at the articular surfaces which are known to be quite low (see below) and which are thus being neglected.

Stress relaxation about human joints

If a segment is fixed at a particular joint angle the passive moment would decline from this initial value to a steady state value over time. This is the pure elastic moment. If one tissue component was involved the decline would be exponential, however, if more than one tissue component were involved the decay may be more complex. This initial reduction in moment is due to the position dependent viscoplastic character of the periarticular tissues (Viidik, 1973). The degree of reduction in the moment is dependent upon the joint and the angle at which the joint is fixed. The stress relaxation about the knee joint has apparently not been studied. Toft, Sinkjaer, Kalund, and Espersen (1989) studied the stress relaxation properties of the ankle joint at extreme dorsiflexion. The ankle joints of 10 male subjects (23-31 years) were rotated into dorsiflexion until "a strong sensation of stretch was experienced" at which point the ankle was fixed. The decline in torque over a five minute interval was recorded. The initial moment at the fully stretched position was variable across subjects, ranging from 20 N•m to 68 N•m. After five minutes the mean torque had decreased by 8.0 ± 3.0 N•m. Expressed as a percentage with respect to the torque at time $t=0$, after 30 seconds the mean percentage decrease was 10.1 ± 1.7% and after five minutes the corresponding value was 22.7 ± 2.6%. Due to the large variability of the initial torque and the small variability in the torque reduction, it was concluded by the authors that the results probably reflected a tissue system with properties of viscosity and plasticity independent of individuals.

Wright and Johns (1961) found a 35% reduction in torque at flexion of the MCP joint after a two minute interval. Variability was not indicated.

THE FRICTIONAL PROPERTIES OF HUMAN SYNOVIAL JOINTS

Articular cartilage exhibits almost two orders of magnitude less friction than most oil lubricated metal on metal (Fung, 1981). Dynamic tests with articular cartilage in synovial fluid reveal a mean minimum coefficient of friction of 0.0026 at a normal stress of 500 kPa and a maximum value of 0.0038 at a normal stress of 2 MPa (Fung, 1981). Compare these values to those of oil lubricated metal on metal (0.3 to 0.5) and teflon coated surfaces (0.05 to 0.1).

McCutchen (1962) found that the coefficient of friction for animal joints tested in a simulated *in vivo* condition varied from 0.002 to 0.005. It appears that it is the combination of synovial fluid and articular cartilage which produces the very low coefficient of friction since synovial fluid does not perform much better than water with man made bearings.

Linn (1968) found that the maximum coefficient of friction of bovine ankle joints lubricated with synovia to be 0.0037.

Many mechanisms of joint lubrication have been postulated: fluid film, thick film (hydrostatic, hydrodynamic), boundary film (Linn, 1968), and squeeze film (Unsworth, Dowson, and Wright, 1975). Regardless of the mode of lubrication most investigators agree that the coefficient of friction of human synovial joints is very low. Thus it seems reasonable to assume that, under the conditions of the present investigation, frictional shearing forces within the joint will be negligible.

PHYSIOLOGICAL VARIATIONS IN JOINT STIFFNESS

Before discussing the techniques for determining the passive moments about a joint, various physiological factors which may affect the magnitude and phase of these moments will first be discussed.

Anthropometry

The size and shape of the segments and joints should influence the magnitudes of the passive moments. A larger cross-section of tissue will contain more parallel elements (elastic and damping) and since elements in parallel are additive (Thomson, 1988), larger subjects should exhibit larger moments (all else being equal). However, the degree to which this is the case and the effects of intervening variables such as flexibility and joint angles has not been extensively pursued in the literature.

Such et al., (1975) found that the passive moments increased by approximately 50% as the thigh and knee circumferences increased by approximately 30% and 40%, respectively. It should be noted that these data are associated with a knee angle of 90° and although the moments increased significantly, the absolute magnitudes were very small (maximum 5.5 N·m). Heerkins et al., (1985) found that up to 71% of the variation in the passive moment in extension (of the knee) could be accounted for by various anthropometric parameters of the lower extremity.

Further work is needed to determine the value of various anthropometric parameters as predictors of passive moments over the full range of flexion-extension.

Gender

Males generally exhibit a higher joint stiffness than females (Heerkins et al., 1985; Such et al., 1975; Wright and Johns, 1961). Such et al., (1975) found that even when age and anthropometry were taken into account males still exhibited higher stiffness than females. Wright and Johns (1961) found an average ratio of male joint stiffness to female joint stiffness of 1.66. Anthropometry and muscle and soft tissue compliancy account for at least part of the difference: men have a higher absolute joint size and are generally less flexible. The higher joint dimensions can account for the higher collagen content of male joints (Fischer, 1973). This higher absolute collagen content will result in a higher joint stiffness (Wright and Johns, 1960). However, Hama, Yamamuro, and Takeda (1976) showed that in the joint capsule of sexually mature male animals not only is the absolute amount of collagen higher but also the collagen content per unit net weight of the collagenous tissue (i.e., the relative collagen content). Thus, it appears that hormonal components contributing to connective tissue metabolism may also be a determinant in joint stiffness.

Females are clearly more flexible compared to their age-matched male counterparts. Canada Fitness Survey (1982) results showed that females outperformed males in every age grouping on the standard flexibility indicator (Trunk Forward Flexion).

Aging and maturity

Although the increase in passive joint resistance which is observed with advancing age (Wright and Johns, 1961) can in part be attributable to the increase in joint and segment dimensions as the individual reaches maturity (up to about 20 years), other factors account for the increased stiffness after this period.

The aging process clearly alters the mechanical properties of all connective tissues (Piez, 1968; Vogel, 1978; Yamada, 1970). The most important (or at least the most reported) aging effect is the structural change in the collagen molecule. As the individual advances in age beyond maturity the amount of cross-linking within the collagen molecule increases (Vogel, 1978; Yamada, 1970), resulting in a stiffer tissue.

Also concomitant with the aging process is a decrease in muscle mass (Larsson, Frimby, and Karlsson, 1979) and thus a decrease in the cross-sectional area of the muscles. Hence, the muscle forces (both active and passive) will be correspondingly decreased. The aging process will also affect the connective tissue within the muscle (series and parallel elements).

There exist age related changes in articular cartilage (Gardner, 1978) which manifest themselves as surface irregularities as evidenced by optical scanning. These irregularities may affect the interaction of the cartilage with the synovial fluid.

Age related changes have also been reported in the components of ground substance (GAGs). The ratios of different types of glycans appears to change with age (Greiling and Bauman, 1973; Matthews and Glagov, 1966). Since the GAGs interact with water to determine the viscosity, age related changes in viscosity may also be expected. Synovial fluid was found to decrease in viscosity with advancing age (Jebens and Monk-Jones, 1959).

Although individual tissue structures show differences with increasing age, these results may not manifest themselves in the measured NPJM since a number of effects may neutralize each other (Such et al., 1975).

Temperature

Wright and Johns (1961) showed that local cooling of the metacarpophalangeal (MCP) joint to 18°C increased the stiffness by 10% to 20%. The effect of localized heating was also tested. It was demonstrated that there was a 20% decrease in stiffness at 45°C compared to that at 33°C.

Oedema

To investigate the effects of local oedema, Wright and Johns (1961) injected saline into the region of the joint capsule and the effect on the joint stiffness (MCP joint) was measured. Stiffness on extension increased by 13% while a 33% increase was observed on flexion. The results of the effects of oedema and temperature support the contention that a significant portion of the stiffness around a joint is attributable to the joint itself (proper) since local temperature and fluid changes in the joint produce clear changes in stiffness while the temperature and fluid levels of more remote structures such as muscles remains constant. This hypothesis is also supported by data from Johns and Wright (1962).

Mobilization and immobilization

Ligaments and tendons adapt to the mechanical demands placed upon them; they become stronger and stiffer when subjected to increased stress and weaker and more compliant when the stress is reduced (Noyes, 1977; Tipton, James, Mergner, and Tcheng, 1970). Exercise has been found to increase the tensile strength and the tendon tangent modulus in the toe region (Woo et al., 1980, 1981; Woo, Gomez, Woo, and Akeson, 1982). Certain types of exercise also increase muscle mass (Goldberg et al., 1975) which may lead to increased passive forces.

Pharmacological agents

Various drugs can affect the connective tissues. In particular, the nonsteroidal anti-inflammatory drugs (NSAIDs; e.g., aspirin, acetaminophen, indomethacin) were found to increase the tensile strength and the total collagen content in rat tail tendons (Vogel, 1977). Carlstedt, Madsen, and Wredmark (1986a, 1986b) found that indomethacin treatment increased the tensile strength in developing and healing plantaris longus tendons in the rabbit .

Pathology

Connective tissue diseases can alter the normal passive resistance of an articulation. Indeed, joint stiffness is used an indicator of rheumatoid arthritis (Chandler, Wright, and Hartfall, 1958; Wright and Johns, 1960). While connective tissue diseases directly affect the joint stiffness, other pathologies, mostly structural in nature (see Nordin and Frankel, 1989), indirectly affect the joint stiffness by altering the kinematics of the joint. Thus, a large number of diseases, both metabolic and structural, can create abnormal joint resistance.

Wright and Johns (1961) tested the elastic and viscous stiffness of the MCP joint of normals and those afflicted with connective tissue disease. Elastic and viscous components were approximately 1.5 times higher in the pathological subjects.

Flexibility and muscle compliancy

The joint stiffness is also significantly affected by the flexibility of the individual. Individuals vary considerably in their flexibility (Barter et al.,1957) and females are generally more flexible than males (Canada Fitness Survey, 1982; Webb associates, 1978). For two individuals of the same sex and age but differing in size to be of equal flexibility, the larger subject must have more compliant tissues to compensate for the increased number of parallel elements.

Toft et al., (1989) found that PNF (proprioceptive neuromuscular facilitation) stretching lowered the magnitude of the passive moment (ankle) at full dorsiflexion in 10 males aged 23-31 years. The stretching program was found to predominantly affect the elastic component.

Diurnal variations

It is known that biological tissues undergo a variation in stiffness throughout the course of a day. The most common example of this phenomenon is usually associated with the lumbar discs and ligaments (Adams, Dolan, and Hutton, 1987) which are stiffer in the morning. Wright (1959) also noticed so called "morning stiffness" in the MCP joint.

From the above discussion it is clear that many factors affect the passive resistance about a joint such as anthropometry, gender, age, temperature, oedema, drugs, exercise, pathological conditions, time of day, and muscle compliancy. Some of these variables are relatively easy to control while others are more difficult to deal with.

DETERMINATION OF THE NET PASSIVE ELASTIC JOINT MOMENT

In this section the various studies which have been conducted on the passive elastic properties of the knee joint will be discussed with respect to methods, advantages, disadvantages, and results.

Kinematic and biomechanical parameters

Successful measurement of the elastic component requires careful control of three kinematic parameters: velocity, acceleration, and ICOR, as well as several biomechanical variables.

If the velocity becomes too high viscous effects will bias the results. Although no definite minimum velocity threshold has been established, most investigators agree that angular velocities of less than 0.5 $rad \cdot s^{-1}$ will minimize viscous effects. Yoon and Mansour (1982) tested the effects of angular velocity on the passive elastic moment about the hip joint. Angular velocities of 0.017, 0.20, 0.41, 0.81, and 1.62 $rad \cdot s^{-1}$ were tested. No differences in the passive moments were found at the different velocities. Vrahas et al., (1990) tested angular velocities of 0.174, 0.522, and 1.044 $rad \cdot s^{-1}$ on the passive moment at the hip. Similar results were observed, i.e., the passive moments were insensitive to the tested velocities. Of course, all of the tested velocities could have been below some minimum threshold. Hayes and Hatze (1977) observed that repeated trials revealed that constancy of angular velocity was not a critical factor in the determination of the elastic moment about the elbow, provided the deviations did not exceed 30 to 40% of the mean velocity, and no jerk ($\dddot{\theta}$) occurred. The cited reason for this insensitivity of the elastic moment to changes in angular velocity was the fact that the mean velocity had an extremely small value (0.04 $rad \cdot s^{-1}$).

Isolation of the elastic moments also requires either the elimination (or minimization) of inertial moments or the inclusion of an inertial correction factor. The latter choice requires the determination of the moment of inertia of the segment as well as that of the apparatus. This procedure will introduce errors; thus it seems simpler and more accurate to monitor the acceleration and keep it at a very low (i.e., negligible) and constant value.

Since human articulations do not possess a fixed centre of rotation errors can be introduced in an attempt to align the approximate centre of rotation of the joint with that of the apparatus. Vrahas et al., (1990) tested the effects of purposely misaligning the centre of rotation of the apparatus with that of the hip joint. Measurements were repeated on a single subject with the apparatus COR displaced as much as 4 cm (anterior, posterior, rostral, and caudal) from what was judged to be the true ICOR of the hip joint (rostral tip of the greater trochanter). The passive elastic moments changed by a maximum of 4.0 N•m, which was about 25% of the maximum moment measured over the joint range studied. The day-to-day variability displayed results of similar magnitude and was therefore attributed to the variable positioning of the subject on different days rather than to any inherent day-to-day differences.

The moments produced by gravity acting on the segment have been discussed in the literature. Some investigators (Heerkins et al., 1985; Such, 1971; Such et al., 1975) used an apparatus which oriented the subject in a vertical position. This position required that the mass of the segment be determined and the gravitational moments subsequently subtracted out. This was accomplished using counterweights. Two procedures have been used to determine the location of the counterweights. Such (1971) empirically positioned the counterweights until balance was achieved. This method presents a problem since not only is the segmental mass corrected for but the passive moment is also included in the correction. Heerkins et al., (1985) attempted to overcome this problem by estimating the mass and the location of the centre of gravity of the leg using data from Clauser, McConville, and Young (1969) and positioning the counterweights based on these data. It is known, however, that these sources of anthropometric data, although useful, introduce various error sources due to the small skewed samples used (Hinrichs, 1985; Miller and Nelson, 1973). Thus, it is a difficult task to separate out purely gravitational effects. Of course, this problem is easily circumvented by using a horizontal apparatus (Thompson et al., 1978).

Passive musculotendinous tension is most likely a significant contributor to the NPEJM. Therefore the passive moment will be a function of joint angle. Explicit in the NPEJM function is the knee angle (θ), however, the hip and ankle angles (θ_H and θ_A) will also influence the NPEJM, to a lesser degree, since various muscles cross both the hip and knee and the ankle and knee joints (Heerkins et al., 1985; Mansour and Audu, 1986).

Another factor which must be eliminated, or at least minimized, to ensure a truly passive measurement is muscle activity. Voluntary activity can usually be significantly eliminated once the subject is relaxed and accustomed to the experimental apparatus and environment. Reflex activity, however, is difficult to control. Slow rotations with no rapid changes in muscle length should ensure that reflex activity is at least kept to a minimum. It has been reported (Heerkins et al., 1985; Thompson, 1978) that the experimental position is a factor in the subject's ability to relax (a vertical position being more conducive to relaxation). Some investigators choose to monitor the EMG activity of representative muscles crossing the joint (Heerkins et al.,1985; Otahal, 1971) while others argue that muscle activity is easily detected by checking for disturbances on the normally smooth passive moment-angle response curve (Such et al.,1975). Smith (1957) completely circumvented this issue by using anesthetized subjects.

Measurement of the NPEJM

The net passive elastic joint moment has been measured by three general (and similar) methods: i) the sinusoidal oscillation technique (forced harmonic motion); ii) positioning apparatus and iii) the manual rotation technique. All three of these techniques are similar in that they all can be classified as direct stiffness approaches (DSA) of structural mechanics. The DSA measures the moment produced for a known angular displacement. The following paragraphs will discuss each of the three techniques with respect to advantages, disadvantages and results.

Sinusoidal oscillation technique (SO)

This technique involves orienting the subject in either a horizontal or vertical position and securing the segment to a drive arm. The drive arm, which is controlled by a torque motor, can be preset to harmonically drive the segment through a specified angular displacement at a specific frequency for a given number of cycles. Since the mathematics of harmonic motion is well established the analysis becomes facilitated and is easily standardized. At the extremes of the motion the acceleration is at a maximum while the velocity is zero; when the system passes through the equilibrium position the velocity is at a maximum while the acceleration is zero.

The most commonly used apparatus configuration has been the vertical knee arthrograph. As was discussed previously, with this configuration, the mass of the leg must be corrected for. Also, unless the frequency is kept low enough so that inertial moments can be neglected, a correction factor for the moment of inertia must also be incorporated. Vrahas et al., (1990) found that inertial effects inevitably come into play due to the large velocity change required to reverse directions. Also, since the segment is being controlled by a motor, safety measures must be incorporated into the system at different levels (i.e., software, mechanical, etc.). Since the oscillation amplitude cannot be too large the experiment must be performed for small intervals over the range of motion and the results pieced together.

Such et al., (1975) used a vertical knee arthrograph to determine the passive elasticity of the knee joint via the SO technique. A total of 70 subjects (49 male, 21 female) between the ages of 21 and 65 years were tested. The ankle was fixed at 0° while the hip angle was not indicated. The leg was oscillated about a knee angle of 90° (amplitude of 11° according to Thompson et al., 1978) at an angular velocity of 0.078 $rad \cdot s^{-1}$ for five trials. On average, the passive elastic moment was found to be 4.0 $\pm$ 1.5 $N \cdot m$ for the 25 year old male subsample. Inertial moments were considered negligible and the gravitational moments were corrected for by the use of empirically positioned counterweights. The major weakness of this investigation was the single knee angle tested. The knee angle of 90° is, from a modelling perspective, relatively uninteresting since the passive moments and stiffness are quite low (negligible for modelling purposes). It should also be noted that Such et al., (1975) used the term stiffness loosely to indicate passive moments and not in the strict engineering sense as a rate.

Thompson et al., (1978) described the design criteria for a horizontal knee arthrograph and presented the results of six male and six female subjects between the ages of 20 and 30 years. The leg was oscillated at a frequency of 0.1 Hz and at an amplitude of 5° in 10 degree steps from 50° to 120° of flexion. The hip angle was set at 0° and the ankle at 0°. The authors stated that testing knee angles below 50° was not feasible due to excessive ICOR displacement and I-E rotation while apparatus constraints did not allow measurements beyond 120°.

Heerkins et al., (1985) performed a very thorough study of passive knee resistance as related to subject anthropometry using the sinusoidal oscillation technique (vertical apparatus). A sample of 29 males and 20 females between the ages of 18 and 56 years was tested. The leg was oscillated at an angular velocity of 0.51 $rad \cdot s^{-1}$ and an amplitude of 7.5°. The test was repeated in 5° steps from 5° to 110° of flexion. Although no distinction was made between viscous and elastic components it is assumed that the results represent mostly elasticity due to the relatively low angular velocity used. The passive moments were characterized by a number of parameters (resistance variables) including the centre moment (CM) which was the moment at the centre of the hysteresis loop, the extension moment, EM (at 5°), the flexion moment, FM (at 110° of flexion). The centre moments were fitted to a cubic function and the equilibrium angle (EA) was defined as the knee joint angle at which the cubic function crossed the x-axis (CM=0). The mean EA (at θ_H=90° and θ_A=0°) was found to be 64.4° (± 6.1°) for males (n=29) and 56.2° (± 6.9°) for females (n=20). The effects of changing the hip joint angle were consistent with anatomical considerations. As the hip angle was decreased from 90° to 80° to 55° the extension moments (for the same knee angle) increased while the flexion moments decreased. The change in hip angle also had the effect of shifting the equilibrium angle.

A multiple linear regression analysis revealed that for males 35-77% of the variance in the resistance parameters could be accounted for by the anthropometric parameters. More specifically, during flexion 57% of the variance in the CM could be accounted for by the anthropometric parameters. During extension, this figure increased to 71%. The best predicted resistance variable was FM (77%) while the worst predicted was EM-FM (35%). There are numerous possible reasons why the R^2 values are so variable. First, it is known that hormonal factors can contribute to joint stiffness (Fischer, 1973; Hama et al., 1976) and anthropometric parameters are not necessarily good indicators of relative collagen density. Also, since the situation is one of successive engagement and disengagement of the various tissues, the appropriateness of the predictors may vary throughout the range of motion. It should also be noted that although a correlation analysis was performed by Heerkins et al., (1985), prediction equations were not generated.

The sinusoidal oscillation technique is a useful technique for measuring the passive elastic moments about an articulation. Since a mechanical motor is involved, however, various safety measures must be incorporated into the system at various levels. Also, no data is available on the effects of angular frequency to the viscous contribution, hence the oscillations should be performed at a low frequency to ensure negligible velocity dependent viscous effects. This technique best lends itself to the study of the time dependent viscoelastic properties (hysteresis, creep, and stress relaxation) since these are best studied under cyclic loading conditions (Fung, 1981). Figure 1 is a graphical summary of the results of the three studies using the small oscillation technique to determine the passive elastic moments about the knee joint. The data of Heerkins et al., (1985) represent the centre moments for a typical male subject with the hip angle at 90^{0} and the ankle at 0^{0}. The data for Thompson et al., (1978) are the average values of the six male subjects while the single symbol (**X**) represents the average data of young males from Such et al., (1975).

Positioning apparatus (PA)

This technique is similar to the SO method in that the segment is rotated by a motor or other mechanical device. However, the apparatus does not harmonically oscillate the segment, rather it sweeps the limb through a desired angular displacement while measuring the resistive moment. This approach is less time consuming than the SO technique since a continuous moment-angle curve is generated. The most sophisticated of this type of apparatus has been developed by Engin (1985) and Engin and Peindl (1980). The apparatus is a global force applicator (GFA) and was used to study the three-dimensional passive resistive properties of all major human articulations over the full range of joint motion. The GFA is capable of correcting for gravitational moments. It should be noted that the GFA is actually a

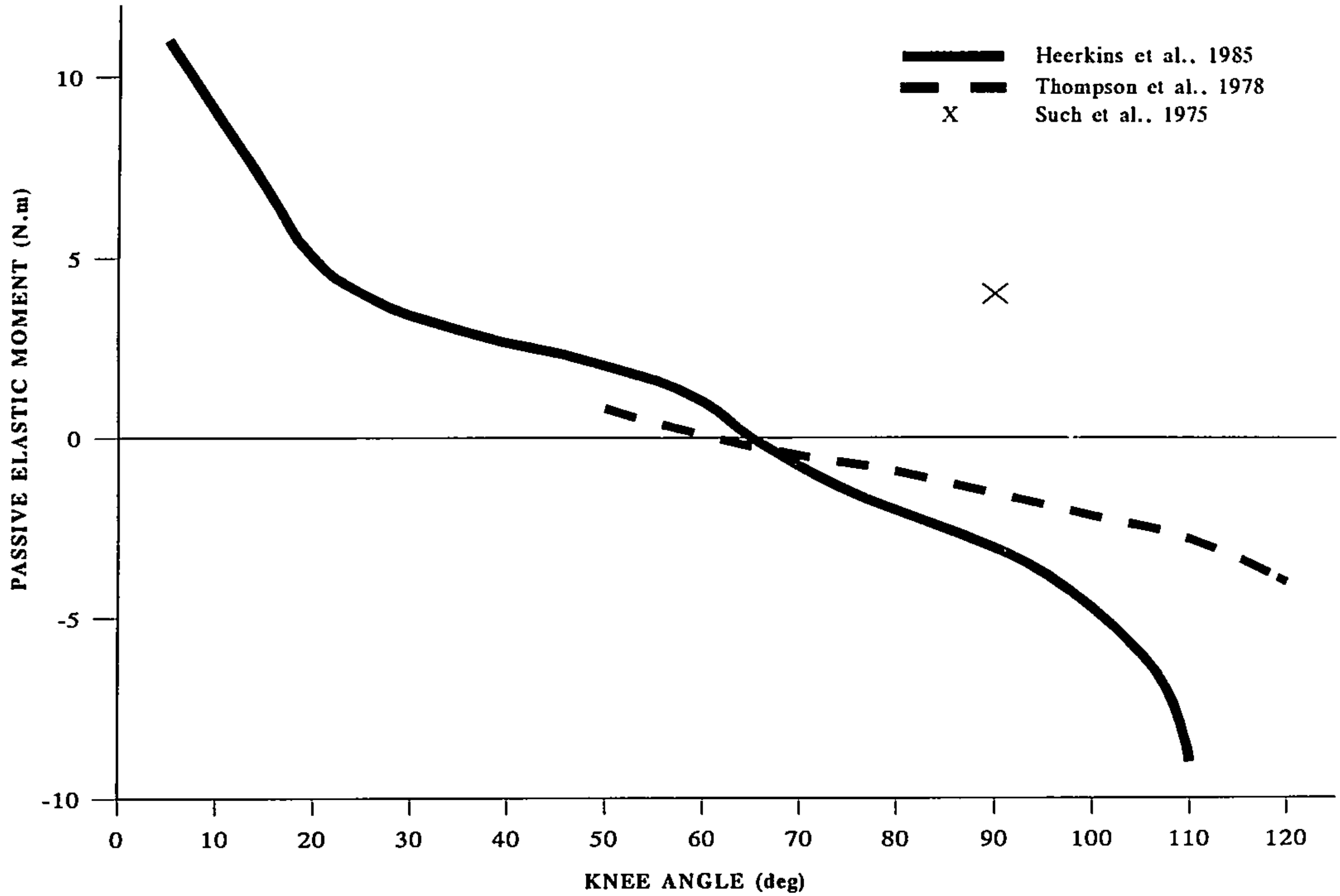

Figure 1. Literature summary of the NPEJM measured using the sinusoidal oscillation technique. See text for details; A negative sign indicates an extension producing moment.

hand-operated device and could also be classified as a manual rotation technique (described in the next section); but since the GFA setup involves a complex track mounted pulley and linkage system, it was arbitrarily classified here as a positioning apparatus. Three male subjects (age not indicated) were studied over the full range of knee joint motion and beyond (0° to 160°) for three trials. The hip and ankle angles as well as the velocity of rotation were not specified. The moment-angle curves were sigmoidal and the magnitudes of the passive moments increased to significant values as the mechanical limits of the joint were approached.

Otahal (1971) also used this technique (PA) to measure the passive elastic moment about the knee of 26 subjects (gender and age not indicated). The subject was positioned in a horizontal configuration which eliminated gravitational effects. The hip was set 0° while the ankle angle was not indicated. The joint was tested from full extension to 120° of flexion at an angular velocity of 0.175 $rad \cdot s^{-1}$. No statistics were presented despite the reasonable sample size.

Figure 2 graphically summarizes the results of the above two studies. The results presented are those of a typical subject. In the data of Otahal (1971) slight hysteresis was present at some knee angles, thus the data point represents an average between the flexion-extension and extension-flexion cycles. The data show the potential for large inter-individual differences in the passive elasticity of the knee joint.

Manual rotation technique (MR)

This technique involves the same type of apparatus as the other techniques

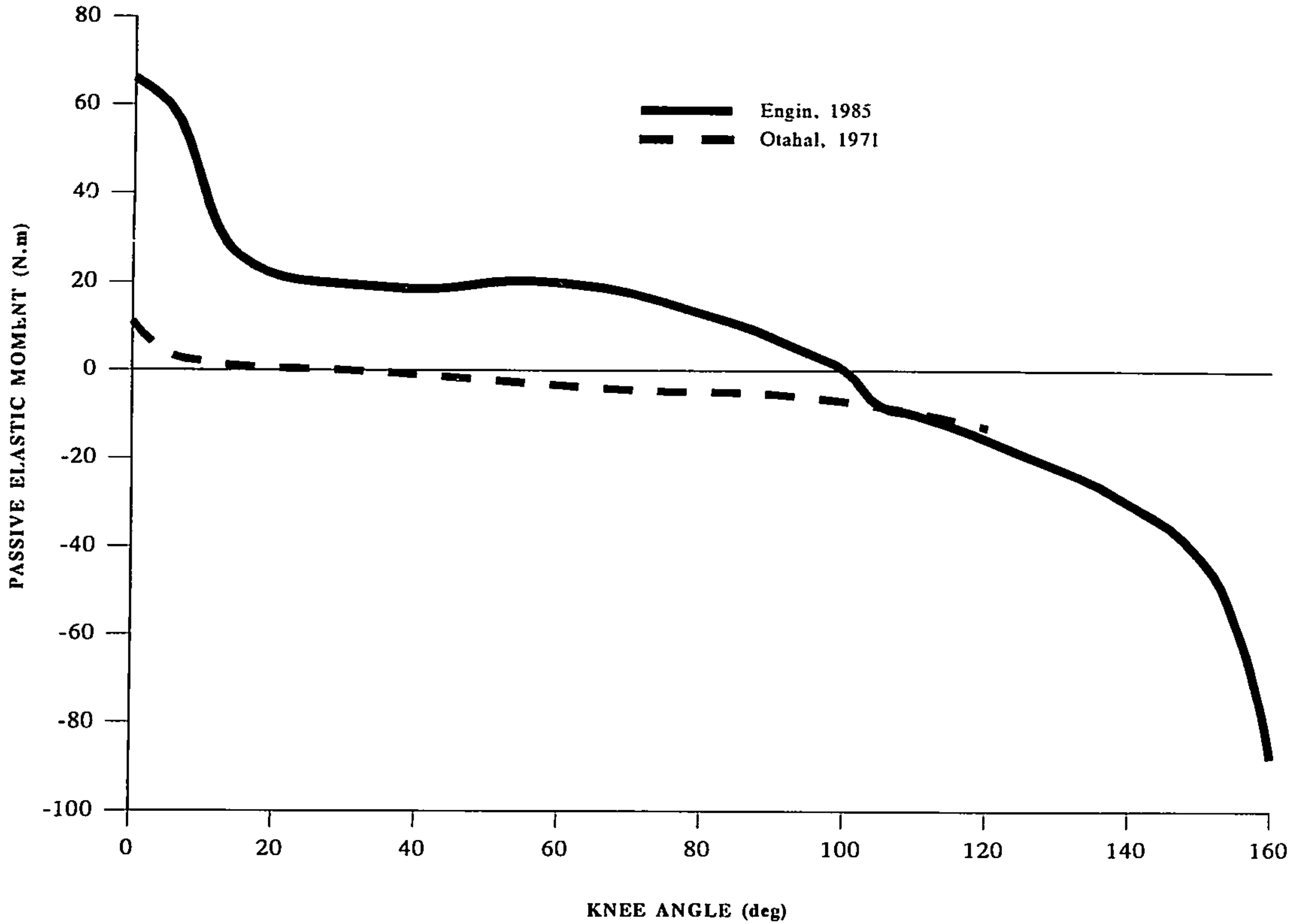

Figure 2. Literature summary of the NPEJM measured using the PA technique. See text for details; A negative sign indicates an extension producing moment.

except that the limb is driven by a human operator; usually by an instrumented lever or a cable-strain gauge linkage. The obvious drawback with this method is the reliability of the experimenter to apply force at a constant velocity. However, as Hayes and Hatze (1977) have pointed out, the constancy of velocity is not critical as long as the average velocity remains small. Similar to the positioning apparatus, this method generates a continuous moment-angle curve. Compared to motor driven apparatii, this technique provides a safer and more cautious approach when testing human articulations at their mechanical limits.

Mansour and Audu (1986) used the manual rotation method to determine the passive elastic moment of the knee joint of four male subjects ranging in age from 23-30 years. A horizontal apparatus was used. The foot was secured to a rotating stool that was instrumented with a strain gauge load cell and which was separate from the rest of the apparatus. The knee joint angle was measured using an electrogoniometer (ELGON) fixed to the subject's knee. Measurements were carried out by having one of the experimenters rotate the stool by following a light beam which was moving at a constant angular velocity on the floor. This experimental setup can add stiffness to the system due to the frictional resistance of the stool wheels on the floor and of the ELGON. The main limitation of this study, however, was the limited range of motion (in flexion) studied. The joint was tested from full extension to about 100° of flexion. The passive elastic moment was observed to be approximately an exponentially increasing function of knee joint angle from $\theta=0°$ to $\theta=100°$. The effect of changing the hip and ankle joint angles was also tested. The ankle was tested at full dorsiflexion and full plantarflexion; the hip was set at either 0°, 10°, or 20° of flexion (approximately). As the ankle changed position from plantar to dorsiflexion the flexion moments increased, presumably due to lengthening of the gastrocnemius. Flexion of the hip caused a shift of the passive moment to generally higher values. It is interesting to note that the passive moment curves at different hip angles converged to the same value in extension indicating that, for the subjects tested, the passive moment in extension was independent of hip angle (for $0° \leq \theta_H \leq 20°$). It was also noted that of the four subjects tested one was significantly larger (body mass criterion) than the other three. Inspection of the data revealed that this subject had a much stiffer joint than the other three.

Hatze (1975a) also used the manual rotation technique to determine a passive elastic moment function of the knee joint of one 23 year old male subject. It must be pointed out that although the single subject sample is definitely a weakness, determination of the elastic moment was not the primary goal of the study. The function was to be used as subject specific input into a dynamic muscle model. The apparatus used was of a horizontal configuration. The leg was rotated by an instrumented (strain gauge) lever through a range of 0° to 130°. The resulting curve was stated to be independent of the length of the biarticular muscles since the effects of these muscles were previously determined and subsequently subtracted out.

Smith (1957) used a novel approach to determine the passive resistance of the knee of three young male subjects who were anesthetized for unrelated surgery. Due to the objective of the study only the terminal extension phase was tested (-10° to

40°). The subject was placed on a trolley in the prone position with the knee just over the edge. The leg lay passively in a sling which was connected above to a precalibrated tension spring. Through a pulley system the experimenter rotated the leg through the desired range. The length of the spring and the knee angle were recorded on cine film at 16 frames per second. The experiment was repeated with the subject in a supine position. Through trigonometric considerations the NPEJM function was calculated. Apparently the ankle angle was not controlled and may have varied during the testing. The results for the three subjects were very similar in magnitude and phase.

Figure 3 illustrates the results which were obtained from the three studies using the MR technique. The data of Mansour and Audu (1986) represents the results of a typical subject averaged over four trials with the hip at 12°and the ankle at 10° of dorsiflexion (-10°). Since hysteresis was observed the data points represent the average of the flexion-extension and extension-flexion values. The data of smith (1957) represents the average of the three subjects tested. The curve of Hatze (1975a) showed some interesting qualities. Between the knee angles of 10° and 115° of flexion the passive moments were very low, i.e., the knee was very compliant. However, beyond these positions the stiffness increases very rapidly. Contrast this with the more gradual increase in stiffness in extension of the subject of Mansour and Audu (1986). Note also the comparably low values in extension for the data of Smith (1957). These results again reveal the potential for a large variability in passive moment data and point to the need for a large statistical database.

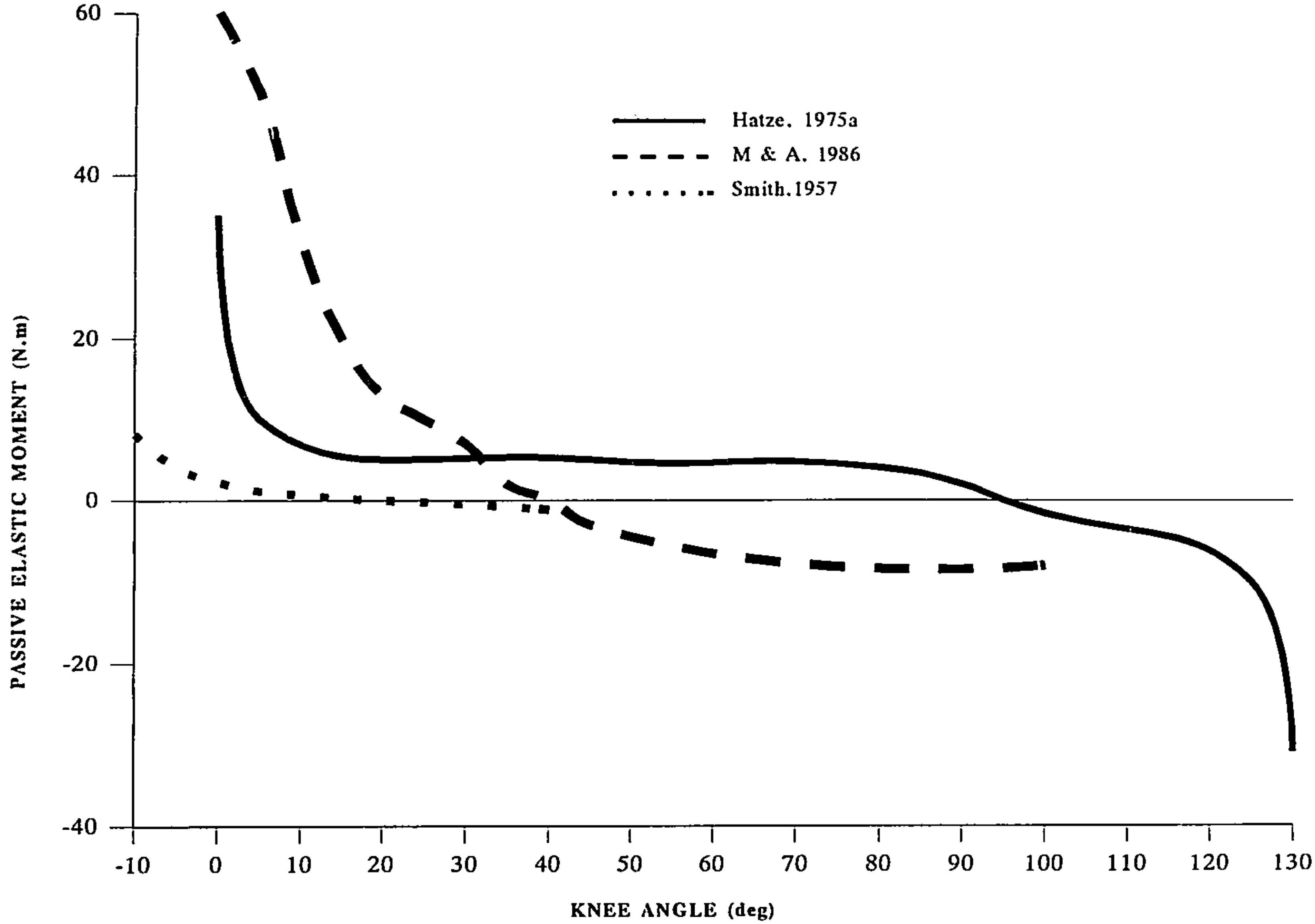

Figure 3. Literature summary of the NPEJM measured using the manual rotation technique. See text for details; A negative sign indicates an extension producing moment.

In summary, the NPEJM can be measured by the direct stiffness approach (as opposed to the compliancy approach) using a number of different experimental apparatii. A torque motor can be used to rotate the leg but safety measures must be implemented to avoid possible injury to the joint. A manually operated apparatus is a more cautious and less intimidating approach to measuring moments about a joint near its mechanical stops. A horizontal configuration is preferred over a vertical setup since gravitational moments (in the sagittal plane) do not enter into the analysis. Also, a small mean angular velocity is critical for proper isolation of the elastic moment and avoidance of inertial moments. Although many investigators did not utilize EMG to monitor the muscles which could potentially contaminate the results (Engin, 1985; Hatze, 1975a; Mansour and Audu, 1986; Such et al., 1975; Thompson et al., 1978) it may be worthwhile to do so since the probability of a protective response increases as the joint limits are approached. It is interesting to note that the data of smith (1957) (at full extension) is at least five times lower and up to 29 times lower than data from other studies. The muscles of anesthetized subjects are completely flaccid with no nervous input. It is possible that some of the studies which obtained very high moments at 0° (Engin, 1985; Mansour and Audu, 1986) may have inadvertently also measured an active protective response.

Hysteresis, which along with stress relaxation, is a property of viscoelasticity and is usually always present to varying degrees when using the SO technique. Hysteresis, however, was not present in all of the studies reviewed. The appearance of hysteresis may be a function of a number of different parameters such as the number of cycles, the amplitude of oscillation, the speed of rotation, the kinematic history, the reversal time, the subject, the knee, ankle, and hip angles and other factors. The effects of various parameters on the degree of hysteresis is the subject of a separate study.

As is evident from the above review, the main gaps in the literature regarding the NPEJM of the knee joint are limited range of motion, small samples, and lack of statistical analyses. It is clear that the potential for inter-individual variability is high and a large statistical database is required so that models of the human system can be supplied with more realistic input.

Characterization of the NPEJM function

For modelling purposes most investigators prefer to express biomechanical functions as mathematical relations and/or to characterize them with various parameters.

Modelling equations

From the preceding review it is evident that the passive elastic moment function of the knee joint, although highly variable, assumes a definite functional character when tested over the full range of motion. This functional nature has also been observed in other human articulations (Boon, Hof, and Wallinga-de Jonge, 1973; Engin, 1985; Engin, Akkas, and Kaleps, 1980; Engin and Chen, 1986; Engin and Peindl, 1987; Hayes and Hatze, 1977; Nashold, 1966; Siegler, Moskowitz, and Freedman, 1984; Vrahas et al., 1990; Wright and Johns, 1961; Yoon and Mansour, 1982). The midrange of joint motion is generally characterized as a low stiffness, low moment region. As the leg rotates into the terminal phases of flexion or extension the moments rise sharply. The rapid increase in the passive moments as the joint limits are approached has been modelled as an exponential function(s) by many investigators (Audu and Davy, 1985; Hatze, 1975a; Hof and Van Den Berg, 1981; Yoon and Mansour, 1982).

Soft joint stops and the equilibrium angle

As the limb moves through the range of motion it will encounter points of increased resistance. These points, called soft joint stops or breakpoints, have been of interest to modellers in the area of crash simulation and aerospace research (Fleck et al., 1975; Obergefell, Avula, and Kaleps, 1988; Prasad and Chou, 1989; Wismans, Griffioen, and Nieboer, 1988). The location of the soft stops is not fixed but rather dependent on the criteria used to determine them. Even for a given criteria some variability will exist due to the history-dependent viscoelastic nature of the tissues.

In the orthopaedic literature qualitatively similar curves are obtained in V-V and I-E studies. Markolf, Mensch, and Amstutz (1976) measured the stiffness and laxity of cadaver knee joints in I-E. The moment-angle curves were separated into three phases. The neutral stiffness was defined as the slope of the best fit line in the midrange of joint motion. The extremes of motion were represented by terminal stiffnesses which were defined as the slope of the tangent line to the terminal data points. The soft stops were defined as the points of intersection of the extrapolated neutral and terminal stiffness lines. Figure 4 depicts an idealized NPEJM curve. The location of the soft stops are identified along with another elastic parameter called the

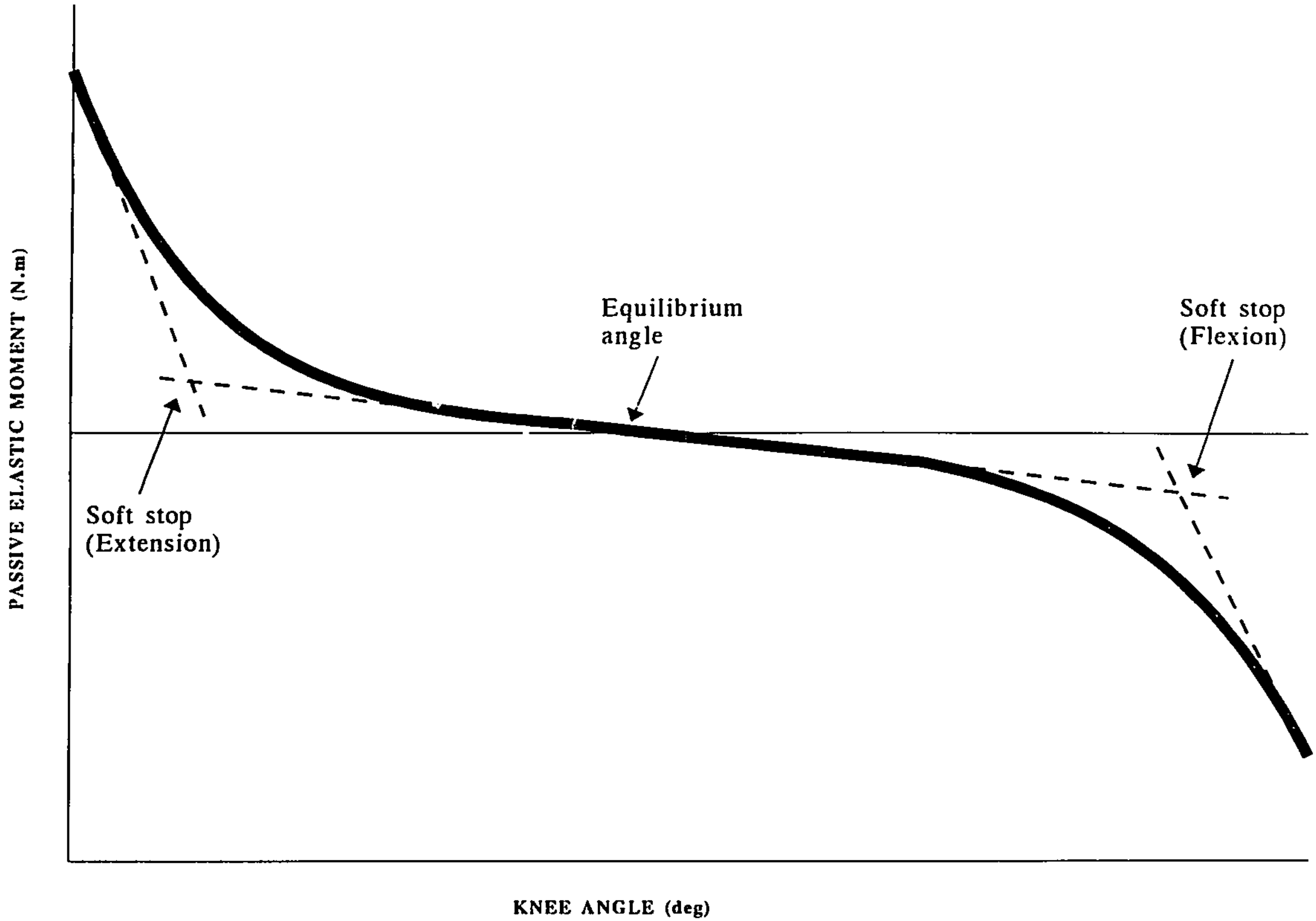

Figure 4. Idealized NPEJM function with associated elastic parameters. Dotted lines are extrapolations of the midrange and terminal moment equations.

equilibrium angle which is the point at which the NPEJM=0.

DETERMINATION OF THE NET PASSIVE VISCOUS JOINT MOMENT

In this section the studies dealing with the viscous properties of the knee joint will be discussed. The measurement of the damping coefficient by the small oscillation technique, due to some mathematical detail, will only be discussed with respect to results, advantages, and disadvantages in this section; a subsequent section will detail the theoretical aspects of this technique.

Measurement approaches

Three techniques have been used to measure the viscous properties of human articulations.The first technique, which was used on the MCP joint by Wright and Johns (1960) employs the same sinusoidal oscillation method which was previously discussed with respect to the NPEJM. Since the velocity is maximal as the leg passes through the equilibrium position, the viscous moment, which is a function of the velocity, will also be maximum (based on a linear model). Also, since the elastic moment is known at this position it can be subtracted out and the remainder will supposedly be the viscous moment. The results can be pieced together to form the NPVJM function.

Another approach is the systems identification (SID) method (Kearney and Hunter, 1990; Weiss et al., 1986). An electrohydraulic actuator delivers a pseudo-random perturbation to the limb over a certain time interval while the moment and angle are simultaneously measured. The mechanical behaviour of the joint is modelled as a second-order underdamped system having inertial, elastic, and viscous terms.

Nonlinear minimization techniques are used to estimate the parameters which best fit the compliance impulse response functions. The perturbations are performed at a number of angles over the joint range. This method allows determination of both the elastic and viscous stiffness.

The final approach, the small oscillation technique (Engin, 1984; Hatze, 1975b), is similar to the SID method in that the articulation is also modelled as a second-order underdamped system. The small oscillation technique (SOT) is based on standard linear vibration theory (Thomson, 1988). Conventional analysis of vibrating mechanical systems usually proceeds with what has been termed by biomechanists as a forward solution: the kinetics (spring force, viscous force, etc.) are known and the system kinematics are calculated. As is common in biomechanics some or all of the kinetic parameters are unknown and are calculated from the resulting system kinematics; this type of solution is known as an inverse solution. The small oscillation technique uses an inverse solution approach to calculate the angular damping coefficient of the knee joint from the kinematics of the oscillation. The segment is distally suspended from a linear spring-load cell assembly, with the spring being of accurately known stiffness. The segment is then slightly displaced from the equilibrium position and allowed to oscillate under the restoring forces of the spring and the passive moments of the articulation. The viscosity of the periarticular structures will cause the amplitude of the oscillations to diminish over time. The damping coefficient can be calculated from the amplitude decay history. It must be noted that since human articulations generally behave nonlinearly the oscillations must be small enough so as to allow a local first-order approximation by linearization about the equilibrium position. The results can be pieced together to form a damping coefficient versus joint angle function. The NPVJM can be calculated by multiplying the damping coefficient by the angular velocity. The mathematical details of this technique will be described in a subsequent section. The general nonlinearity of the knee joint has been dealt with in this way by numerous investigators (e.g., Andriacchi, Mikosz, Hampton, and Galante, 1983; Jans, Dortmans, Sauren, and Huson, 1988; Moffatt, Harris, and Haslam, 1969).

Hatze (1975a, 1975b) appears to have been the first investigator to use the technique on the knee joint; the results are displayed in Figure 5. The data of this figure represent the data from the one subject tested (the same subject as in Figure 3). Although no definite conclusions can be drawn from a single subject study, the results of this technique on other joints (Engin, 1984; Hatze, 1975a; Hayes and Hatze, 1977) indicate that the damping coefficient function is approximately quadratic in nature. It should be noted that the damping curve in Figure 5 appears to contain extrapolations to the extremes of joint motion since positions of hyperextension and flexion angles around 150° to 160° are very difficult to obtain in the laboratory under the constraints of the small oscillation technique.

Problems and limitations with the small oscillation technique

The small oscillation technique is not without some problems and limitations. One of the major concerns involves the possibility of the oscillations eliciting a stretch reflex and thereby contributing to the damping. Sinkjaer and Hayashi (1989) have

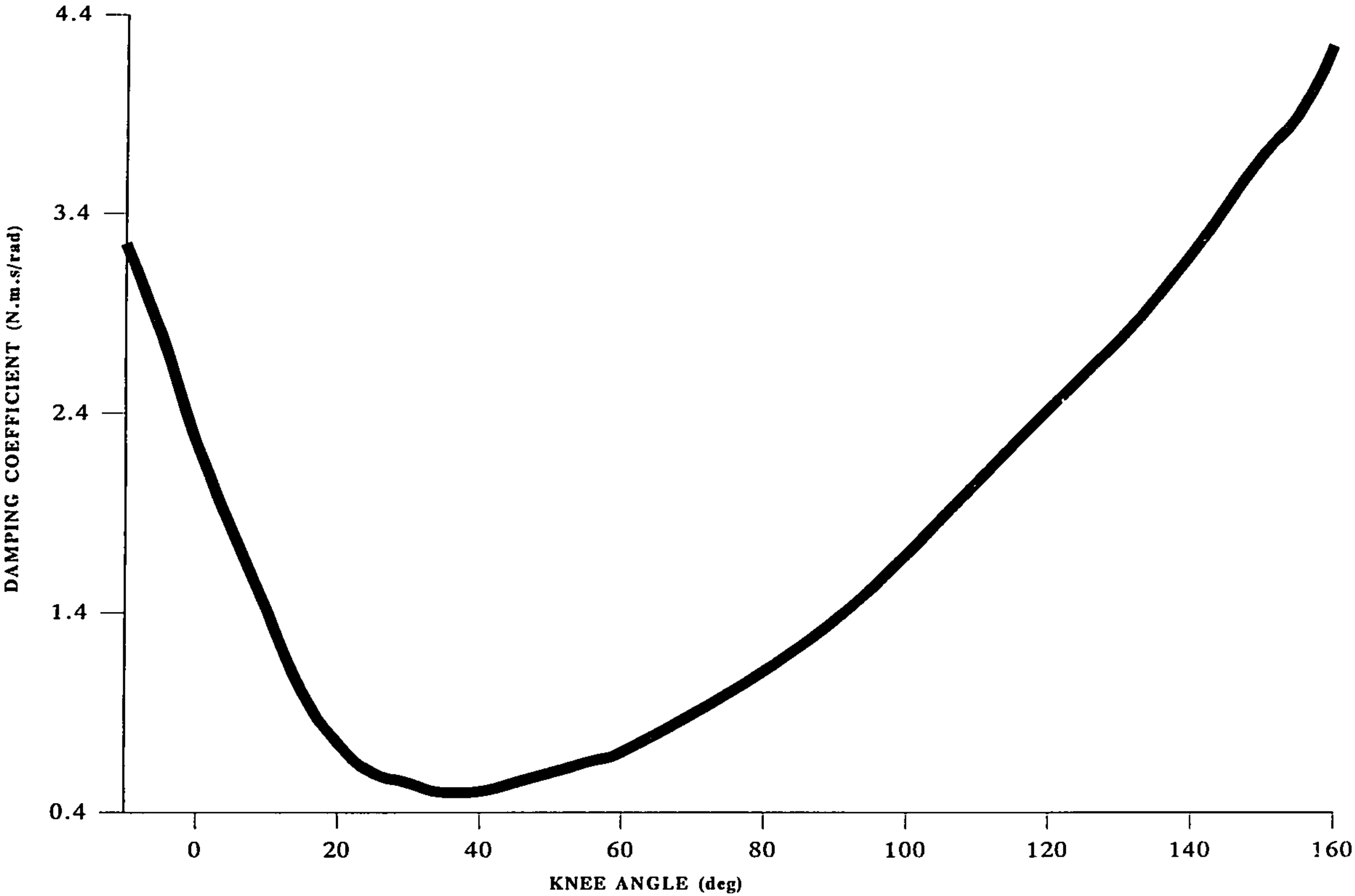

Figure 5. The damping coefficient as a function of knee angle. Adapted from the work of Hatze (1975a).See text for details.

found that the stretch reflex can have a considerable effect on restoring a segment to an equilibrium position. To test for the possibility of stretch reflex involvement, Hayes and Hatze (1977) used two reflex facilitation procedures, namely the Jendrassik manoeuvre (Hayes, 1972) and the tonic neck reflex, TNR (Hayes, 1976) to aid in the detection of reflex activity. It was reasoned that any increase in the damping coefficient as a result of the facilitation procedures could be attributed to stretch reflex activity. The results were subject dependent. In those subjects who had no problem relaxing prior to oscillation the facilitation procedures did not make a significant difference. However, with those subjects who had difficulty maintaining relaxation, a distortion in the oscillogram was apparent. This reflex activity, which appeared only if electrical silence was not achieved prior to release of the limb, was most likely due to an elevated gain of the muscles stretch servomechanism during an active contraction (Marsden, Merton, and Morton, 1972). The authors made the conclusions that if electrical silence can be maintained prior to release of the limb and that remote muscle groups are relaxed then the results of the small oscillation technique should not be significantly contaminated by reflex activity. Both Engin (1984) and Hatze (1975b) noticed that the first peak on the oscillogram was much larger than subsequent peaks, indicating relatively large initial damping probably attributable to the stretch reflex. Thus, the first peak was not used for any of the damping coefficient calculations.

A peculiar problem was revealed by Stijnen, Willems, Spaepen, Peeraer, and Van Leemputte (1983). The results appeared to be a function of the spring stiffness and the suspension distance. The technique was tested on the whole arm (arm and forearm) and the whole leg (thigh and leg) for different values of spring constant and suspension length. As will be discussed in the following section, the moment of inertia of the oscillating segment is an intermediate variable in the SOT. Thus, a partial validation would be to test the technique on a solid of known physical parameters. Hence, along with the above mentioned segments the test was also repeated on an iron rod of a theoretically known moment of inertia under the same experimental conditions. The tests were carried out for spring stiffnesses of 184, 1080, 1264, and 2170 $N \cdot m^{-1}$ at a fixed suspension distance. The tests on the iron rod revealed a high degree of reliability and validity with all calculated values of moment of inertia being within 0.5% of the theoretical value. When the technique was tested on the human segments various discrepancies appeared. The moment of inertia appeared to be a function of the spring stiffness. The largest difference in the moment of inertia was found to be 61% between the most compliant (184 $N \cdot m^{-1}$) and stiffest (2170 $N \cdot m^{-1}$) springs while the smallest difference (6.6%) appeared between the 1080 and 1264 $N \cdot m^{-1}$ springs. The results using the 184 $N \cdot m^{-1}$ spring showed the largest variations compared to the other springs. A spring stiffness of 184 $N \cdot m^{-1}$ represents a very compliant spring under the experimental loading conditions and it is possible that the elastic limits were exceeded and the spring was beginning to behave nonlinearly.

Similar findings were revealed when the effects of suspension length (d) were tested for a fixed spring stiffness. Three different positions of d were tested:

proximal, mid, and distal. The moment of inertia differed by 15.2% between the proximal and distal conditions and by 6.5% between the proximal and mid distances.

Possible causes of the discrepancies were stated to be moving muscle mass during the oscillations, the specific shape of the joint, and out-of-plane rotations. Since the small oscillation technique assumes the segment to be a rigid body it is possible that the observed discrepancies reflect variable rigidity of the segments; that is, it is possible that the different suspension positions and spring stiffnesses modulated the 'effective' rigidity of the segment. It should also be noted that the tests done by Stijnen et al., (1983) were done on multilink segments which require splinting to prevent angular motion between the segments.

Peyton (1986) has pointed out that the small oscillation technique can determine the moment of inertia of an isolated, solid object, of an appropriate size with an error not exceeding 2%. Also, the elasticity crossing a joint will alter the moment of inertia unless it is accounted for. Thus, accurate measurement of the NPEJM is required and any error involved in this measurement will be carried into the calculations of the small oscillation technique.

One of the major advantages of the small oscillation technique is that only two transducers are required: the springs and the load cell. Thus, the effect of cumulative errors in multi-transducer designs can be minimized.

The small oscillation technique: Theoretical considerations

The following section outlines some of the mathematical details involved in the small oscillation technique. A small nomenclature section defining some of the terms and units used in the subsequent analysis is first presented. Figure 6 also illustrates some of the joint angle definitions and the coordinate system employed.

Nomenclature

θ The knee joint angle (radians). See also Figure 6.

θ^* The knee angle about which the small oscillations are taking place (radians).

ϕ The knee joint angle defined with respect to the horizontal (radians). See also Figure 6. $\theta(t)=\theta^* \pm \phi(t)$.

K The stiffness of the spring assembly ($N \cdot m^{-1}$).

d The distance between the lateral femoral epicondyle and the suspension point of the right leg (m).

m_l The mass of the leg-foot segment (kg).

m_a The mass of the apparatus to which the leg-foot is attached (kg).

g The acceleration due to gravity ($9.81\ m \cdot s^{-2}$).

I_l The moment of inertia of the leg-foot segment about the y-axis through the knee joint centre ($kg \cdot m^2$).

I_a The moment of inertia of the apparatus components about the y-axis through the knee joint centre ($kg \cdot m^2$).

τ The time period of the damped oscillations (s).

δ The logarithmic decrement of the damped oscillations (dimensionless).

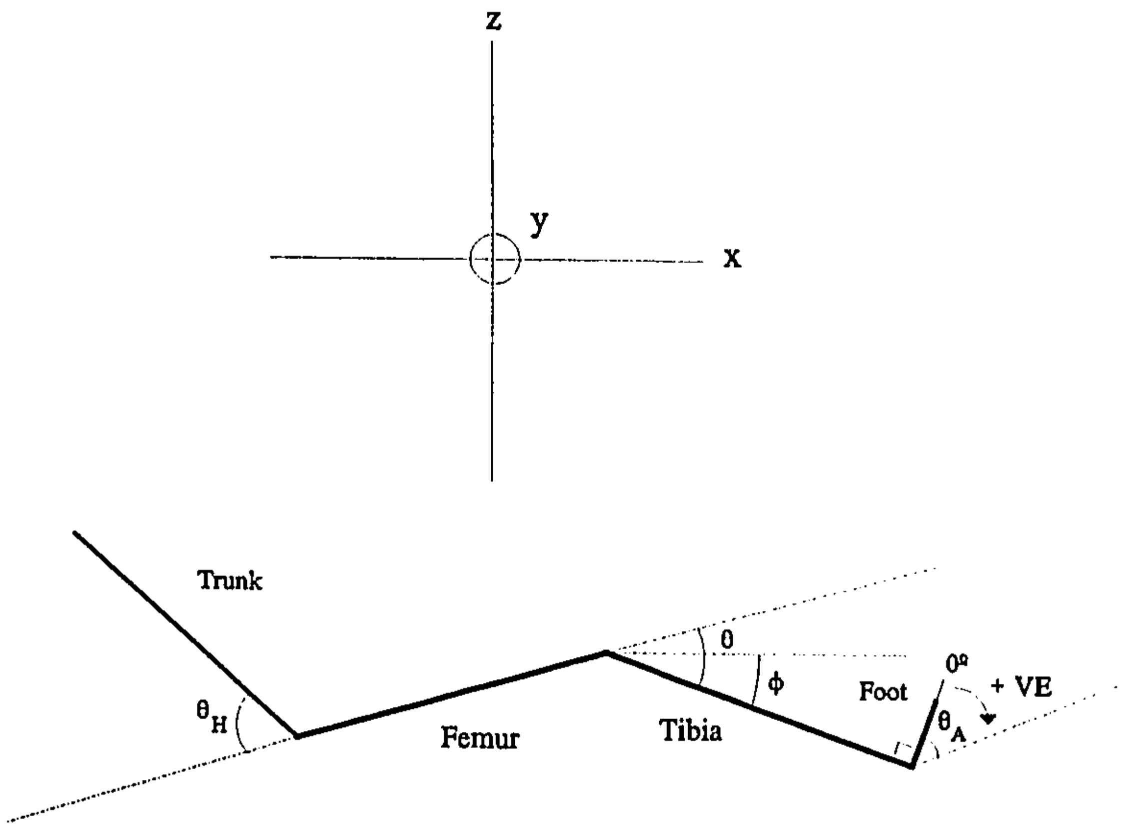

Figure 6. Definitions of the knee (θ, ϕ), Hip (θ_H), and ankle (θ_A) angles and the coordinate system used in the analysis. The Y - axis is perpendicular to the plane of the page.

The functional nature of the passive moments

The total viscoelastic moment function (NPJM or $M_p(\theta,\dot{\theta})$) acting about the approximate centre of rotation of the knee joint is given by:

$$M_p(\theta,\dot{\theta}) = M_e(\theta) + M_v(\theta,\dot{\theta}) \tag{1}$$

Both of the functions on the right hand side of equation (1) are known to be nonlinear functions of joint angle, θ (Engin, 1984; Engin, 1985; Hatze, 1975a, 1975b; Heerkins et al., 1985; Mansour and Audu, 1986).

As previously discussed, the passive elastic moment function has been shown to exhibit an exponential nature as the terminal regions of joint range are approached. Due to the velocity dependence of the viscous moment the exact nature of the function is difficult to determine and is therefore not clearly understood. In a typical viscously damped mechanical system the viscous forces are written as a separable function which takes the form (Thomson, 1988):

$$F_d = -b\dot{x} \tag{2}$$

where b is the linear damping coefficient which is a constant for a given damper. With respect to the human system, *in vivo* experimental evidence (Engin, 1984; Hatze, 1975b) indicates that, within limits, the viscous moment function can also be expressed as a separable function:

$$M_v(\theta,\dot{\theta}) = C_k(\theta)\dot{\theta} \tag{3}$$

where $C_k(\theta)$ is the angular damping coefficient of the knee joint (in $N \cdot m \cdot s \cdot rad^{-1}$)

which is a nonlinear function of the knee joint angle. The assumption of the independence of $C_k(\theta)$ on $\dot{\theta}$ in equation (3) will be justified in a later section since forthcoming information is required to understand the reasoning.

From the above discussion it is evident that both $M_e(\theta)$ and $M_v(\theta,\dot{\theta})$ are generally nonlinear. Therefore, the equation of motion of the oscillating system will be nonlinear. While nonlinear differential equations (NDE) can be solved, the theory is not as well developed as linear theory. Also, the exact nature of the nonlinearity of $M_v(\theta,\dot{\theta})$ is not clear. In many cases it is possible to replace a nonlinear equation by a related linear equation which approximates the actual nonlinear situation (either over the whole range of values or over a restricted interval) closely enough to give useful results (Kahn, 1990; Ross, 1964; Thomson, 1988). This linearization approach forms the basis of the small oscillation theory (Goldstein, 1981; Wells, 1967) and will be used in the present analysis.

Linearization of the NPEJM function: The series approximation. Even though the oscillations are small, $M_e(\theta)$ cannot be assumed constant. Hence, a linear approximation of $M_e(\theta)$ must be incorporated into the differential equation. The Taylor series expansion of an infinitely differentiable continuous function f in incremental form (Beyer, 1984) is:

$$f(x+h) = f(x) + hf'(x) + \frac{h^2}{2!}f''(x) + \frac{h^3}{3!}f'''(x) + \ldots \tag{4}$$

If the system is oscillating about a given knee joint angle, θ^*, over the interval ($\Delta\theta$ sufficiently small):

$$\theta^* + \Delta\theta \geq \theta \geq \theta^* - \Delta\theta \tag{5}$$

the function $M_e(\theta)$ can be represented by:

$$M_e(\theta^* + \theta) = M_e(\theta^*) + \theta\left[\frac{dM_e(\theta)}{d\theta}\right]\Bigg|_{\theta^*} + \frac{\theta^2}{2!}\left[\frac{d^2M_e(\theta)}{d\theta^2}\right]\Bigg|_{\theta^*} + \frac{\theta^3}{3!}\left[\frac{d^3M_e(\theta)}{d\theta^3}\right]\Bigg|_{\theta^*} + \ldots \tag{6}$$

If the first two terms of the series expansion are retained, a local first-order (linear) approximation of $M_e(\theta)$ at $\theta=\theta^*$ is obtained:

$$M_e(\theta^* + \theta) = M_e(\theta^*) + \theta\left[\frac{dM_e(\theta)}{d\theta}\right]\Bigg|_{\theta^*} \tag{7}$$

The bracketed component of the second term on the right hand side of equation (7) represents the tangential angular elastic stiffness (TAES in $N \cdot m \cdot rad^{-1}$) of the knee joint at $\theta=\theta^*$, hence, let

$$\left[\frac{dM_e(\theta)}{d\theta}\right]\Bigg|_{\theta^*} = K_e(\theta^*) \tag{8}$$

and equation (7) is then rewritten as:

$$M_e(\theta^* + \theta) = M_e(\theta^*) + \theta K_e(\theta^*) \tag{9}$$

Linearization of the NPVJM function: The piecewise linear approximation technique. To linearize $M_v(\theta,\dot{\theta})$ over a small interval ($\Delta\theta$) various assumptions must be made. Recalling equation (3):

$$M_v(\theta,\dot{\theta}) = C_k(\theta)\dot{\theta} \tag{3}$$

It is clear that it is assumed that $M_v(\theta,\dot{\theta})$ varies linearly with velocity, $\dot{\theta}$. It is expected that most of the damping will be the result of the viscosity of the relaxed musculotendinous units and soft tissues surrounding the knee joint and also due to the viscosity of the joint synovia. Most biofluids are non-Newtonian (Fung,1981) hence, one may expect the linearity assumption to be invalid. However, it is known (Giles, 1977; King, 1966; Ribitsch, 1990) that non-Newtonian fluids can be approximated as Newtonian (linear) at low shear stresses. Many investigators have assumed linear viscosity in their muscle models (Glantz, 1974; Loeffler and Sagawa, 1975).

In equation (3) $C_k(\theta)$ is the angular damping coefficient of the knee joint which is a nonlinear function (continuous and differentiable) of the knee joint angle, θ. It is expected that the function $C_k(\theta)$ will be well behaved and will not locally be a strong function of θ in the sense that $dC_k(\theta)/d\theta$ will not be of high magnitude (i.e., will not change rapidly) or contain singularities (Engin, 1984). Hence, for a small oscillation of the leg-foot segment about an equilibrium position, θ^*, $C_k(\theta^*)$ can be taken as constant. Based on this assumption the function $C_k(\theta)$ can be mapped out over the whole range of knee joint motion. This method is called piecewise linear approximation.

Derivation of the equation of motion

If the thigh is fixed and the leg is secured distally in an apparatus (SOA) which allows oscillations about the knee in the sagittal plane, the free body diagram (FBD) of the forces and moments acting on such a system can be depicted as in Figure 7. The frictional forces in synovial joints, as was previously discussed and which should not be confused with articular viscosity, are known to be quite low and are not included the FBD of Figure 7. In the subsequent sections the equation of motion of the system depicted in Figure 7 will be developed and the solution to this equation will be used to derive equations to calculate the system damping.

Spring force. The linear restoring force due to a linear deflection z of the spring of stiffness K is:

$$F_s = Kz \tag{10}$$

For small angular displacements the linear displacement can be approximated by the arc length:

$$z = d\phi \tag{11}$$

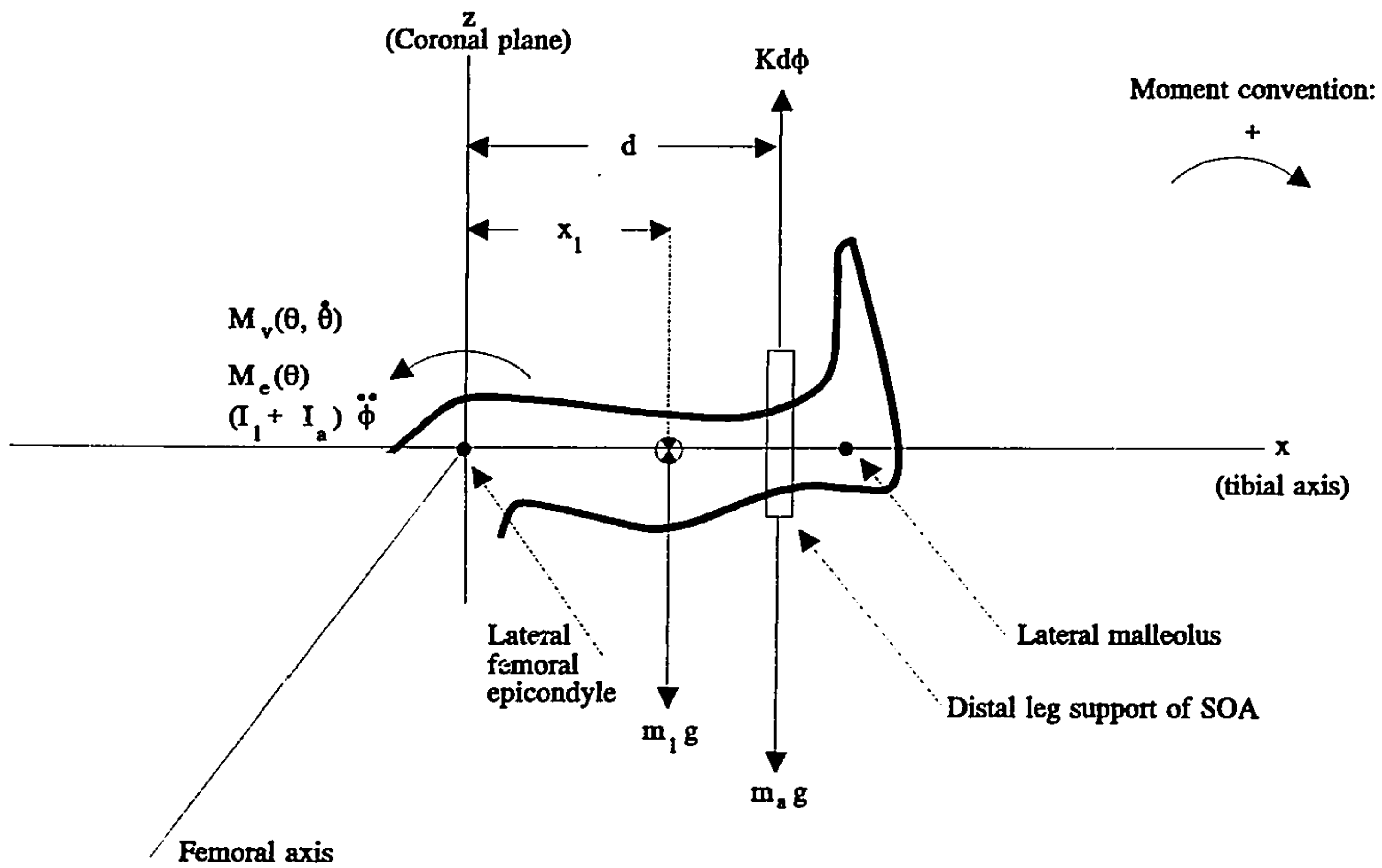

Figure 7. Free body diagram of the forces and moments acting on the leg-foot-SOA system. Refer to Figure 6 for the definition of the angle ϕ.

For $\phi=8^{\circ}$ the difference between the linear and angular displacements is 0.325%. The spring force can now be expressed in terms of the angle ϕ:

$$Kz = Kd\phi \tag{12}$$

And the restoring moment of force due to the spring force about the y-axis is:

$$(Kd\phi)d = Kd^2\phi \tag{13}$$

Gravitational moments. If the leg-foot-apparatus system is always oscillated about a horizontal equilibrium position, then small oscillation theory allows the approximation:

$$\cos\phi \approx 1 \qquad \mathit{for}\ \phi \leq 0.14\ \mathit{rad}\ (8^{\circ}) \tag{14}$$

The maximum error associated with this approximation is 0.983%. The moment due to gravity of the leg-foot segment about the y-axis is given by:

$$m_l g x_l \cos\phi \approx m_l g x_l \tag{15}$$

Similarly, the moment due to gravity of the apparatus (distal leg support and lower spring support) about the y-axis is given by:

$$m_a g d \cos\phi \approx m_a g d \tag{16}$$

The gravitational moments are therefore constant and maximum for small oscillations.

Equation of motion. The angular analog of Newton's second law is:

$$\sum M_y = I\ddot{\phi} \tag{17}$$

From the FBD of Figure 7, with clockwise (flexion) moments taken as positive, equation (17) expands to:

$$-Kd^2\phi - M_e(\theta) - M_v(\theta,\dot{\theta}) + m_l g x_l + m_a g d = I_l\ddot{\phi} + I_a\ddot{\phi} \tag{18}$$

Incorporating the linear approximations of the passive moments, equations (3) and (9), into equation (18) yields:

$$-Kd^2\phi - [M_e(\theta^*) + \theta K_e(\theta^*)] - C_k(\theta^*)\dot{\theta} + m_l g x_l + m_a g d = I_l\ddot{\phi} + I_a\ddot{\phi} \tag{19}$$

The total angular damping coefficient, $C_t(\theta^*)$, is given by:

$$C_t(\theta^*) = C_k(\theta^*) + C_a(d) \tag{20}$$

where $C_a(d)$ is the angular damping coefficient of the apparatus (springs, lower spring support, and distal leg support) which is expected to be a linear function of the suspension length, d, (Hatze, 1975b). This value can be determined experimentally (see methods) and subtracted out later. Thus, for the remainder of the analysis $C_t(\theta^*)$ will be used in place of $C_k(\theta^*)$. Also, since θ and ϕ are related (see Figure 6 and nomenclature subsection) they are interchangeable. After some rearrangement, equation (19) becomes:

$$(I_l + I_a)\ddot{\phi} + [C_t(\theta^*)]\dot{\phi} + [Kd^2 + K_e(\theta^*)]\phi = (m_l x_l + m_a d)g - M_e(\theta^*) \tag{21}$$

The right hand side of equation (21) will be either a positive or negative constant for small values of ϕ (depending on the subject and the joint angle). Thus, let

$$h = (m_l x_l + m_a d)g - M_e(\theta^*) \tag{22}$$

Equation (21) then becomes:

$$(I_l + I_a)\ddot{\phi} + [C_t(\theta^*)]\dot{\phi} + [Kd^2 + K_e(\theta^*)]\phi = h \tag{23}$$

Equation (23) is a second-order nonhomogeneous linear ordinary differential equation (ODE). It can be shown (Fowles, 1986; Thomson, 1988) that constant external forces have no other effect on a harmonically oscillating system other than to shift the equilibrium position. Thus, if the equilibrium position is redefined to account for these forces, equation (23) becomes:

$$(I_l + I_a)\ddot{\phi} + [C_t(\theta^*)]\dot{\phi} + [Kd^2 + K_e(\theta^*)]\phi = 0 \tag{24}$$

Equation (24) is a standard second-order homogeneous linear ODE with constant coefficients (Tierny, 1979). If the system is released from rest and from an initial angular displacement ϕ_o at time t=0, equation (24) will be subject to the initial conditions:

$$\phi(t) = \phi(0) = \phi_o \tag{25}$$

and

$$\dot{\phi}(t) = \dot{\phi}(0) = 0 \tag{26}$$

The complete procedure for finding a solution to equations (24), (25), and (26) can be found in Tierny (1979). The following is a brief outline of that process.

Solution of the homogeneous ODE. Dividing each term on both sides of equation (24) by $(I_l + I_a)$ yields:

$$\ddot{\phi} + \left[\frac{C_t(\theta^*)}{(I_l + I_a)}\right]\dot{\phi} + \left[\frac{(Kd^2 + K_e(\theta^*))}{(I_l + I_a)}\right]\phi = 0 \tag{27}$$

Equation (27) is in standard linear form. The roots of the auxiliary equation are given by:

$$r_1, r_2 = \frac{-\dfrac{C_t(\theta^*)}{(I_l + I_a)} \pm \sqrt{\dfrac{C_t(\theta^*)^2}{(I_l + I_a)^2} - \dfrac{4(Kd^2 + K_e(\theta^*))}{(I_l + I_a)}}}{2} \tag{28}$$

Three cases are possible depending on the signs of the constants under the radical. However, human articulations appear to behave in an underdamped fashion (Engin, 1984; Hatze, 1975b; Peyton, 1986). Thus, in the present investigation underdamping is expected and required. Underdamping corresponds to the case of light damping in which the elastic term predominates over the viscous term, or:

$$\frac{C_t(\theta^*)^2}{(I_l + I_a)^2} - \frac{4(Kd^2 + K_e(\theta^*))}{(I_l + I_a)} < 0 \tag{29}$$

Hence, the underdamping case involves complex roots:

$$r_1 = \alpha + i\beta \tag{30}$$

and

$$r_2 = \alpha - i\beta \tag{31}$$

where α and β are real and $i = \sqrt{-1}$. It can be shown that:

$$\alpha = -\frac{C_t(\theta^*)}{2(I_l + I_a)} \tag{32}$$

and

$$\beta = \frac{\sqrt{4(I_l + I_a)(Kd^2 + K_e(\theta^*)) - C_t(\theta^*)^2}}{2(I_l + I_a)} \tag{33}$$

The solution is:

$$\phi(t) = e^{-\alpha t}\left[\left(\frac{\alpha\phi_o}{\beta}\right)\sin\beta t + \phi_o\cos\beta t\right] \tag{34}$$

Equation (34) is the solution to the equation of motion of the system in terms of the system parameters K, d, I_l, I_a, $K_e(\theta^*)$, and $C_t(\theta^*)$. However, it is preferable to express the results in a form which is more in line with standard vibration theory (Thomson, 1988). This form is often called the nondimensional form. In the case where the viscous term predominates over the elastic term overdamping occurs. The limiting case between overdamping and underdamping is called critical damping, $\mathbf{C_c}$, which corresponds to (refer to equation (28)):

$$\frac{C_t(\theta^*)^2}{(I_l + I_a)^2} = \frac{4(Kd^2 + K_e(\theta^*))}{(I_l + I_a)} \tag{35}$$

The viscous damping factor or damping ratio, ζ, is defined as the ratio of the damping of a system, C, to the critical damping, or (Thomson, 1988):

$$\zeta = \frac{C}{C_c} \tag{36}$$

The undamped natural frequency of the system, ω_n, is defined as:

$$\omega_n = \sqrt{\frac{(Kd^2 + K_e(\theta^*))}{(I_l + I_a)}} \tag{37}$$

From equations (35), (36), and (37), ζ can be expressed in terms of the system parameters:

$$\zeta = \frac{C_t(\theta^*)}{2(I_l + I_a)\omega_n} \tag{38}$$

The damped natural frequency, ω_d, is defined as:

$$\omega_d = \omega_n\sqrt{1 - \zeta^2} \tag{39}$$

Equation (34) can now be expressed in standard nondimensional form:

$$\phi(t) = \phi_o e^{-\zeta\omega_n t}\left[\left(\frac{\zeta\omega_n}{\omega_d}\right)\sin\omega_d t + \cos\omega_d t\right] \tag{40}$$

Determination of the system damping, $C_t(\theta^*)$

Figure 8 illustrates the response curve of equation (40). Calculation of the damping coefficient begins with the determination of the ratio of successive amplitudes of the response curve. Let ϕ_1 be the value of the positive peak at time t_1 and ϕ_2 be the value at time t_2, one period later, i.e.:

$$t_2 - t_1 = \tau \tag{41}$$

Hence substitution of (t_1, ϕ_1) and (t_2, ϕ_2) into equation (40) yields, respectively:

$$\phi(t_1) = \phi_1 = \phi_o e^{-\zeta\omega_n t_1}\left[\left(\frac{\zeta\omega_n}{\omega_d}\right)\sin\omega_d t_1 + \cos\omega_d t_1\right] \tag{42}$$

and

$$\phi(t_2) = \phi_2 = \phi_o e^{-\zeta\omega_n t_2}\left[\left(\frac{\zeta\omega_n}{\omega_d}\right)\sin\omega_d t_2 + \cos\omega_d t_2\right] \tag{43}$$

Dividing equations (42) and (43) results in the cancellation of the periodic terms since $\cos(t_1)=\cos(t_2)$ and $\sin(t_1)=\sin(t_2)$ because t_1 and t_2 are separated by one time period or 2π. Thus:

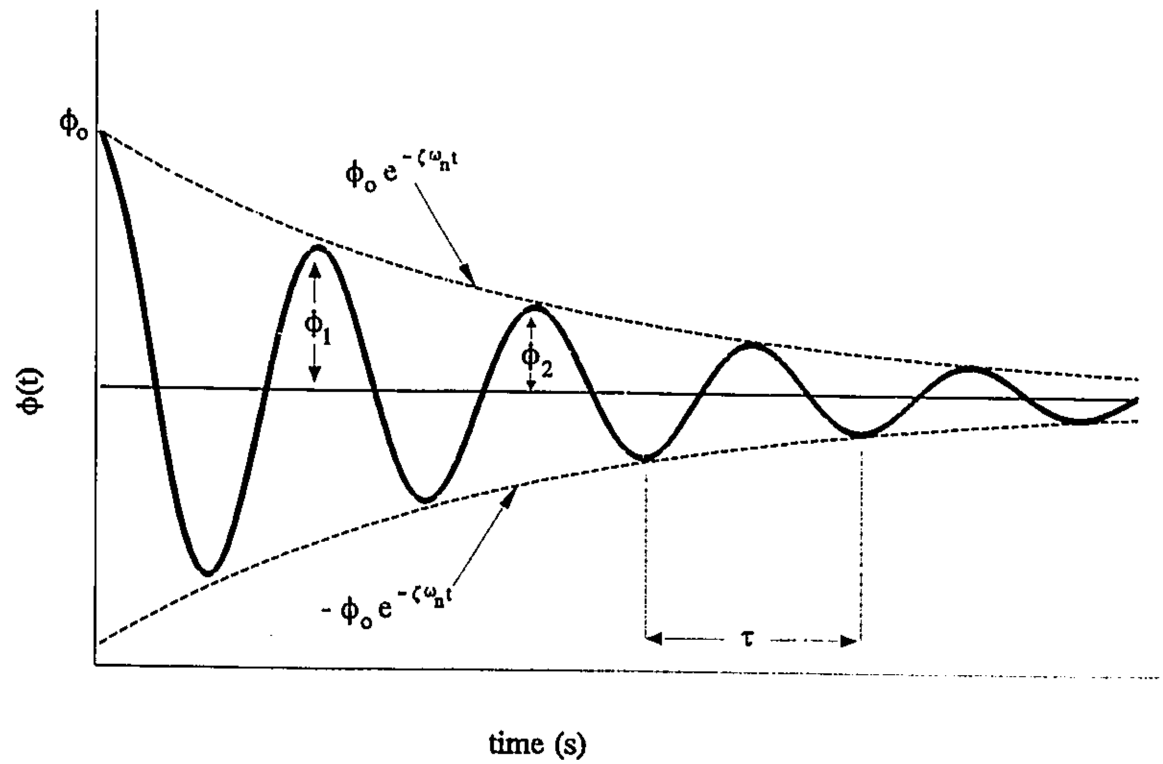

Figure 8. Expected response curve of the underdamped biomechanical system. Dotted lines are the exponential envelopes of the amplitude decay history.

$$\begin{aligned}\frac{\phi_1}{\phi_2} &= \frac{e^{-\zeta\omega_n t_1}}{e^{-\zeta\omega_n t_2}} \\ &= e^{(-\zeta\omega_n t_1)-(-\zeta\omega_n t_2)} \\ &= e^{\zeta\omega_n (t_2 - t_1)}\end{aligned} \tag{44}$$

and

$$\frac{\phi_1}{\phi_2} = e^{\zeta\omega_n \tau} \tag{45}$$

The time period is given by:

$$\tau = \frac{2\pi}{\omega_d} \tag{46}$$

and equation (45) then becomes:

$$\frac{\phi_1}{\phi_2} = e^{\frac{2\pi\zeta\omega_n}{\omega_d}} \tag{47}$$

Substituting equation (39) into equation (47) will result in an expression with $\frac{\phi_1}{\phi_2}$ in

terms of ζ only:

$$\frac{\phi_1}{\phi_2} = e^{\frac{2\pi\zeta}{\sqrt{1-\zeta^2}}} \tag{48}$$

The logarithmic decrement, δ, is defined as (Thomson, 1988):

$$\delta = \ln\left[\frac{\phi_1}{\phi_2}\right] \tag{49}$$

or more generally:

$$\delta = \left(\frac{1}{n}\right)\ln\left[\frac{\phi_i}{\phi_{i+n}}\right] \quad \textit{for } n>0 \tag{50}$$

Substituting equation (48) into equation (49) yields:

$$\delta = \ln\left[e^{\frac{2\pi\zeta}{\sqrt{1-\zeta^2}}}\right] \tag{51}$$

or

$$\delta = \frac{2\pi\zeta}{\sqrt{1-\zeta^2}} \tag{52}$$

Substituting equation (39) into equation (52) yields:

$$\delta = 2\pi\zeta\left[\frac{\omega_n}{\omega_d}\right] \tag{53}$$

But since $\tau=2\pi/\omega_d$, equation (53) becomes:

$$\delta = \zeta\omega_n\tau \tag{54}$$

hence,

$$\zeta\omega_n = \frac{\delta}{\tau} \tag{55}$$

Also, it can be shown that:

$$\zeta\omega_n = \frac{C_t(\theta^*)}{2(I_l + I_a)} \tag{56}$$

Equating equations (55) and (56) yields:

$$\frac{\delta}{\tau} = \frac{C_t(\theta^*)}{2(I_l + I_a)} \tag{57}$$

Solving for $C_t(\theta^*)$ yields:

$$C_t(\theta^*) = \frac{2\delta(I_l + I_a)}{\tau} \tag{58}$$

Once the value of the damping coefficient of the apparatus , $C_a(d)$, is known (see methods) then from equation (20) the angular damping coefficient of the knee joint at $\theta=\theta^*$ can be determined:

$$C_k(\theta^*) = C_t(\theta^*) - C_a(d) \tag{20a}$$

Determination of the moments of inertia

Of the four parameters in equation (58), δ and τ will be the output of the experimental apparatus/electronics. The moment of inertia of the apparatus, I_a ,can also be easily determined. The moving components of the apparatus (for small spring deflections), with mass m_a, are coupled to the oscillating leg-foot segment at a distance d from the approximate centre of the knee joint and thus the inertial contribution of the apparatus is given by:

$$I_a = m_a d^2 \qquad (59)$$

Note that I_a will be different for each subject due to the subject specific parameter d.

The moment of inertia of the leg-foot segment, I_l, may be obtained from standard regression equations (e.g., Hinrichs, 1985; Yeadon and Morlock, 1989) or it may be calculated from the presently developed system of equations. Indeed, the small oscillation technique has been used to specifically determine the moment of inertia of various segments (Hatze, 1975b; Peyton, 1986). Through various substitutions and rearrangements it can be shown that:

$$I_l = \left[\frac{\tau^2 (Kd^2 + K_e(\theta^*))}{(4\pi^2 + \delta^2)} \right] - m_a d^2 \qquad (60)$$

The value of I_l can then be substituted into equation (58).

Justification of the assumption of the independence of the damping coefficient on the angular velocity

The necessary theory has now been covered to justify the assumption of the independence of $C_k(\theta^*)$ on $\dot{\theta}$ as in equation (3). The equation of motion of the system, equation (40), indicates that the motion is periodic with an exponentially decaying amplitude. The velocity of the oscillating system is also periodic with exponentially decaying amplitude, but is 90° out of phase (leading) with the displacement. Thus, the velocity is varying over time. If the system damping were dependent on the velocity then the logarithmic decrement, δ, would also vary over time. Hence, an appropriate test for independency would be to measure δ at different instances in time over the oscillation. This is exactly what Hatze (1975b) and Engin (1984) did and, except for a brief initial increase in damping (most likely due to stretch reflex activity), no significant variation in δ (within the limits of an approximation technique) was observed for ratios ϕ_i/ϕ_{i+n} sampled at different times. These findings were taken as proof of the independence of the angular damping coefficient on the angular velocity for small oscillations as in equation (3).

CHAPTER III

METHODOLOGY

The following sections will detail the experimental and post-experimental methods which are based partly on the previous literature review. The first two sections describe the particulars of the subject sample as well as the various anthropometric parameters which were measured. Subsequent sections involve the measurement and data processing of the elastic and viscous components of the net passive joint moment. Due to the differing experimental protocols each component will be treated in a separate section. The final section describes the statistical treatment of all experimental results.

SUBJECTS

The subject sample consisted of 17 males between the ages of 22 and 31 years with no known history of knee injury or pathology. Each subject was required to complete three forms (Appendix A): Informed consent, Sports/Exercise History, and Medical/Orthopaedic History. Table 1 lists the particulars of the subject sample.

ANTHROPOMETRIC PARAMETERS

Prior to experimental testing, with the subject barefoot and wearing jogging shorts, the greater trochanter and the lateral femoral epicondyle of the right femur were located and marked with a felt marker. These marks were used to measure segment lengths and for positioning the subject in the aparatii. A series of 22 anthropometric parameters (right side joint and segment dimensions) as well as age, height,

Table 1. Mean values and variability of selected anthropometric parameters of the subject sample (n=17 males).

Parameter	Mean	CV *	Range
Age (years)	26.3	10.4	22 - 31
Height (m)	1.75	3.4	1.66 - 1.87
Mass (kg)	77.9	16.6	59.4 - 109.0
Knee circumference (cm)	38.1	8.2	34.0 - 45.0
Ankle circumference (cm)	22.5	5.8	20.5 - 25.0
Upper thigh circumference (cm)	59.7	10.6	50.5 - 74.0
Lower thigh circumference (cm)	44.3	11.7	37.0 - 54.0
Calf circumference (cm)	38.0	8.2	33.0 - 45.5

* CV = Coefficient of Variation = (S.D./Mean) x 100 %

and mass were obtained from each subject using an anthropometer (GPM), flexible tape, and a standard medical scale. A flexibility parameter (Trunk forward flexion, Canadian Standardized Test of Fitness, 1987) was also obtained. All information was entered into a data sheet (Appendix B). To avoid gross errors, joint and segment dimensions were measured until three readings agreeing to the nearest millimetre were obtained. Appendix C provides descriptions of the anthropometric and flexibility parameters. Table D1 (Appendix D) contains the complete set of anthropometric data of the subject sample. Due to equipment availability the two components (elastic and viscous) were tested separately in all but three subjects. For these 14 subjects the mean time between testing sessions was 4.1 months (S.D. = 0.55 months). All anthropometric and flexibility parameters were also remeasured during the second testing session.

DETERMINATION OF THE NET PASSIVE ELASTIC JOINT MOMENT

The following sections describe the apparatus and the data collection and processing techniques which were used to determine the NPEJM.

Apparatus: the horizontal knee arthrograph (HKA)

The apparatus used to determine the NPEJM function was a manually driven apparatus similar to that used by Hatze (1975a) and was called the horizontal knee arthrograph (HKA). The HKA was built at the University of Ottawa Science Workshop and is depicted in Figures 9, 10, and 11 (not to scale). The HKA consisted of two main units: 1) the subject table and manipulandum platform which were constructed of 3.9 cm square tubing and 2) the manipulandum, most of which was constructed of 1.2 cm thick interlocking aluminium plates. The base of the manipulandum slides in lockable tracks on top of the manipulandum platform.

Figures 9 and 10 illustrate the side and top views, respectively, of the HKA. The manipulandum was originally developed to study two articulations which is the reason for the proximal and distal joints. In the present investigation only the distal joint was used; the proximal unit (joint and moveable plate) was locked in place. The distal arm consisted of the upper and lower plates and the leg support. The distal arm rotated freely (complete 360°) about the centre of rotation (COR) of the distal (bearing) joint. The operator rotated the distal arm by applying a bending moment to the sensing member via the plexiglass handle.

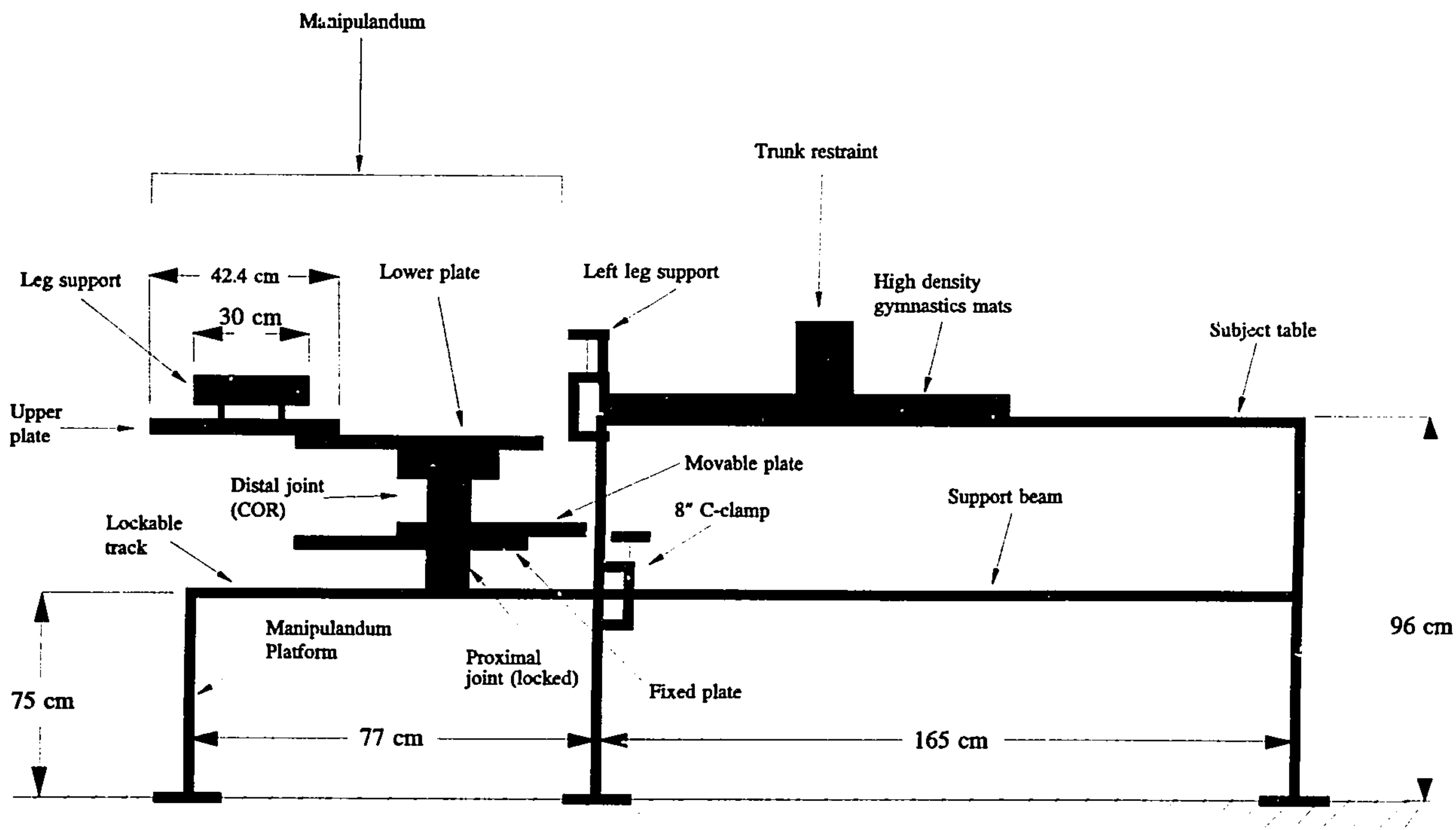

Figure 9. Side view of the horizontal knee arthrograph (HKA)

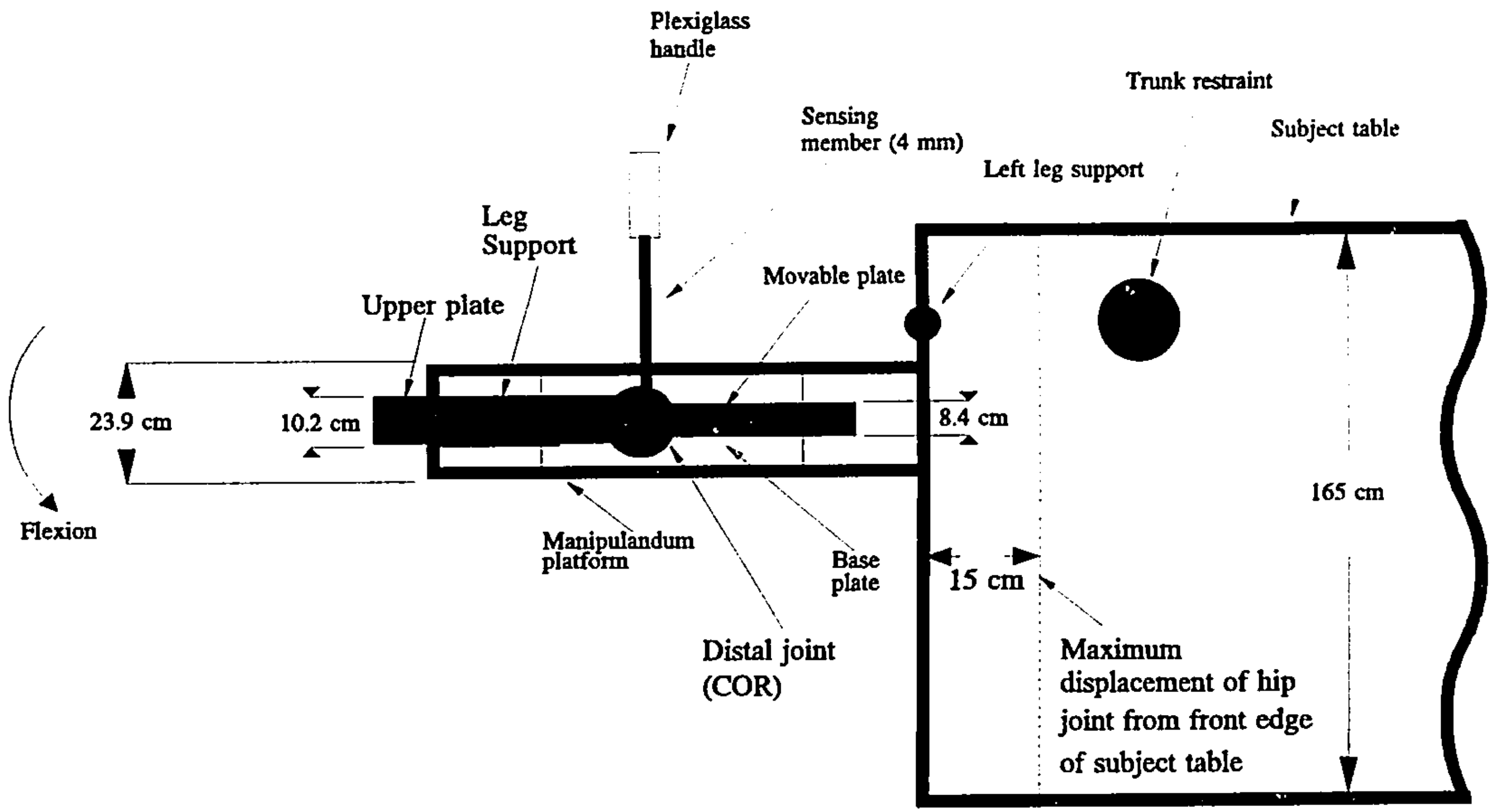

Figure 10. Top view of the horizontal knee arthrograph (HKA). The manipulandum is in the 0º position.

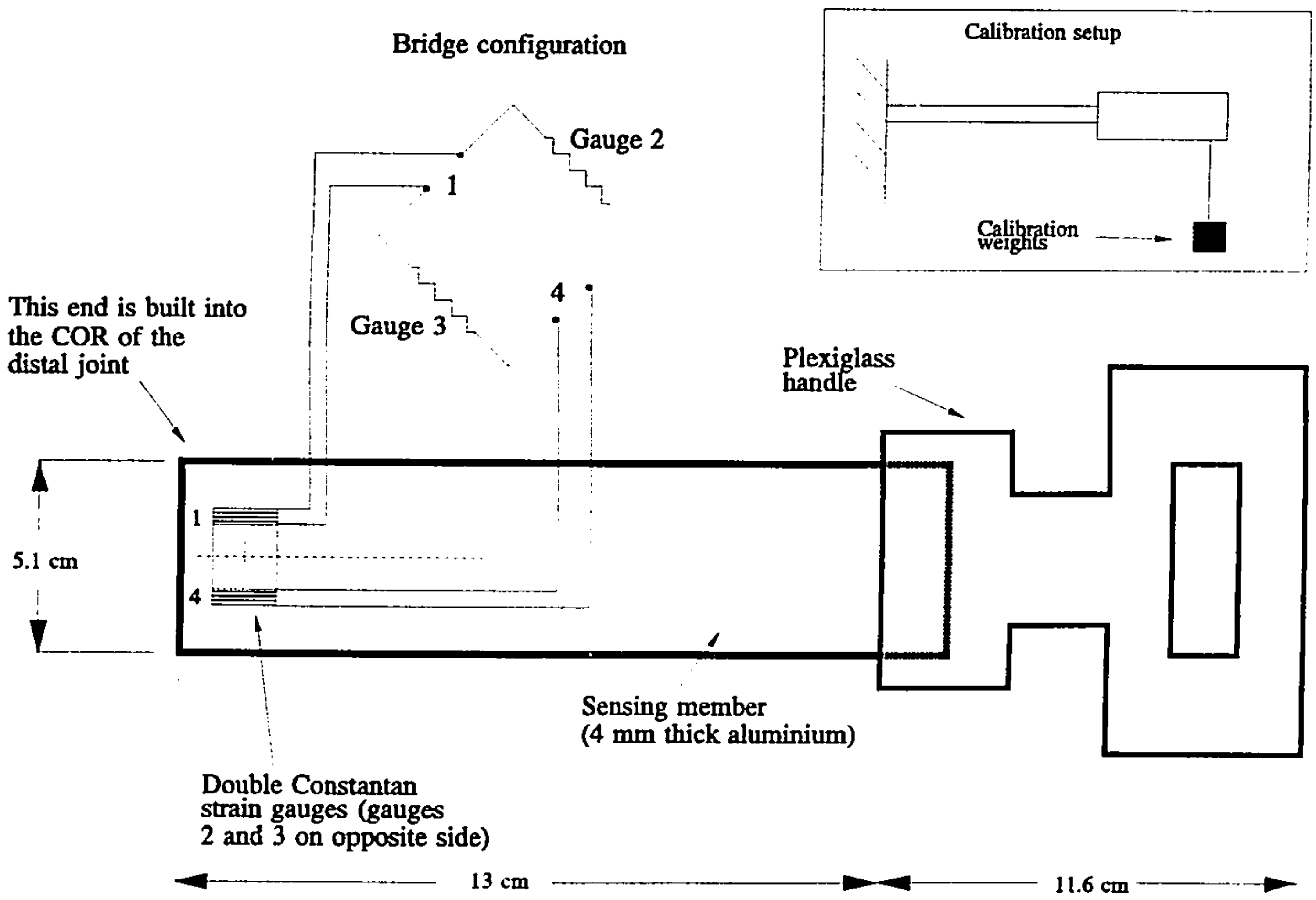

Figure 11. Isolated side view of the strain gauged sensing member of the HKA with the wheatstone bridge configuration. Inset: Calibration setup.

Subject positioning

The subject lay on his right side on the subject table (propped up with high density gymnastics mats so that the leg was parallel to the floor) with his hip joint placed at most 15 cm from the edge of the table. The right leg was extended over the proximal and distal arms and the lateral femoral epicondyle was aligned with the COR (which was marked) using a plumb line. Maintaining this alignment, the leg was then secured to the leg support with two velcro straps. The left leg was hooked over a padded 8" C-clamp on the front edge of the subject table so that the medio-lateral line of the pelvis was approximately perpendicular to the table top (Figure 12). The manipulandum platform was attached to the support beam of the subject table with two 8" C-clamps. This allowed for small adjustments along the front of the table. The trunk restraint was a weighted post which was placed against the subject's back to maintain the hip at 90°. The leg support was approximately a quarter hollow cylinder of 1 mm aluminium covered with 1.5 cm foam rubber. The quarter cylinder configuration was a compromise between providing enough support for the leg so that minimal undesired movement occurred while at the same time leaving the posterior aspect of the calf uncovered (except for the velcro straps) to allow for undisturbed apposition of the posterior thigh and calf which is a natural part of the NPEJM at the limits of flexion. The height of the subject table and the handle of the sensing member were set so as to allow comfortable operation by the experimenter.

Sensing member

Figure 11 is an isolated side view of the strain gauged sensing member (and bridge configuration) which detected the NPEJM. The sensing member was a rectangular piece of 4 mm thick aluminium. The plexiglass handle was attached to one end while the opposite end was built orthogonally into the COR of the distal joint. Therefore, the sensing member and handle were parallel to the floor and perpendicular and anterior to the distal arm/leg segment (as depicted in Figure 10).

Instrumentation and calibration

The HKA was instrumented with two linear transducers: strain gauges and a potentiometer. The following sections will describe the transducers and their associated electronics and calibration.

Strain gauges: configuration and hardware. Two double Constantan strain gauges (Micromeasurements Inc., Raleigh, NC., model EA-06-125TG-350, R=350.0 Ω ± 0.4% at 24°C, gauge factor 2.070 ± 0.5% at 24°C, transverse sensitivity + 0.8 ± 0.2% at 24°C) were bonded to the sensing member (one per side) as configured in Figure 11 based on guidelines given by Measurements Group Education Division (1983). The gauges were wired into a four-arm wheatstone bridge. This design detects bending moments while compensating for temperature effects and axial and torsional components (Beckwith and Marangoni, 1990).

The output signal from the strain gauges was conditioned by an amplifier (University of Ottawa Biomechanics Laboratory, based on Analog Devices model 1B32 signal conditioning component, Analog Devices, 1988; gain setting=100) the output of which was a filtered signal (low-pass, f_c=4 Hz).

Strain gauges: calibration. Since the strain frequency was expected to be very low, a static calibration procedure was employed. The sensing member was removed from the distal joint and fixed to a rigid support. Pre-weighed calibration weights (Mettler PE 3600 Delta-range digital scale) were successively loaded and unloaded at the opposite end of the sensing member (Figure 11, inset) producing a bending moment from 0 to 47 N•m while the voltage output was simultaneously recorded. Each loading/unloading cycle was repeated three times. The complete procedure was then repeated with the sensing member turned over so that the tension/compression modes were reversed.

Potentiometer: configuration and hardware. A linear potentiometer (Bourns, R=10 kΩ) was securely housed inside, and rotated with, the distal joint. The output signal from the potentiometer was conditioned by an amplifier (University of Ottawa Biomechanics Laboratory, based on Analog Devices model 1B32 signal conditioning component, Analog Devices, 1988; Gain setting=100) the output of which was a raw (unfiltered) signal.

Potentiometer: calibration. A manual goniometer was fixed to the manipulandum in such a way as to produce a joint angle (θ) as defined in Figure 6. The manipulandum was rotated in 5° steps from -20° to 180° (and in the reverse direction) while simultaneously recording the voltage output from the potentiometer. The process was repeated for three cycles.

Subject preparation

Prior to testing, EMG electrodes were applied to the subject and the ankle joint was fixed at 0° (neutral). These procedures are described below.

Electromyography (EMG)

To ensure the passive state, the surface EMG of five muscles was recorded. Pairs of Ag-Agcl surface electrodes (MEDI-TRACE) were placed 2.0 cm apart (centre-to-centre) over the motor points of the following muscles: RF, VM, LBF, ST, and MGA; according to the procedures outlined by Delagi, Perotto, Iazzetti, and Morrison (1975). Before applying the electrodes the skin was prepared by shaving the appropriate area and rubbing the skin with alcohol and electrode gel (Hewlett Packard) until erythema appeared. Skin resistance was measured with a digital multimeter using a 2 kΩ criterion. Electrodes were taped to the skin to reduce artifacts. The raw EMG signal of three muscles were input into a bioamplifier (University of Ottawa Biomechanics Laboratory, 10-700 Hz bandpass, input impedance of 10 MΩ) while the other two EMG signals were input into an AC amplifier (Teca Corporation, Pleasantville, NY, 10-1000 Hz bandpass). The five EMG signals were sent to two storage oscilloscopes (Tektronix T912 and 5115) for monitoring purposes and also input to the data collection system for subsequent A/D conversion (described below).

Ankle fixation

A number of methods were attempted in an effort to fix the ankle joint at 0°. It was found that standard adhesive athletic tape was sufficient in providing fixation with the advantage of adding insignificant mass to the system (more important for the small oscillation technique).

Frictional moment of the HKA

The frictional contribution of the distal joint of the HKA was first determined. Since the distal joint contained some slack, a nylon cylinder (mass=4.798 kg; length=0.508 m) was strapped to the leg support (as the leg would be) to take up the slack and obtain a more realistic frictional value. The loaded manipulandum was then rotated through the full range of motion in both directions while the amplified strain gauge and potentiometer signals were digitally converted as described below for the human data collection. Five trials were performed.

Separation of the knee ROM into three phases

Pilot testing indicated that, due to the nature of the HKA, more accurate results would be obtained if the operator only rotated the manipulandum (via the handle of the sensing member) in one direction. Therefore the knee ROM was separated into three phases:

Flexion phase: $\theta \geq 95^{o}$

Extension phase: $\theta \leq 55^{o}$

Midrange phase: $55^{o} < \theta < 95^{o}$

For the flexion and extension phases data collection started at a knee angle located somewhere in the midrange phase and progressed in one direction to either full flexion or extension. The leg was forced into flexion or extension until no further movement occurred despite considerable application of force. The initial portion of the data file (up to the cutoff angle) was not used in the subsequent data analysis. None of the subjects objected to having their knee joint forced into flexion (i.e., >

140°) and extension (< 0°). Since the midrange phase bounds the equilibrium angle, a sign change in the moment will occur within this interval. Therefore data for this phase was collected by performing two sets of trials: one for rotations in the direction of extension and one for rotations in the direction of flexion (also with some overlap).

Final adjustments and EMG check

With the subject positioned in the HKA, final adjustments were made using the subject's feedback with respect to discomfort, shearing of the velcro straps over the leg, shearing of the hip on the subject table, etc. The leg was rotated through the complete range of motion to check for and minimize undesired movements.

Just before actual data collection, with optimal subject positioning, the leg was again rotated through the complete range of motion, including forced flexion and extension, for 6 to 7 cycles to accustom the subject to the testing environment and to decrease the protective response. Observation of the EMG signals on the oscilloscopes clearly showed a gradual decrease in the amplitude of the signals as the cycling progressed.

Data collection

Figure 12 illustrates the complete experimental setup. As the leg was rotated very slowly by the operator through the appropriate phase the amplified strain gauge and potentiometer signals were digitally converted (Labmaster board) at 25 Hz and the EMG signals at 1500 Hz for a period of 10 seconds. The A/D conversion was controlled by BIOAD software (Version 1.1, Lamontagne, Bradley, and Lemaire, 1989) specifically developed for the 16 MHz Compaq 386 microcomputer. After each

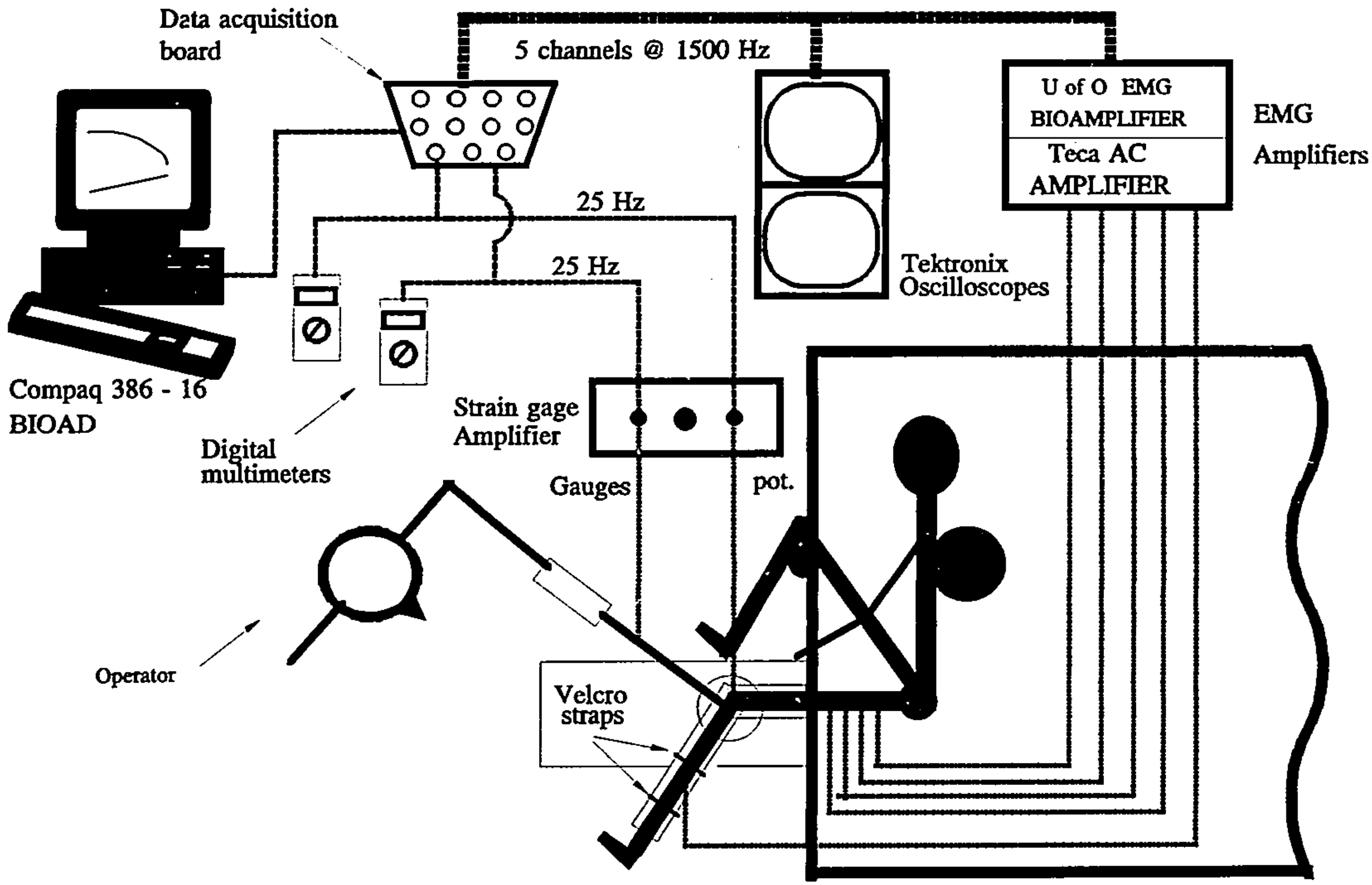

Figure 12. Complete experimental setup (top view) to determine the NPEJM of the human knee joint.

trial was complete it was reviewed on screen to check for EMG activity and disturbances in the transducer signals. Also after each trial, the strain gauge output was checked to ensure no permanent (plastic) deformation had occurred. The process was repeated until five successful trials were obtained. Therefore, for each subject a total of 20 trials were obtained (five flexion, five extension, and 10 midrange). Time between trials was approximately two minutes and the entire testing session lasted about 90 minutes. All data files were stored on floppy disks for future processing. To test the effects of muscle activity on the strain gauge output a number of extra trials were also collected (on subject JT) while the subject purposely performed muscle contractions.

Initial data reduction

All data files (stored in the BIOAD format) were loaded into the companion program BIOPROC version 1.18 (Lamontagne et al., 1989). Each data file contained seven channels (five EMG, two transducer) as functions of time. The potentiometer signal was low-pass filtered (critically damped, fourth-order, f_c=6 Hz). Extraneous end point data were removed and the EMG signals were rechecked. The data were then stored in ASCII format. Each reduced data file contained three arrays: time, strain gauge output (in volts), and the potentiometer output (in volts).

Curve fitting procedures

Theoretical considerations and initial observation of the data indicated that the extension and flexion phases could be fitted to simple exponential functions. Using a transformed least-squares fitting procedure (Giordano and Weir, 1985) each trial of the extension phase was fitted to an exponential function of the form:

$$M_e(\theta) = a_1 e^{a_2 \theta} \tag{61}$$

where a_1 is positive, a_2 is negative, and θ is in radians. Similarly, each trial of the flexion phase was fitted to an equation of the form:

$$M_e(\theta) = a_3 e^{a_4 \theta} \tag{62}$$

where a_3 is negative, a_4 is positive, and θ is in radians. The mean values of the coefficients (a_1, a_2, a_3, a_4) were used to represent the extension and flexion phases of the NPEJM.

The midrange phase showed an approximately linear nature and each trial was fitted with a standard linear least-squares regression line (Giordano and Weir, 1985):

$$M_e(\theta) = a_5 \theta + a_6 \tag{63}$$

where a_5 is negative, a_6 is positive, and θ is in radians. The mean values of a_5 and a_6 were used to represent the NPEJM in the midrange phase. If equations (61), (62), and (63) were pieced together, a curve similar to that illustrated in Figure 4 would result.

Determination of the soft joint stops

The intersections of the dotted lines in Figure 4, the soft stops, were determined from the following equations. The soft joint stop in extension was given by:

$$\theta_{SE} = \frac{a_1 e^{a_2\theta_2} - S_E\theta_2 - a_6}{a_5 - S_E} \tag{64}$$

where

$$S_E = \frac{a_1 e^{a_2\theta_2} - a_1 e^{a_2\theta_1}}{\theta_2 - \theta_1} \tag{65}$$

and $\theta_1=0$ radians (0°) and $\theta_2=0.0174$ radians (1°). The soft joint stop in flexion was given by:

$$\theta_{SF} = \frac{a_3 e^{a_4\theta_4} - S_F\theta_4 - a_6}{a_5 - S_F} \tag{66}$$

where

$$S_F = \frac{a_3 e^{a_4\theta_4} - a_3 e^{a_4\theta_3}}{\theta_4 - \theta_3} \tag{67}$$

and θ_3=2.426 radians (139°) and θ_4=2.444 radians (140°).

Determination of the equilibrium angle

The point where the passive moment crossed the $x(\theta)$-axis (= 0) was called the equilibrium angle (Figure 4) and was given (in radians) by:

$$\theta_e = \frac{-a_6}{a_5} \tag{68}$$

Angular velocity

The angular velocity was determined by differentiating the potentiometer signal with respect to time using second central finite difference equations (Miller and Nelson, 1973).

Macro-driven spreadsheets (ELASTIC.WSP)

Each ASCII data file was imported into a series of linked, pre-programmed, macro-driven spreadsheets which were saved as a workspace (ELASTIC.WSP). This system of spreadsheets contained the transducer calibration equations, the central finite difference equations, the HKA frictional moment factor, the necessary procedures and equations for determining the coefficients (a_1 - a_6) in equations (61) through (63) with the associated R^2 and RMS error values, the analytical derivatives of equations (61) through (63), and equations (64) to (68).

DETERMINATION OF THE ANGULAR DAMPING COEFFICIENT

The following paragraphs detail the apparatus and the experimental protocol used to determine the angular damping coefficient of the knee joint.

Apparatus: the small oscillation apparatus (SOA)

The apparatus used to determine the damping coefficient of the knee joint was called the small oscillation apparatus (SOA). The SOA was built at the University of Ottawa Science Workshop and is depicted in Figures 13 through 18 (not to scale). The SOA consisted of two main units: 1) The subject carriage and 2) the suspension frame/load cell/spring assembly. The subject carriage, constructed of 3.9 cm square steel tubing, consisted of a padded seat and incline frame hinged to a system of two stacked frames (base frame and decline frame) which were also hinged at one end. The base frame had six legs which fit into tracks on the floor. Through a lever system (position adjustment lever in Figure 13) the whole carriage could be moved backward and forward in the tracks and under the suspension frame. The subject carriage (and the suspension frame) could be configured in five positions corresponding to knee angles of 10°, 45°, 90°, 110°, and 130° while maintaining the constraints of $\theta_{H}=$ 90° and $\phi=0°$ (leg horizontal). Knee angles of 10°, 45°, and 90° were obtained by simply adjusting the incline frame and fitting the appropriate support beams (Figures 13, 14, and 15; beams not required for 90°). The knee angle of 110° was obtained by resting the incline frame flat on the decline frame and then raising the decline frame by 20° and inserting the appropriate support beams (Figure 16). A knee angle of 130° could be obtained by raising the decline frame by another 20° (to 40°). However, subject feedback during pilot testing in the laboratory indicated that this position was not comfortable for long durations with some subjects complaining of dizziness and a general feeling of discomfort. Therefore, this position was abandoned and a new setup

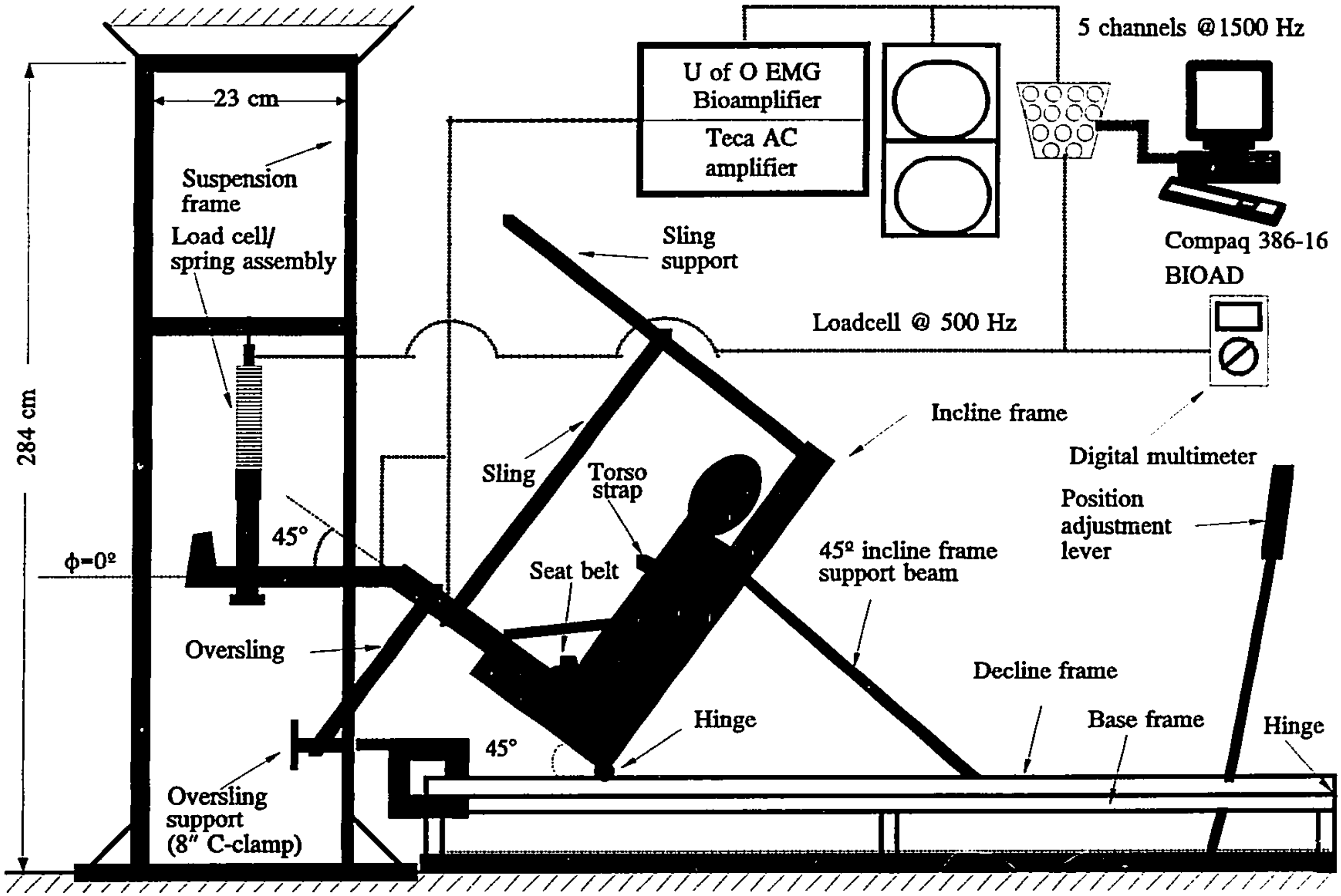

Figure 13. Side view of the small oscillation apparatus with the complete experimental setup for the $\theta = 45^{\circ}$ position

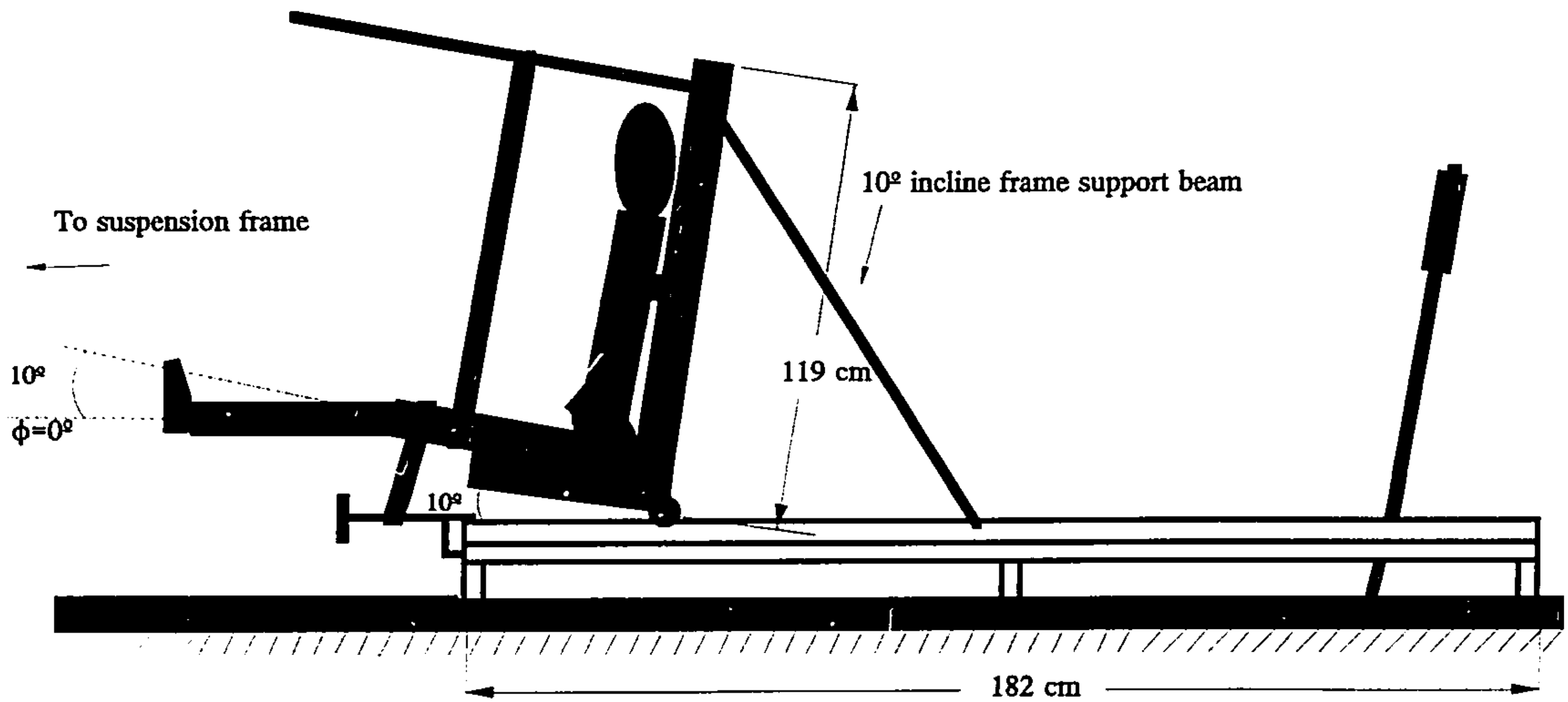

Figure 14. Side view of the subject carriage in the θ = 10º position.

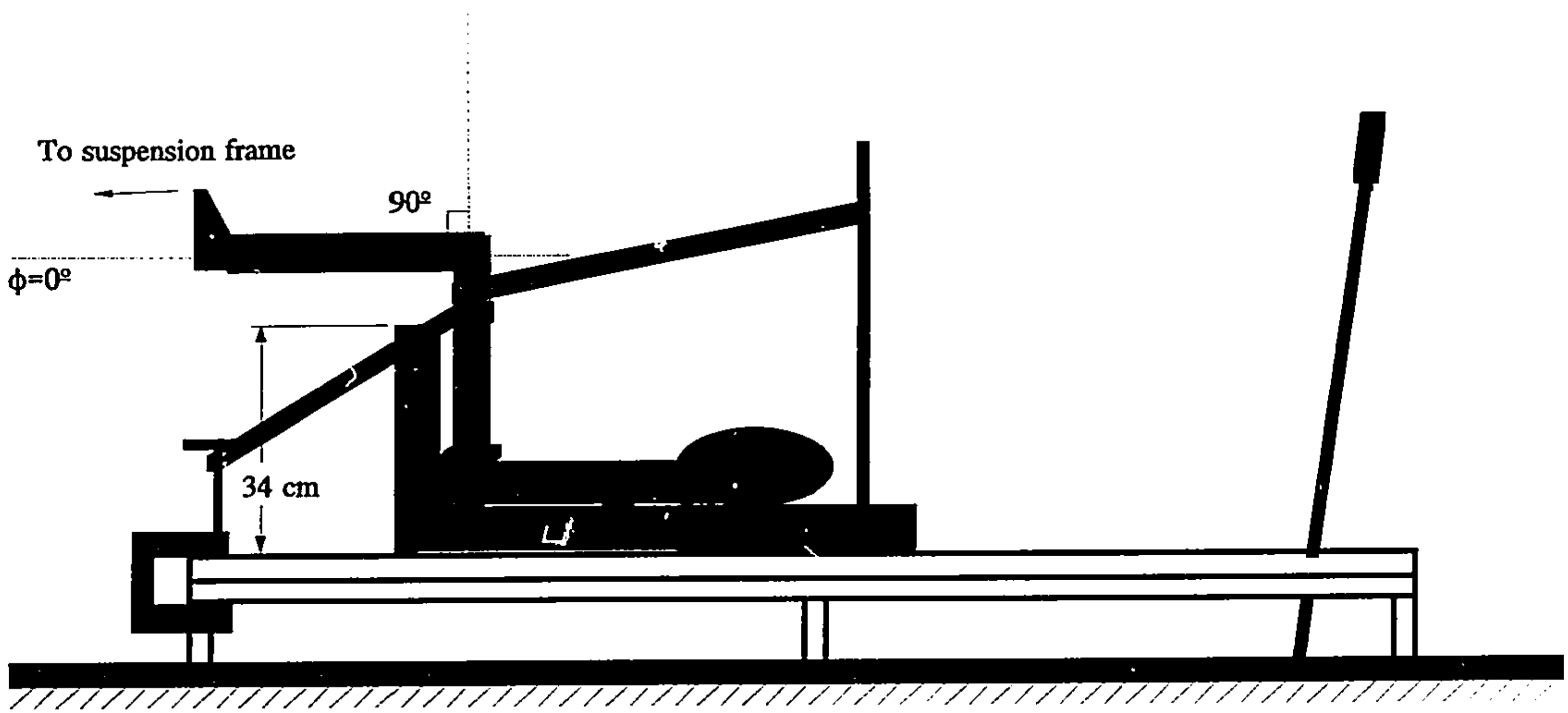

Figure 15. Side view of the subject carriage in the θ = 90º position.

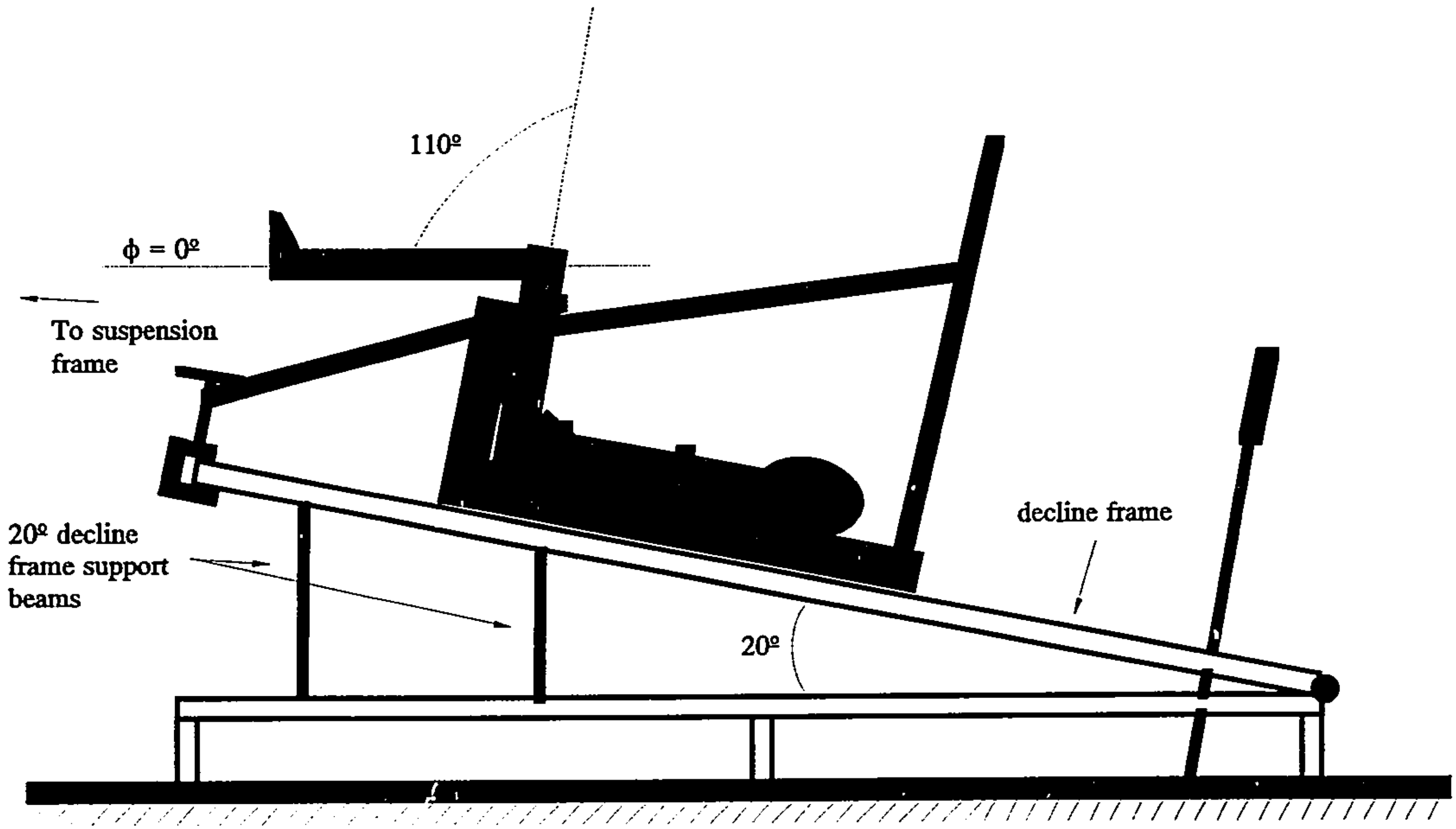

Figure 16. Side view of the subject carriage in the $\theta = 110^{\circ}$ position.

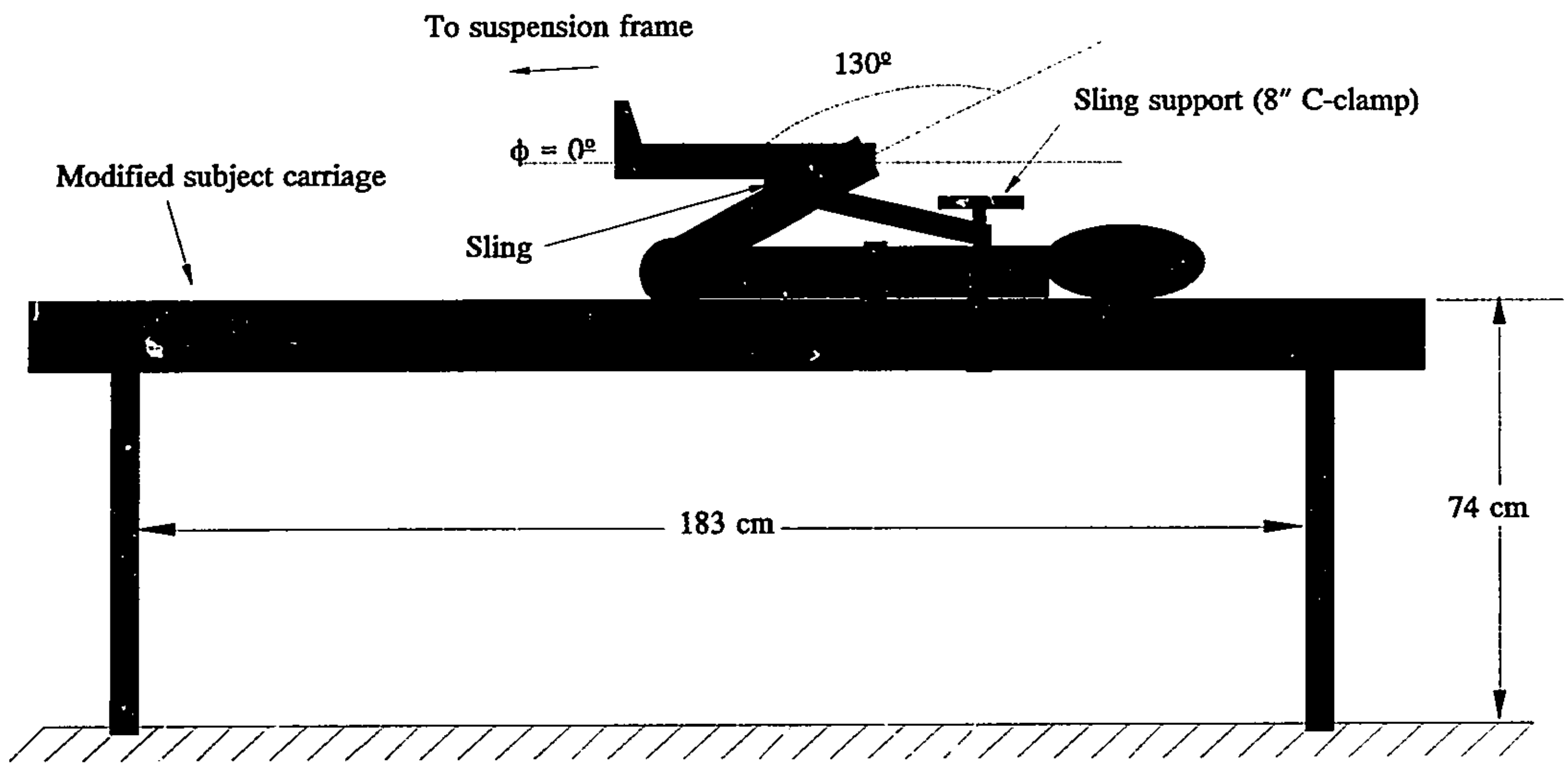

Figure 17. Side view of the subject carriage in the $\theta = 130^{\circ}$ position (modified setup).

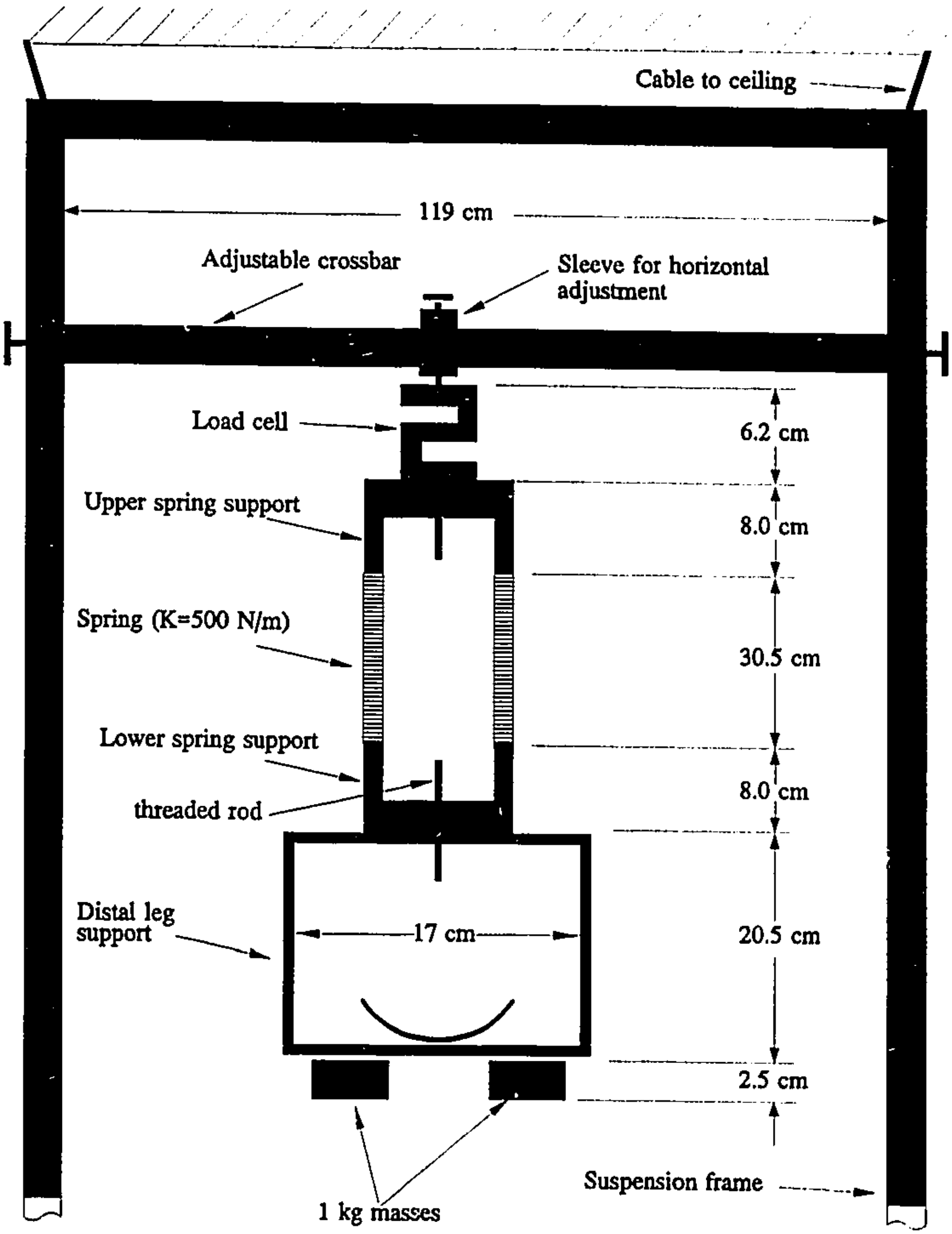

Figure 18. Front view of the suspension frame and the load cell/spring assembly/distal leg support (only about 25% of the length of the suspension frame is shown).

was incorporated for the $\theta = 130°$ position (Figure 17). The subject carriage was simply replaced with a padded table. This new setup violated the constraint of $\theta_H = 90°$ (increasing the hip angle to 130°). The consequences of this violation will be considered in subsequent sections of this document.

The suspension frame (side view in Figure 13, front view in Figure 18) was also mostly constructed of 3.9 cm square steel tubing and was anchored to the ceiling by cables. For scaling purposes, the full length of the suspension frame is not shown in Figure 18. The adjustable crossbar slides up and down along the vertical supports of the frame and could be locked at any height. The crossbar had a sleeve which could slide across the length of the crossbar and could also be locked at any point. A threaded rod was screwed into the bottom of the sleeve. The other end of the threaded rod was attached to the load cell/spring assembly/distal leg support.

Subject positioning

With the subject carriage configured in either the 10°, 45°, 90°, or 110° position the prepared subject (EMG and ankle fixation) was seated with his back against the incline frame. The hips were secured in place with a seat belt attached to the incline frame. The torso was similarly restrained by a large velcro strap. The distal leg, usually just proximal to the malleoli, was placed on the distal leg support. The carriage was moved forward (or backward) until the spring assembly/distal leg support was vertical (i.e., perpendicular to the floor). A small carpenter's level was secured with elastic bands to the anterior border of the tibia at approximately the segment midpoint. The crossbar of the suspension frame was then adjusted until the leg was level (horizontal). Secured to an inner support of the incline frame was an adjustable beam to which a sling was attached. The sling wrapped around the distal third of the thigh. Another sling, the oversling, wrapped over the anterior aspect of the thigh about 5 cm above the superior border of the patella. The oversling was anchored below to two C-clamps attached to the decline and base frames. Both slings could be tightened with velcro loops. Geometrically, the design of the SOA should result in the desired knee angle; however, due to soft tissue compression and subject variability, fine adjustments were required. Given that the leg must remain horizontal, trigonometric considerations revealed the angle at which the thigh segment must be in to obtain the desired knee angle. Thus, a special goniometer was constructed, using a carpenter's inclinometer, which allowed rapid measurement of the angle of the thigh segment with respect to the horizontal. The lengths of the slings were adjusted until the desired inclination was obtained. After this adjustment the level of the leg was usually disturbed and required further adjustments.

For the 130° position, the subject lay supine on the table. The sling was wrapped around the posterior aspect of the distal third of the thigh and anchored on each side by a C-clamp attached to the side of the table. The sling could be tightened so as to pull the thigh back (i.e., flex the thigh) to the desired inclination (as measured by the goniometer). The leg was then levelled as before by adjusting the height of the crossbar.

Instrumentation and calibration

The SOA was instrumented with a load cell and tension springs. Each transducer is described below.

Load cell. An S-shaped strain gauge load cell (Intertechnology Inc., Don Mills, Ontario, Canada, model 363-D3-100-2CP3, output 3 $mV \cdot V^{-1}$ at 445.0 N) was attached via a threaded rod to the adjustable sleeve on the crossbar (Figure 18). The load cell output was sent to an Acrotech (Chino, California) model 308 strain gauge interface and supply with signal conditioning. The output of the signal conditioning unit, an unfiltered (raw) signal, was split into two branches: one branch was sent to a digital multimeter while the other was sent to the data collection system for subsequent A/D conversion (described below).

The average frequency of oscillation was expected to be about 2 Hz and thus a static calibration procedure was used. The load cell was loaded with pre-weighed calibration weights (Mettler PE 3600 Delta-range digital scale) from 0 to 157.0 N and in the reverse direction for three trials.

Spring assembly. Two custom made stainless steel extension springs (HI-BEK Precision Spring Company Ltd., Hamilton, Ontario, Canada) were mounted to the bottom of the load cell via the upper spring support. Each spring was 30.500 cm in length, 3.880 cm outer diameter, 0.376 cm wire thickness and was constructed to have a stiffness of 500 $N \cdot m^{-1}$. The two springs mounted parallel to one another (Figure 18) had a total stiffness of $K = 1000\ N \cdot m^{-1}$. The lower ends of the springs were attached to the lower spring support which was in turn attached to the distal leg support. Pilot testing indicated that less variability was obtained if two one kg masses were added to the bottom of the distal leg support. The mass of the lower spring support, the distal leg support, associated hardware, and the 1 kg masses were measured on a precision digital scale (Mettler PE 3600 Delta-range). The mass of the apparatus was the sum of the masses of these components and was measured to be m_a=4.100 kg. Since the oscillations were small the mass of the moving portion of the springs was considered to be negligible.

Determination of the mechanical constants of the SOA

The SOA constants, the moment of inertia (I_a) and the damping coefficient ($C_a(d)$), are both functions of the suspension distance (d). The procedures used to obtain these constants are described below. The data processing phase was the same as that described below for the human testing.

Determination of the moment of inertia of the SOA (I_a)

Theoretically, the moment of inertia of the SOA should be given by equation (59) as previously described. This theory was tested experimentally to check for its degree of accuracy.

An aluminium rectangular parallelepiped with a mass of 2.950 kg, a length of 0.585 m and a thickness of 0.012 m was attached by a smooth hinge joint to the seat of the incline frame of the SOA. The moment of inertia of the parallelepiped, corrected for the offset of the hinge joint, was calculated to be I_{pp}=0.352 kg$\cdot$m^2 (Fowles, 1986). The other end of the parallelepiped was placed on the distal leg support and a carpenter's level was placed on top of the parallelepiped. The crossbar was adjusted until the parallelepiped was level (horizontal). The bias voltage output of the load cell was noted for later removal and the system was displaced slightly (<

8°) and allowed to oscillate under the restoring force of the springs. The load cell signal was digitally converted at 500 Hz for 10 seconds using BIOAD software (Lamontagne et al., 1989). Five trials were collected for each of the following suspension distances: d=20.0, 30.0, 40.0, 50.0, 54.0, and 57.9 cm. The equation of motion of such a system had the same form as equation (24):

$$(I_a + I_{pp})\ddot{\phi}_{pp} + (C_H + C_a(d))\dot{\phi}_{pp} + Kd^2\phi_{pp} = 0 \tag{24a}$$

where C_H is the damping coefficient of the hinge joint in N·m·s·rad^{-1} and ϕ_{pp} is the angle of the parallelepiped with respect to the horizontal in radians. The moment of inertia of the apparatus was determined from an equation of the form of equation (60):

$$I_a = \left[\frac{\tau_{pp}^2(Kd^2)}{4\pi^2 + \delta_{pp}^2}\right] - I_{pp} \tag{60a}$$

where τ_{pp} and δ_{pp} are, respectively, the time period and logarithmic decrement of the oscillating parallelepiped.

The data were fit to a power curve of the form $I_a=Ad^n$ where n=2 using a least-squares criterion (Giordano and Weir, 1985). If the theory is sufficiently accurate, the value of the coefficient A should approach the numerical value of the mass of the SOA (4.100).

Determination of the damping coefficient of the SOA ($C_a(d)$)

To calculate the damping coefficient of the knee joint, the contribution of the apparatus was first determined. A small portion of the apparatus damping was the result of internal energy dissipation within the spring material as it was being cyclically stressed; this form of damping is known as structural damping (Thomson, 1988). The major forms of damping, however, were inertial and geometrical damping. Inertial damping depends upon the acceleration and inertia of the system and was accounted for in the system of equations. Geometrical damping was the damping which resulted from the effects of the suspension distance (d). Since the leg was coupled to the SOA the apparatus damping was a function of the suspension distance. Hatze (1975b) found the apparatus damping to be a linear function of d.

A threaded rod with a smooth end was screwed into the centre of one end of a right circular cylinder. The cylinder (described below) had a moment of inertia about the proximal end of $0.417\ \mathrm{kg \cdot m^2}$; the offset produced by the threaded rod increased the moment of inertia to $I_c=0.522\ \mathrm{kg \cdot m^2}$. To ensure that no proximal damping occurred and the effects of d were isolated, a procedure similar to that used by Engin (1984) was employed. One edge of a thin sheet of aluminium (3.175 mm thick) was machined down to a knife edge. The sheet was then fastened to the seat of the incline frame with the knife edge on top. The smooth end of the threaded rod was placed on the knife edge and the distal end of the cylinder was placed in the distal leg support. The carpenter's level was placed on top of the cylinder and the crossbar was adjusted until the cylinder was level. The bias voltage of the load cell was recorded for later removal and the system was displaced slightly ($< 8^o$) and allowed to oscillate under the restoring force of the spring assembly. The load cell signal was digitally converted at 500 Hz for 10 seconds using BIOAD software (Lamontagne et al., 1989). Five trials were collected for suspension distances of 20.0, 30.0, 40.0, and 50.0 cm. This oscillating system had an equation of motion given by:

$$(I_a + I_c)\ddot{\phi}_c + C_a(d)\dot{\phi}_c + Kd^2\phi_c = 0 \tag{24b}$$

where ϕ_c is the angle of the cylinder with respect to the horizontal in radians. The damping coefficient was given by an equation of the form of equation (58):

$$C_a(d) = \left[\frac{2\delta_c(I_c+I_a)}{\tau_c}\right] \tag{58a}$$

where τ_c and δ_c are, respectively, the time period and logarithmic decrement of the oscillating cylinder. The average data were fit to a standard least-squares regression line (Giordano and Weir, 1985) with d as the independent variable.

Pilot tests

A number of preliminary tests were required to validate the SOA setup and theory. These tests will be described below. The data processing was the same as that described below for the human testing.

Validation I: vertical mass-spring system (VMSS)

The small oscillation technique incorporates a linear approximation to the angular motion of the leg-foot system. For angles of $\theta \leq 8°$ (0.139 rad) the arc length is approximately equal to the linear dimension and thus the system was assumed to be oscillating in a straight line as in a simple vertical mass-spring system

(VMSS). To obtain an expected base line error of the SOA setup a VMSS was analyzed as a first phase of validation. The SOA was configured as a VMSS by replacing the distal leg support with a calibration weight holder. The system was assumed to oscillate in a single plane with negligible damping governed by the ODE (Fowles, 1986):

$$m\ddot{y} + Ky = 0 \tag{70}$$

The mass could be calculated from the time period of the oscillation:

$$m_{cal} = K\left(\frac{\tau_{ms}}{2\pi}\right)^2 \tag{71}$$

where τ_{ms} is the time period of the oscillating system.

The sysiem was tested at four different masses: m=5.177, 9.177, 13.177, and 19.707 kg which were pre-weighed on a precision digital scale (Mettler PE 3600 Delta-range). The stiffness of the spring assembly remained constant at 1000 $N \cdot m^{-1}$. The load cell/spring assembly was loaded with the appropriate mass and the bias voltage was noted for later removal. The mass was then displaced slightly downwards, released, and allowed to oscillate under the restoring force of the springs. The load cell signal was digitally converted at 500 Hz for 10 seconds using BIOAD software (Lamontagne et al., 1989). Five trials at each mass were collected. Equation (71) was used to compare the actual and calculated masses.

Validation II: determination of the moment of inertia of a solid object of known physical parameters

Since equation (60) was used as an input into equation (58) a partial validation would entail carrying out the procedure on a solid object of known moment of inertia.

The validation solid. The solid object chosen to validate equation (60) was a right circular cylinder made of homogeneous nylon (natural extruded nylon, type 66SA, Canus Plastics Ltd., Ottawa, Ontario, Canada). The cylinder had a mass of 4.798 kg, a length of 0.508 m, and a radius of 0.051 m. Using standard equations (Fowles, 1986) the moment of inertia of the cylinder about one end was calculated to be 0.417 $kg \cdot m^2$.

Protocol. A smooth mechanical joint was threaded into the centre of one end of the cylinder. The offset produced by this joint increased the moment of inertia to I_t=0.477 $kg \cdot m^2$. The mechanical joint was attached to the seat of the incline frame of the SOA. The distal end of the cylinder was placed in the distal leg support. A carpenter's level was placed on top of the cylinder and the crossbar was adjusted until the cylinder was level. The bias voltage was recorded for later removal and the system was then displaced slightly downwards ($< 8^o$) and allowed to oscillate freely under the restoring force of the springs. The load cell signal was digitally converted at 500 Hz for 10 seconds using BIOAD software (Lamontagne et al., 1989). Five trials were collected at each of three suspension distances: d=33.420 cm, d=42.620 cm, and d=51.820 cm. The stiffness of the spring assembly remained constant at K=1000 $N \cdot m^{-1}$. Such a system had an equation of motion of the same form as equation (24):

$$(I_a + I_s)\ddot{\phi}_s + (C_a(d) + C_J)\dot{\phi}_s + Kd^2\phi_s = 0 \tag{24c}$$

where C_J is the damping coefficient of the mechanical joint in $N \cdot m \cdot s \cdot rad^{-1}$ and ϕ_s is the angle of the oscillating cylinder with respect to the horizontal. The equation used to determine I_s was of the same form as equation (60):

$$I_{s(cal)} = \left[\frac{\tau_s^2(Kd^2)}{4\pi^2 + \delta_s^2}\right] - I_a \tag{60b}$$

where τ_s and δ_s are, respectively, the time period and logarithmic decrement of the oscillating cylinder. The output of equation (60b) was compared to the theoretical value of I_s.

Testing the effects of the tightness of the oversling

The sling system (sling and oversling) was required since without it coupled oscillations occurred at other more compliant sites. Pilot work in the laboratory indicated that this effect was most pronounced at $\theta = 10°$ since the knee joint was relatively stiff and the upper part of the posterior compartment was in contact with the seat. It was expected that if the oversling was too tight increased damping would result due to compression of the quadriceps and the quadriceps tendon. Thus, the effect of the tightness of the oversling was tested on one subject (JT) at $\theta = 10°$.

Protocol. The actual data collection process was the same as that used for the complete human testing sessions and will be described in a subsequent section. With the subject positioned in the SOA and with the thigh supported by the sling, three oscillation trials were collected with no oversling (N). The oversling was then attached very loosely (L) and three more trials were collected. The process was repeated for three more qualitative levels of tightness: moderate (M), tight (T), and very tight (VT). During these tests all other parameters remained constant: $K=1000$ $N \cdot m^{-1}$, $d=45.000$ cm, and $\theta=10^{\circ}$.

A one-way ANOVA (Spiegel, 1975) was performed ($\alpha=0.05$) using Number Cruncher Statistical System (1987) software to detect possible differences between means. Newman-Keuls post-hoc analysis was used to locate any differences.

Subject preparation

The subject was again prepared with EMG electrodes and the ankle joint was taped at 0°. These procedures were described previously with respect to the elastic component.

Data acquisition

Positioning the subject properly in the SOA often took up to 20 minutes due to difficulties in obtaining the exact knee angle and the optimal tightness of the oversling. With the subject properly positioned, the suspension distance (d) was measured (three times to within 1.0 mm) using an anthropometer and recorded on the data sheet (Appendix B).

Figure 13 illustrates the complete experimental setup. With the leg level the voltage output of the load cell was recorded for later removal. The system was displaced slightly downwards ($< 8^{\circ}$) by a small cable connected to the bottom of the distal leg support. The system was held in place for a few seconds during which time the EMG signals were viewed on the oscilloscopes. When electrical silence was observed the limb was released and allowed to oscillate under the restoring forces of the spring assembly and the passive moments. For subjects who had difficulty in achieving muscle relaxation, a number of warm-up trials were performed to accustom the subject to the testing environment. The load cell signal was digitally converted (Labmaster board) at 500 Hz and the five EMG signals at 1500 Hz for a period of 10 seconds. The A/D conversion was controlled by BIOAD software (Version 1.1, Lamontagne et al., 1989) specifically developed for the 16 MHz Compaq 386 microcomputer. After each trial was complete it was reviewed on screen to check for EMG activity and disturbances in the load cell signal. The process was repeated until five successful trials were obtained. Time between trials was approximately one minute. The subject was removed from the apparatus and the next configuration was set up. The entire process was repeated for the other four configurations (knee angles) and the entire testing session took about three to four hours. All data files were stored on floppy disks for later processing. To test the effects of muscle activity on the load cell output a number of trials were also collected (on subject JT) while the subject purposely performed muscle contractions.

Data processing

Described below are the procedures used to reduce the raw data and to calculate the angular damping coefficient.

Initial data reduction

All data files (25 per subject, stored in the BIOAD format) were loaded into the companion program BIOPROC version 1.18 (Lamontagne et al., 1989). Each data file contained six channels (five EMG, load cell) as functions of time. The load cell signal was low-pass filtered (critically damped, fourth-order, f_c=6 Hz) and the bias voltage was removed. End point data was removed in such a way as to exclude the first positive peak and to obtain as many useful cycles of oscillation as possible. To obtain an estimate of the difference between the initial peak and the subsequent peaks, the front end of the data file was maintained for four subjects (FH, GK, JC, PP). The EMG signals were rechecked and the data were then stored in ASCII format. Each reduced data file contained two arrays: time and load cell output (in volts).

Peak finding

Each of the 425 ASCII files were loaded into a FORTRAN peak finding program. This program reads an ASCII input data file and outputs an ASCII file which contains the maxima, minima, and their times of occurrence.

Macro-driven spreadsheets (VISCOUS.WSP)

Each output file from the peak finding program was imported into a series of linked, pre-programmed, macro-driven spreadsheets which were saved as a workspace (VISCOUS.WSP). The load cell output data did not have to be converted to newtons since all calculations were relative and could be performed using the units of volts. The following is a brief description of the calculations which were performed within VISCOUS.WSP.

This system of spreadsheets created a separate file for each knee angle for each subject (85 files). For each of the five trials the time period (τ) between each successive positive peak and each successive negative peak for all cycles was calculated. A global mean (across cycles and trials) was then calculated along with the standard deviation and other statistics.

Also for each trial, the logarithmic decrements (δ) of the positive and negative peaks were calculated using equation (50) for up to $n=1, 2, 3, 4, 5$ (if enough cycles were available). An overall mean value of δ was calculated (the mean of the mean positive and negative values) and finally a global mean across trials was computed. Standard deviations and other statistics were also calculated along with the means.

Since the positive and negative envelopes of the oscillations should be exponential in nature, a linear regression of $ln(\phi_i)$ versus time was performed for all trials as a check for exponential decay.

VISCOUS.WSP also contained 17 files (one for each subject) which incorporated the necessary procedures for calculating the damping coefficient of the knee joint. Each file extracted the mean τ and δ values from the previous 85 files and the value of $K_e(\theta^*)$ was extracted from ELASTIC.WSP. The value of d was obtained from a file which contained a matrix of the values of the suspension distance for each subject for each angle. All of these parameters were input into the regression equations for I_a and $C_a(d)$ and equations (58), (60), and (20a) to calculate the damping coefficient.

Since the hip angle was changed for the $\theta=130°$ position the value of $K_e(\theta^*)$

taken from the derivative of equation (62) may not be an appropriate input into equation (60) due to the effects of the biarticular muscles. Therefore, the value of I_t was determined using the nonlinear regression equations of Yeadon and Morlock (1989).

Variability of the oscillation parameters (τ and δ)

Two types of variability in τ and δ exist: within trials and across trials. Depending on the knee angle each trial contained up to 13 cycles of oscillation. Variability of τ and δ over these cycles within a single trial represents the within trials variability while the variability over the five trials represents the across trials variability. The variability was represented by the coefficient of variation (CV in %) which was given by:

$$CV(\%) = \left(\frac{S.D.}{mean}\right) * 100 \tag{72}$$

To determine if the variabilities were dependent on the knee joint angle the data (average CVs) were submitted to four one factor (knee angle) ANOVA's: one for each type of mean (τ-within, τ-across, δ-within, δ-across). Newman-Keuls pcst-hoc analysis was used to locate differences between the mean CVs. The analyses were carried out on Number Cruncher Statistical System (1987) software. The alpha level was set at α=0.05.

STATISTICAL ANALYSIS

The following section describes the regression analysis performed on both the elastic and viscous components of the NPJM. All analyses were performed using Number Cruncher Statistical System (NCSS,1987) software.

Multiple linear regression analysis (MLR)

The ultimate goal was to generate prediction equations based on one, two, or three anthropometric parameters. The statistical model takes the form (Mendenhall, 1983):

$$y = \beta_o + \beta_1 x_1 + \beta_2 x_2 + \beta_3 x_3 + \epsilon \qquad (73)$$

and the regression procedure described below determined the best estimates of the regression coefficients ($\hat{\beta}_o$, $\hat{\beta}_1$, $\hat{\beta}_2$, $\hat{\beta}_3$).

Dependent variables (DV)

Since the predictability probably varies over the range of motion, 12 separate regression analyses were performed at fixed knee angles. For the elastic component the dependent variables were the net passive elastic joint moment in newton-metres (N·m) at each of the following knee angles: $\theta=0°$, 10°, 45°, 90°, 110°, 130°, and 140°. Although most subjects attained knee angles greater than 140° and less than 0°, 0° and 140° were chosen as the limits since all subjects attained at least these positions. For the viscous component the dependent variables were the angular damping coefficients in newton-metre-seconds per radian ($N \cdot m \cdot s \cdot rad^{-1}$) at the knee angles of $\theta=10°$, 45°, 90°, 110°, and 130°.

Independent variables (IV)

The main independent variables included body mass, height, knee breadth, knee depth, knee circumference, ankle circumference, ankle breadth, thigh length, upper-thigh circumference, gluteal furrow depth, gluteal furrow breadth, midthigh circumference, midthigh depth, midthigh breadth, lower-thigh circumference, lower-thigh depth, lower-thigh breadth, calf length, calf circumference, calf depth, calf breadth, and trunk forward flexion. Also, a number of combination (multiplicative), second-order, and third-order terms were derived from the main IVs. All of the anthropometric parameters (main and derived) are described and tabulated in Appendices C and D. All parameters (31 IVs and 12 DVs) were input into a database within NCSS.

Variable selection

Of the 31 potential independent variables, one, two, or three of the best were required for each dependent variable. To select these IVs scatter plots and a correlation matrix were generated for every potential IV against every DV. Based on a sample size of 17 and an alpha level of 0.05, the minimum correlation (*r*) required for significance is 0.412 (Spiegel, 1975). Only those IVs which displayed linear trends and met the *r* criterion were considered for further analysis.

Regression procedures: forward and backward stepping procedures

The above process usually trimmed the list of potential IVs down to about 10 to 15. To reduce the list further and find the best predictors, a stepwise regression technique was employed. This procedure continued adding predictors until the mean squared error (MSE) did not change by more than one percent (user defined). More often than not this process added more variables than was desired. Predictors were then systematically removed based on their influence on the cumulative R^2-statistic. The program also calculated a t-statistic giving the probability of each coefficient being equal to zero. To produce stable coefficients an equation was maintained only if all coefficient probabilities were less than 0.125 (Hinrichs, 1985). An attempt was also made to include predictors (in the same equation) which were not highly correlated with each other (collinearity).

Robust regression analysis (RR)

Initial observation of the data indicated a number of points which were potential outliers. Since outliers can have a considerable influence on the estimates of the regression coefficients, a robust regression technique (Number Cruncher Statistical System, 1987; Rousseeuw and Leroy, 1987) was also employed. Robust regression techniques are iterative techniques which seek to find outlying points and minimize their influence on the parameter estimates. At each step of the iteration each data point was assigned a weight (scaled to one). Small weights were assigned to extreme outliers while larger weights were given to points which were close to the regression line.

A robust regression was run on all the data using the Andrew's Sine robustifying function with a truncation constant of 2.1 (Number Cruncher Statistical System, 1987). Iterations were halted when the maximum change in any regression parameter was less than 5% (user defined). The weights were stored in the database and the stepwise regression techniques were rerun, as described above, using the weighted data.

CHAPTER IV

RESULTS

The following sections present the experimental results. Again, the elastic and viscous components are treated separately. Statistical results for both components are presented in the final section.

THE NET PASSIVE ELASTIC JOINT MOMENT

The main results of the experiments designed to determine the passive elastic moment will be described in the subsequent paragraphs.

Calibration: strain gauges

Two slightly different calibration curves were obtained: one for each orientation of the sensing member (Figure E1, Appendix E). The mean positive output (flexion producing moments) was linear ($r = 0.990$) with a root mean squared error (RMSE) of 0.180 N•m and hysteresis of 0.400% of full scale. The mean negative output (extension producing moments) was similar ($r = 0.990$, RMSE = 0.301 N•m, and hysteresis = 0.300% of full scale). One subject produced passive moments exceeding the upper bound of the initial calibration range (47 N•m). Therefore, after all experimentation was complete, the strain gauges were recalibrated beyond the maximum moment obtained (86.141 N•m). Linearity was still observed between 47 N•m and 87 N•m.

Calibration: Potentiometer

The potentiometer signal was very stable (Figure E2, Appendix E). The mean output was linear ($r = 0.990$) with an RMS error of 0.593°. Hysteresis was not detected.

Frictional moment of the HKA

The frictional moment of the loaded HKA was relatively constant throughout the operating range. The mean frictional moment was measured to be 1.118 N•m (± 0.267 N•m).

Muscle activity

Most subjects had no difficulty in relaxing their muscles after a number of test cycles were performed to accustom them to the HKA. A few subjects, however, did show a protective response as the joint limits were approached and more time was required to obtained the desired number of trials. Figure 19 displays the raw EMG signals of the RF and LBF muscles along with the strain gauge and potentiometer signals for a passive rotation into flexion for a typical subject (GW). When a subject (JT) purposely performed small contractions disturbances in the strain gauge output were apparent (Figure 20).

Range of motion

Table 2 displays the range of motion obtained for each subject. These values were obtained by forcing the leg into flexion or hyperextension. In flexion, the maximum knee angle ranged from 140° to 170°. These values were consistent with the anthropometry of the subject. All subjects were able to achieve some degree of hyperextension ranging from -1.5° to -10°. It should be noted that the coefficients generated for equations (61) and (62) are valid for these ranges for each subject.

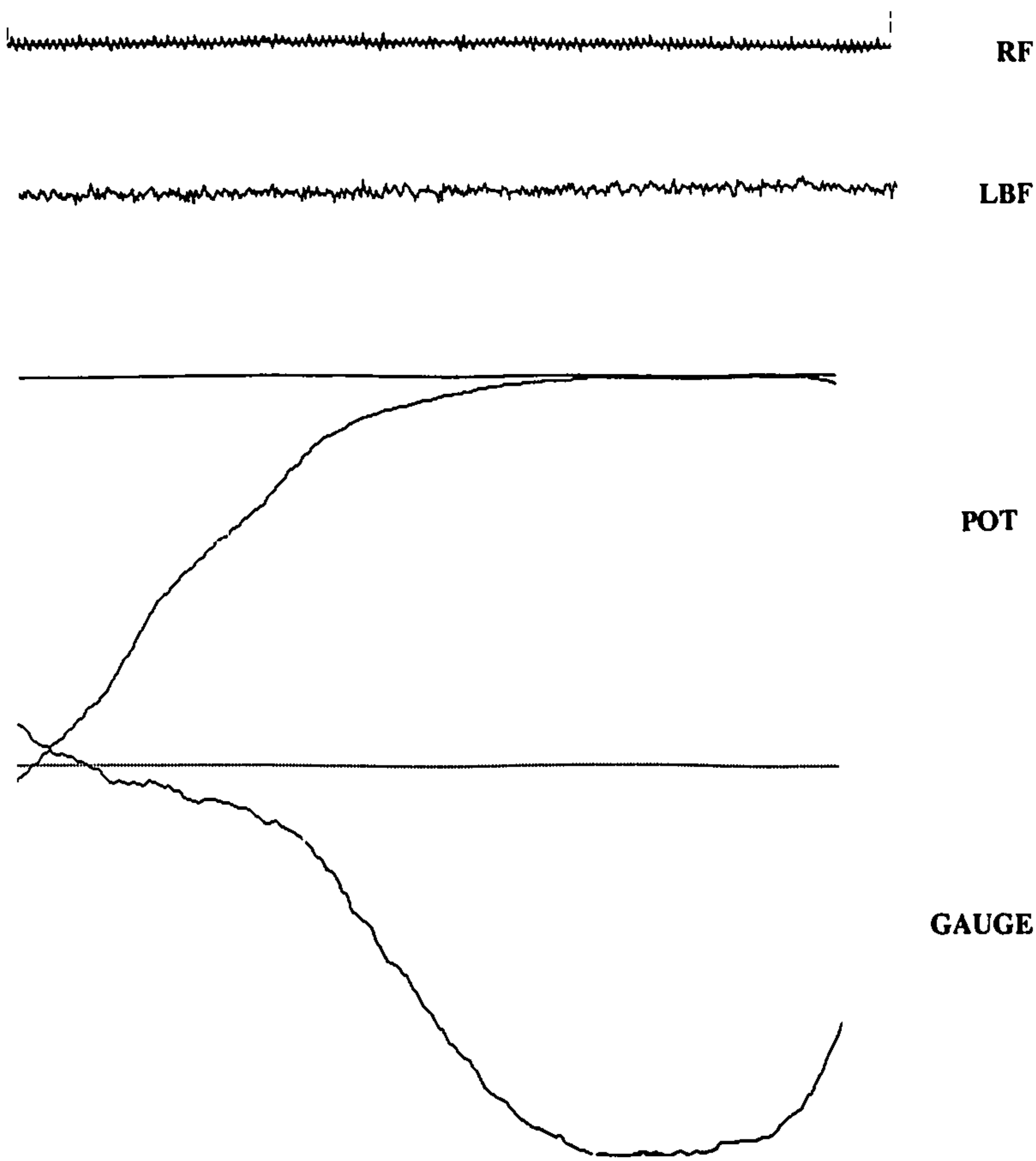

Figure 19. Raw EMG signals of the RF and LBF muscles during a passive rotation in the flexion phase for subject GW. The lower traces are the strain gauge and potentiometer signals. The other muscles showed similar behaviour.

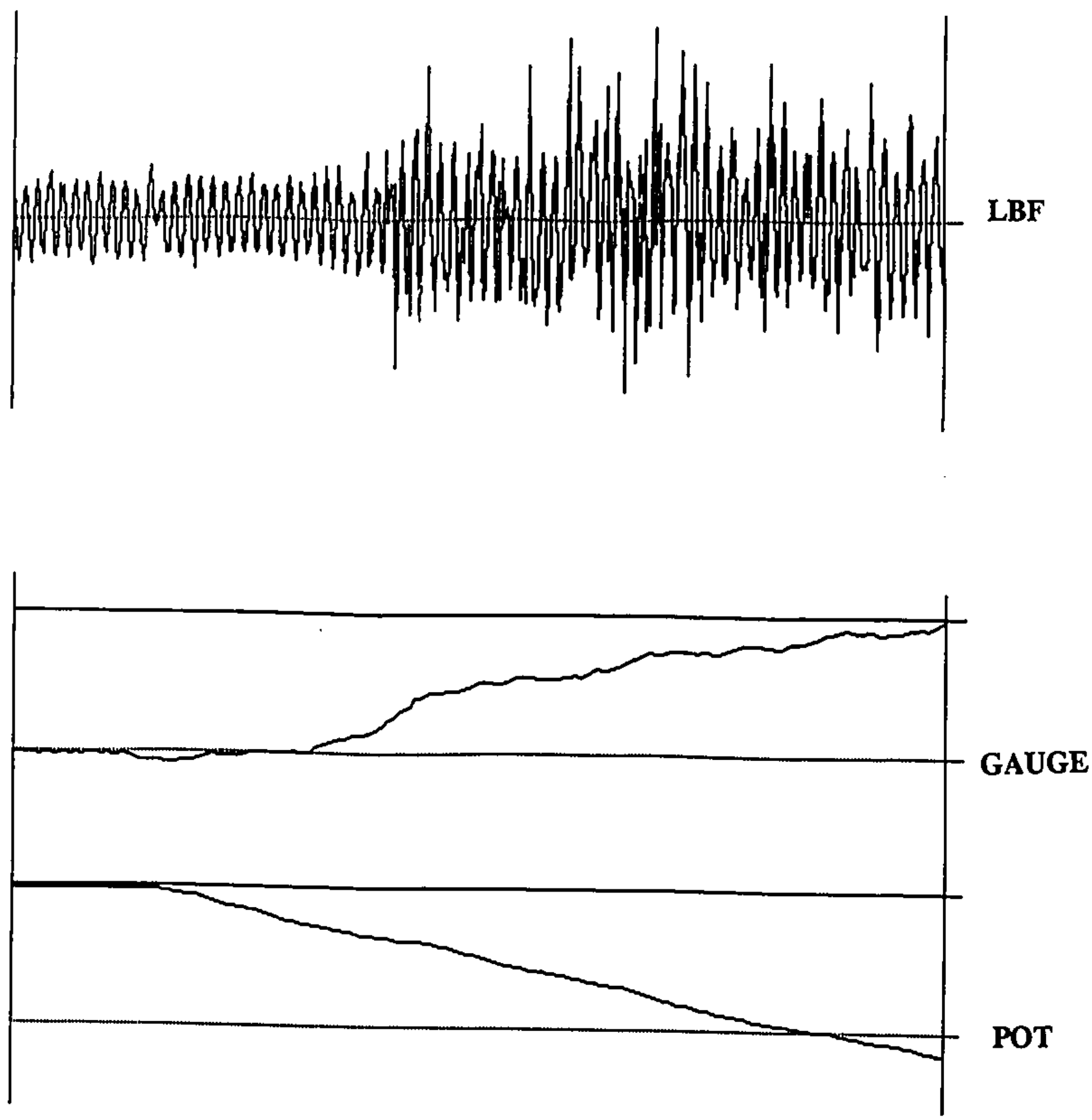

Figure 20. The effect of small muscle contractions on the output of the HKA transducer signals. Subject JT; muscle: LBF.

Table 2. Maximum range of motion obtained for the subject sample.

Subject	Hyperextension (°)	Flexion (°)
DS	-2.0	167.0
JF	-8.5	140.0
AR	-3.0	165.0
BG	-10.0	158.0
EM	-7.5	153.0
RC	-4.0	170.0
RV	-3.0	157.0
JB	-8.5	163.0
BC	-1.5	159.0
JT	-10.0	165.0
GK	-8.0	163.0
GW	-8.0	154.0
PP	-10.0	155.0
CH	-4.0	167.0
FH	-1.5	153.0
JC	-10.0	153.0
YF	-6.0	146.0
Mean	-6.2	158.1
S.D.	3.2	8.0
CV(%)	51.6	5.1

Angular velocity

For the extension phase the mean angular velocity was 0.225 $rad \cdot s^{-1}$ ($\pm$ 0.039). For the flexion phase the mean angular velocity was 0.258 $rad \cdot s^{-1}$ ($\pm$ 0.077) while the average value for the midrange phase was 0.233 $rad \cdot s^{-1}$

($\pm$ 0.049). For a given trial the velocity remained relatively constant as evidenced by the linear nature of the potentiometer versus time signal (see Figure 19). Only during the final 5-10° of flexion or extension did the velocity decrease, mostly due to the encountering of increased resistance. During the midrange testing the velocity decrease was essentially non-existent since the end points did not impose a large increase in resistance.

Curve fitting

As expected, the data for the extension and flexion phases were very well represented by simple exponential models of the form of equations (61) and (62). Figure 21 depicts a typical trial during the extension phase for subject AR. The solid squares are the experimental data points while the solid line is the fitted curve. Note that as the motion progresses into the final phase of extension the data points cluster together due to the increased resistance which was encountered. Figure 22 displays a typical trial for the flexion phase of joint motion for subject PP. Note the extremely good curve fit. Tables 3 and 4 list the mean values (S.D.) of the coefficients of equations (61) and (62) along with the R^2-statistic of the transformed regression and the RMS error between the fitted curve and the data points. All of the curve fits were very good with the RMS errors ranging from 0.333 to 1.604 $N \cdot m$ for the extension phase and from 0.265 to 2.211 $N \cdot m$ for the flexion phase.

It should be noted that for one subject (BC) the extension phase could not be adequately fitted (R^2=0.200) with an exponential function of the form of equation (61). For this subject the pattern in extension was very unusual yet consistent over

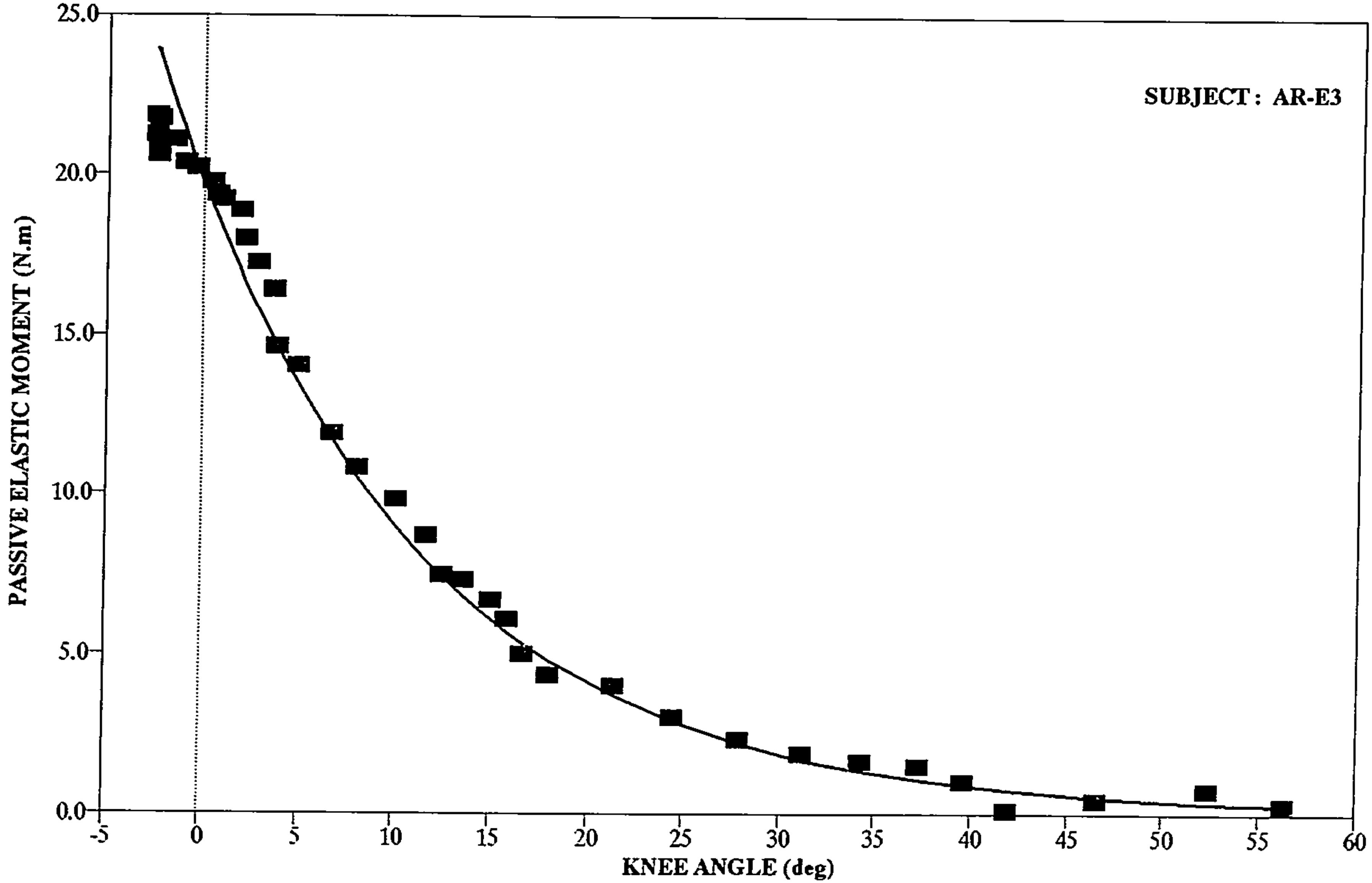

Figure 21. Extension phase passive elastic moments for subject AR. Filled squares are the experimental data points; solid line is the best fitting least-squares exponential function (equation 61).

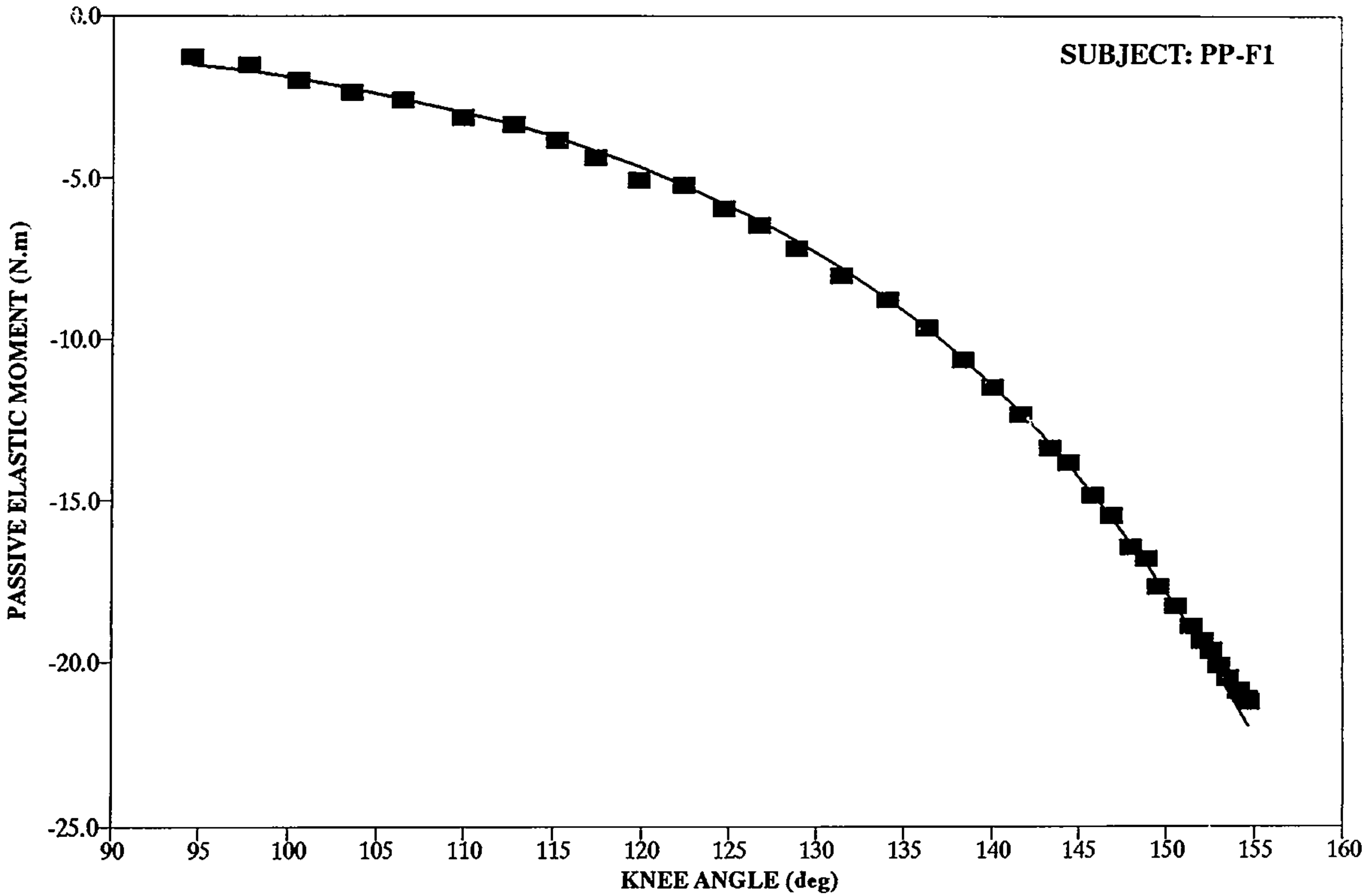

Figure 22. Flexion phase passive elastic moments for subject PP. Filled squares are the experimental data points; solid line is the best fitting least-squares exponential function (equation 62).

Table 3. Average values (S.D.) of the coefficients a_1 and a_2 in equation (61) for the extension phase of the net passive elastic joint moment function.*

Sub-ject	a_1 (S.D.)	a_2 (S.D.)	R^2	RMSE (N•m)
DS	8.572 (0.508)	-3.015 (0.219)	0.944	0.369
JF	22.460 (3.254)	-2.092 (0.556)	0.976	0.433
AR	19.720 (1.599)	-4.497 (0.549)	0.941	1.172
BG	11.484 (0.828)	-3.623 (0.557)	0.980	0.590
EM	12.417 (0.650)	-1.744 (0.163)	0.808	1.604
RC	9.582 (0.699)	-3.092 (0.794)	0.853	0.864
RV	13.250 (0.962)	-3.967 (0.122)	0.978	0.905
JB	8.439 (1.092)	-4.585 (0.095)	0.836	0.764
BC**	-87.581 (3.503)	8.224 (0.288)	0.969	0.732
JT	10.075 (0.760)	-2.209 (0.068)	0.986	0.383
GK	10.024 (0.503)	-3.012 (0.610)	0.990	0.372
GW	9.663 (1.000)	-2.280 (0.164)	0.989	0.348
PP	9.980 (1.093)	-3.229 (0.416)	0.965	0.846
CH	6.756 (0.103)	-3.767 (0.189)	0.911	0.333
FH	17.980 (2.428)	-4.002 (1.180)	0.925	1.174
JC	7.427 (0.862)	-3.730 (0.081)	0.948	0.867
YF	7.723 (1.655)	-4.153 (0.799)	0.825	1.003

* These coefficients are valid for the ranges of motion presented in Table 2.

** For this subject only equation (61) takes the form $M_e(\theta) = a_1\theta + a_2$ *for* $\theta \leq 5^\circ$. See text for details.

the five trials. The moments tended to increase approximately linearly with low stiffness up to about 5° of flexion after which (i.e., into extension) the moment also increased linearly but with much higher stiffness (very similar to the subject of

Table 4. Average values (S.D.) of the coefficients a_3 and a_4 in equation (62) for the flexion phase of the net passive elastic joint moment function.*

Sub-ject	a_3 *(S.D.)*	a_4 *(S.D.)*	R^2	RMSE (N•m)
DS	-0.002 (0.000)	3.219 (0.261)	0.987	1.240
JF	-0.002 (0.001)	4.367 (0.570)	0.997	2.031
AR	-0.133 (0.018)	1.825 (0.116)	0.984	0.810
BG	-0.188 (0.156)	1.887 (0.492)	0.938	2.148
EM	-0.053 (0.040)	2.311 (0.335)	0.921	2.111
RC	-0.031 (0.005)	2.254 (0.208)	0.987	1.275
RV	-0.077 (0.032)	2.166 (0.399)	0.978	1.079
JB	-0.018 (0.001)	2.533 (0.141)	0.923	2.211
BC	-0.108 (0.045)	1.746 (0.203)	0.948	0.664
JT	-0.141 (0.018)	2.049 (0.648)	0.950	1.853
GK	-0.004 (0.000)	3.120 (0.064)	0.988	1.116
GW	-0.001 (0.000)	3.795 (0.168)	0.987	1.312
PP	-0.023 (0.002)	2.539 (0.188)	0.997	0.265
CH	-0.003 (0.000)	3.137 (0.397)	0.980	1.694
FH	-0.094 (0.025)	2.117 (0.093)	0.987	0.966
JC	-0.048 (0.026)	2.456 (0.257)	0.962	1.400
YF	-0.081 (0.058)	2.410 (0.325)	0.994	0.427

* These coefficients are valid for the ranges of motion presented in Table 2.

Hatze (1975a), depicted in Figure 3). Therefore, for this subject only, the midrange phase was extended and defined as $5^{\circ} < \theta < 95^{\circ}$ while the extension phase was narrowed to $\theta \leq 5^{\circ}$ and equation (61) was changed to a function of the form $M_e(\theta) = a_1\theta + a_2$.

Also as expected, the midrange phase was a low moment, low stiffness region and could be adequately modelled as a linear function of the knee angle. Figure 23 depicts a typical curve fit for subject JF. Table 5 presents the mean (S.D.) coefficients for equation (63) for each subject along with the R^2-statistic and the RMS error between the experimental data points and the least-squares regression line. Again, the curve fits were very good with the RMS errors ranging from 0.167 to 1.860 N·m.

Soft joint stops

Table 6 presents the results of applying equations (64) and (66) to the passive elastic moment data. Based on these definitions it can be seen that the soft stop in flexion had very little variability over the subject sample as evidenced by the low coefficient of variation (1.6 %). The soft stop in extension, however, had somewhat more variability across subjects (CV = 41.4 %). For subject BC the soft stop in extension was taken as 5°.

Equilibrium angle

Table 6 also presents the equilibrium angle as calculated by equation (68). The mean knee angle at which the anterior and posterior passive structures balance each other was 64.5°.

Variability and magnitudes of the passive elastic moments

Within the subject sample studied in the present investigation considerable variation existed in the passive elastic moments even for the same gender within a relatively narrow age range. Figures 24, 25, and 26 are plots of the mean net

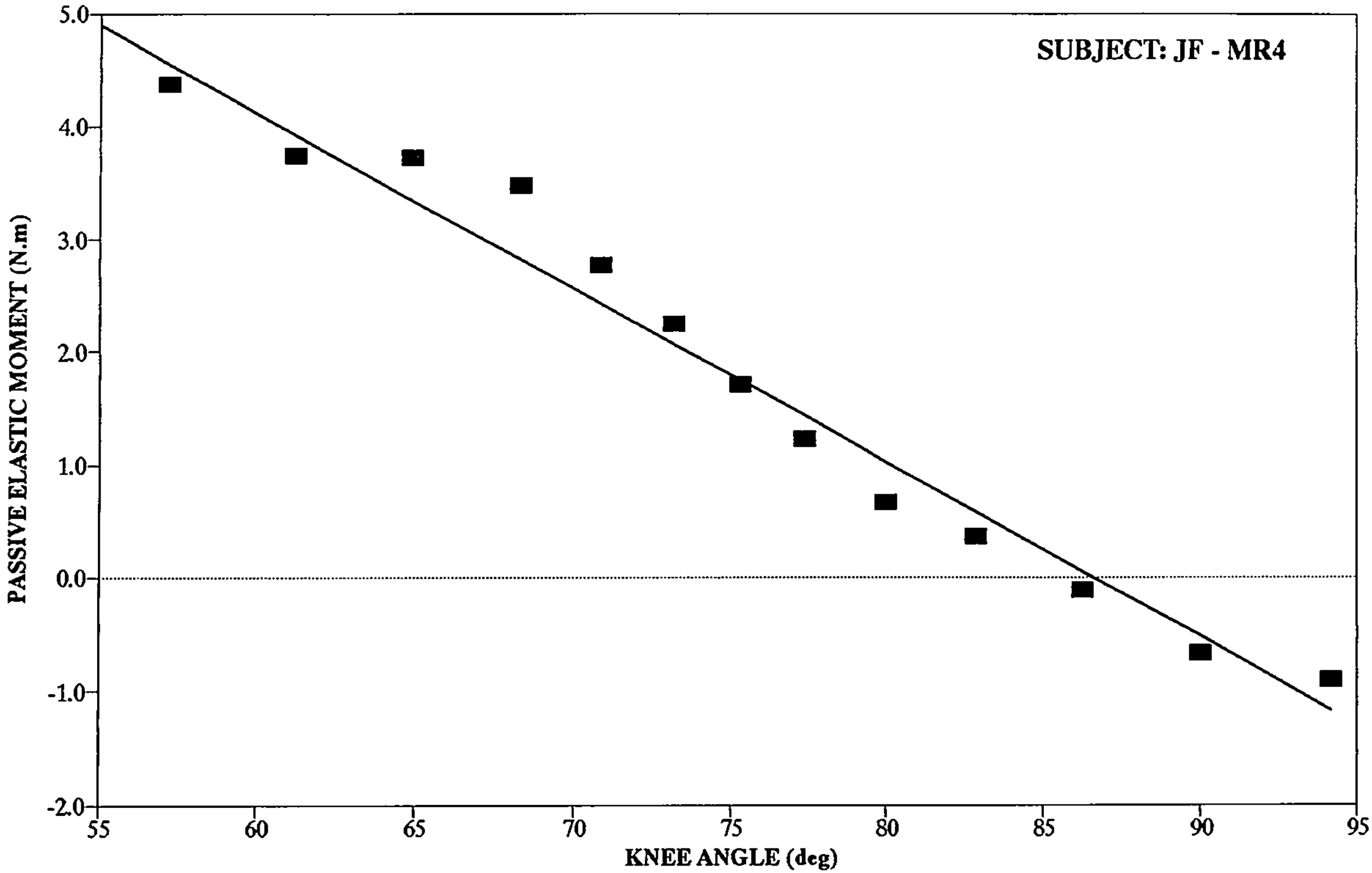

Figure 23. Midrange phase passive elastic moments for subject JF. Filled squares are the experimental data points; solid line is the best fitting linear regression line (equation 63).

Table 5. Average values (S.D.) of the coefficients a_5 and a_6 in equation (63) for the midrange phase of the net passive elastic joint moment function.

Subject	a_5 *(S.D.)*	a_6 *(S.D.)*	R^2	RMSE (N•m)
DS	-0.846 (0.059)	1.087 (0.108)	0.923	0.167
JF	-9.698 (0.388)	12.637 (0.382)	0.973	0.296
AR	-4.396 (1.002)	4.538 (1.821)	0.794	0.211
BG	-6.827 (2.079)	7.003 (0.093)	0.934	0.127
EM	-6.873 (2.756)	8.973 (1.077)	0.865	1.860
RC	-2.605 (0.380)	3.012 (0.248)	0.920	1.070
RV	-4.549 (1.105)	4.721 (0.607)	0.980	0.992
JB	-1.934 (0.126)	1.985 (0.076)	0.880	1.500
BC*	-2.568 (0.390)	2.110 (0.079)	0.960	0.700
JT	-7.922 (1.089)	8.905 (0.945)	0.970	1.120
GK	-1.824 (0.124)	2.310 (0.024)	0.990	1.500
GW	-2.318 (0.127)	3.306 (0.073)	0.990	0.830
PP	-2.928 (0.292)	3.287 (0.265)	0.980	0.560
CH	-1.068 (0.051)	1.214 (0.009)	0.950	1.014
FH	-5.189 (0.959)	5.432 (0.486)	0.960	1.100
JC	-4.489 (0.881)	4.582 (0.291)	0.960	1.134
YF	-6.771 (2.129)	6.751 (1.107)	0.910	0.720

* For this subject only equation (63) is defined over the interval $5° < \theta < 95°$. See text for details.

passive elastic joint moment functions (from Tables 3, 4, and 5, respectively) and the standard deviation envelopes for the extension, flexion, and midrange phases, respectively. Figures 27, 28, and 29 give examples of the range of magnitudes of passive moments obtained (maximum, minimum, and intermediate) for the

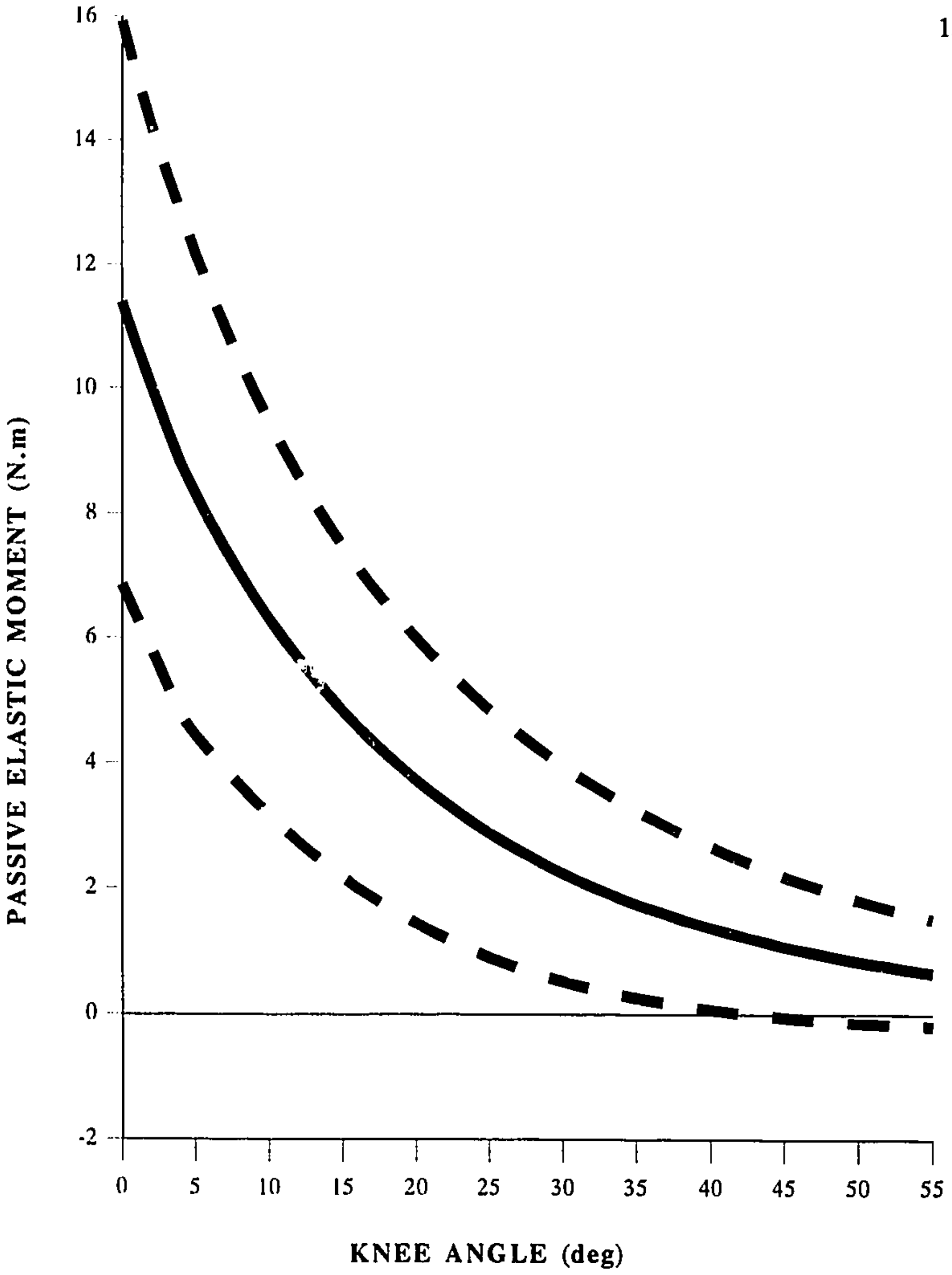

Figure 24. Variability in the extension phase passive elastic moments. Solid line is the mean function while the upper and lower dotted lines are the ± 1 standard deviation envelope.

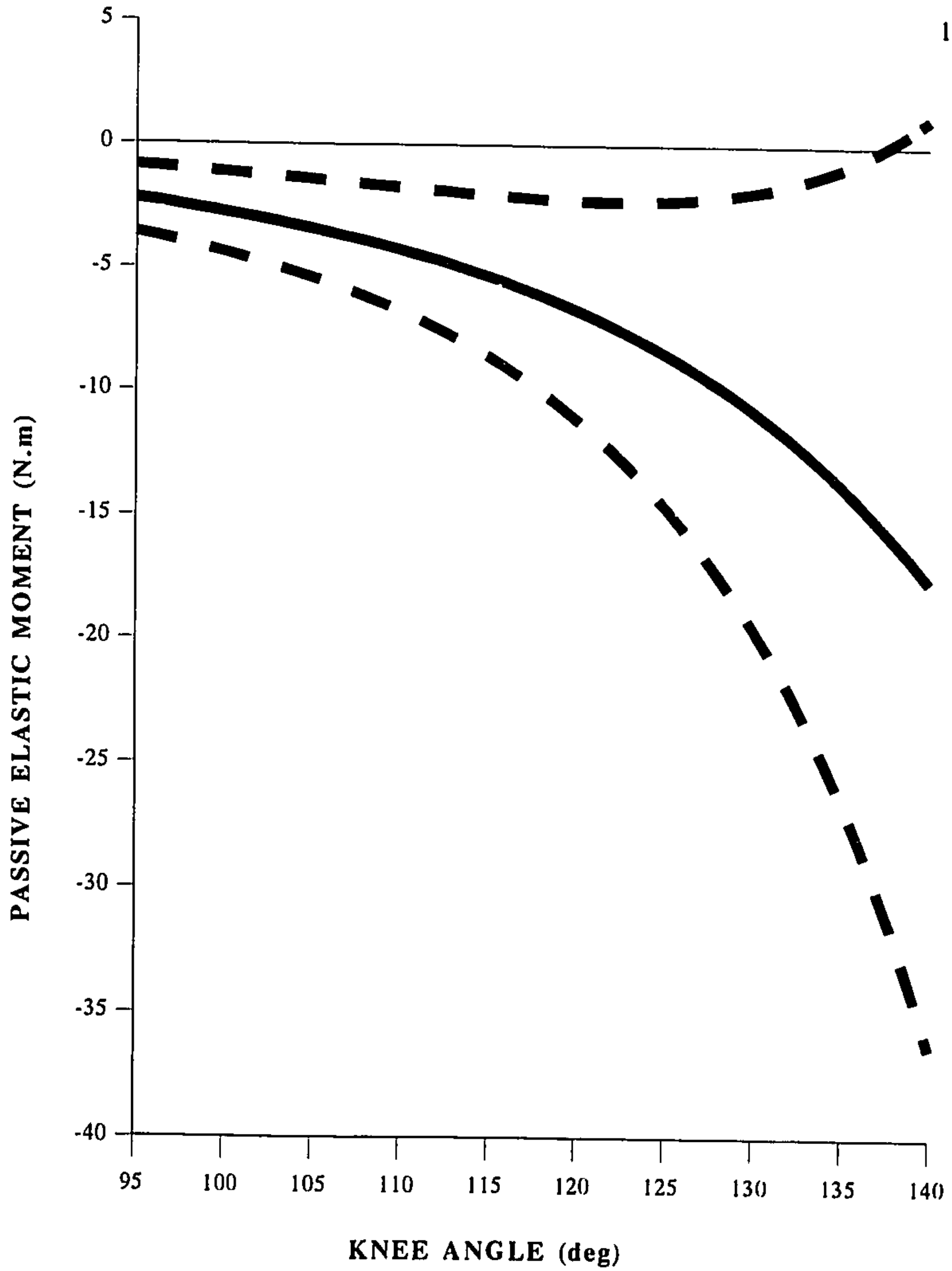

Figure 25. Variability of the flexion phase passive elastic moments. Solid line is the mean function while the upper and lower dotted lines are the ± 1 standard deviation envelope.

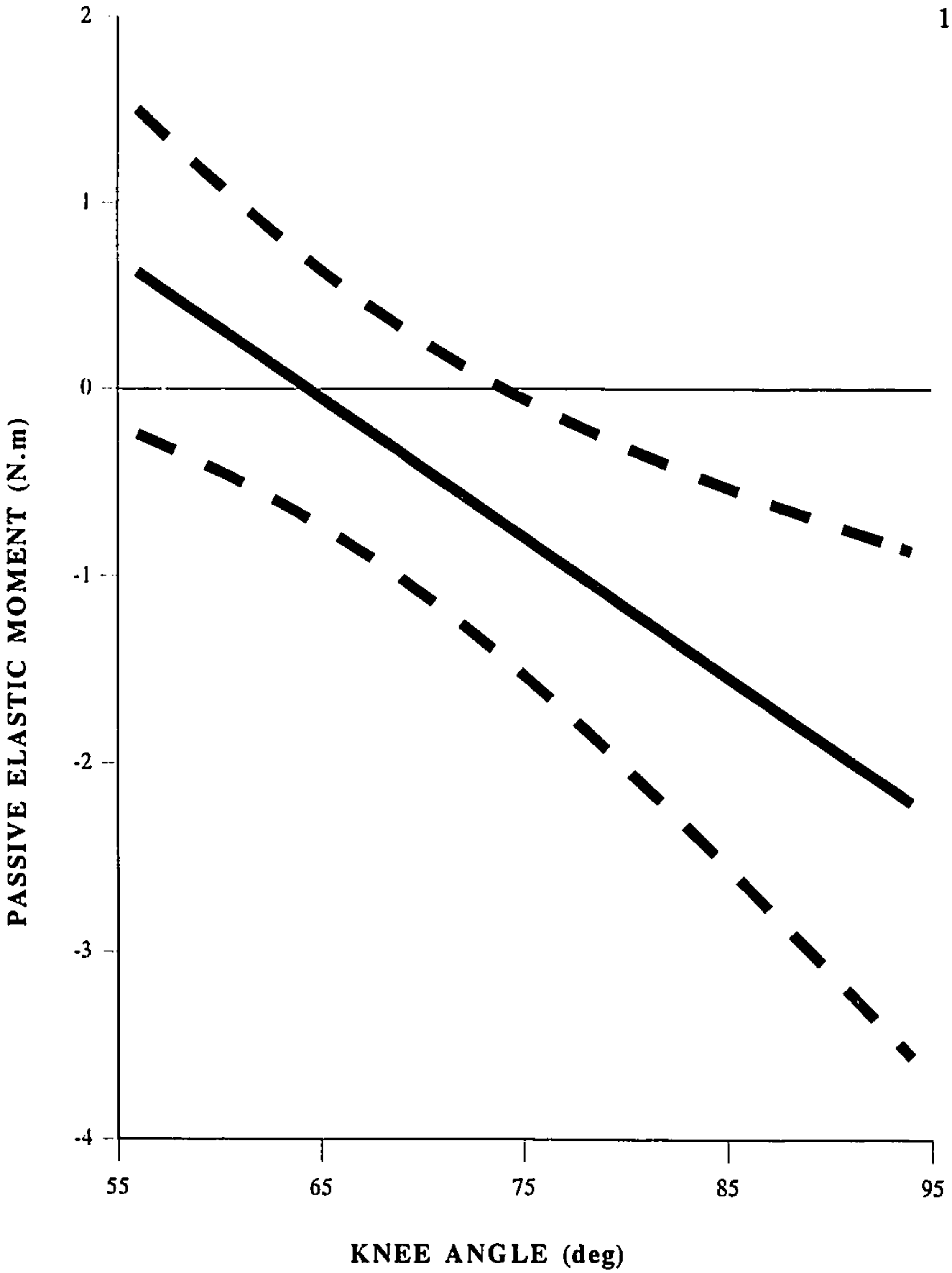

Figure 26. Variability of the midrange phase passive elastic moments. Solid line is the mean function while the upper and lower dotted lines are the ± 1 standard deviation envelope.

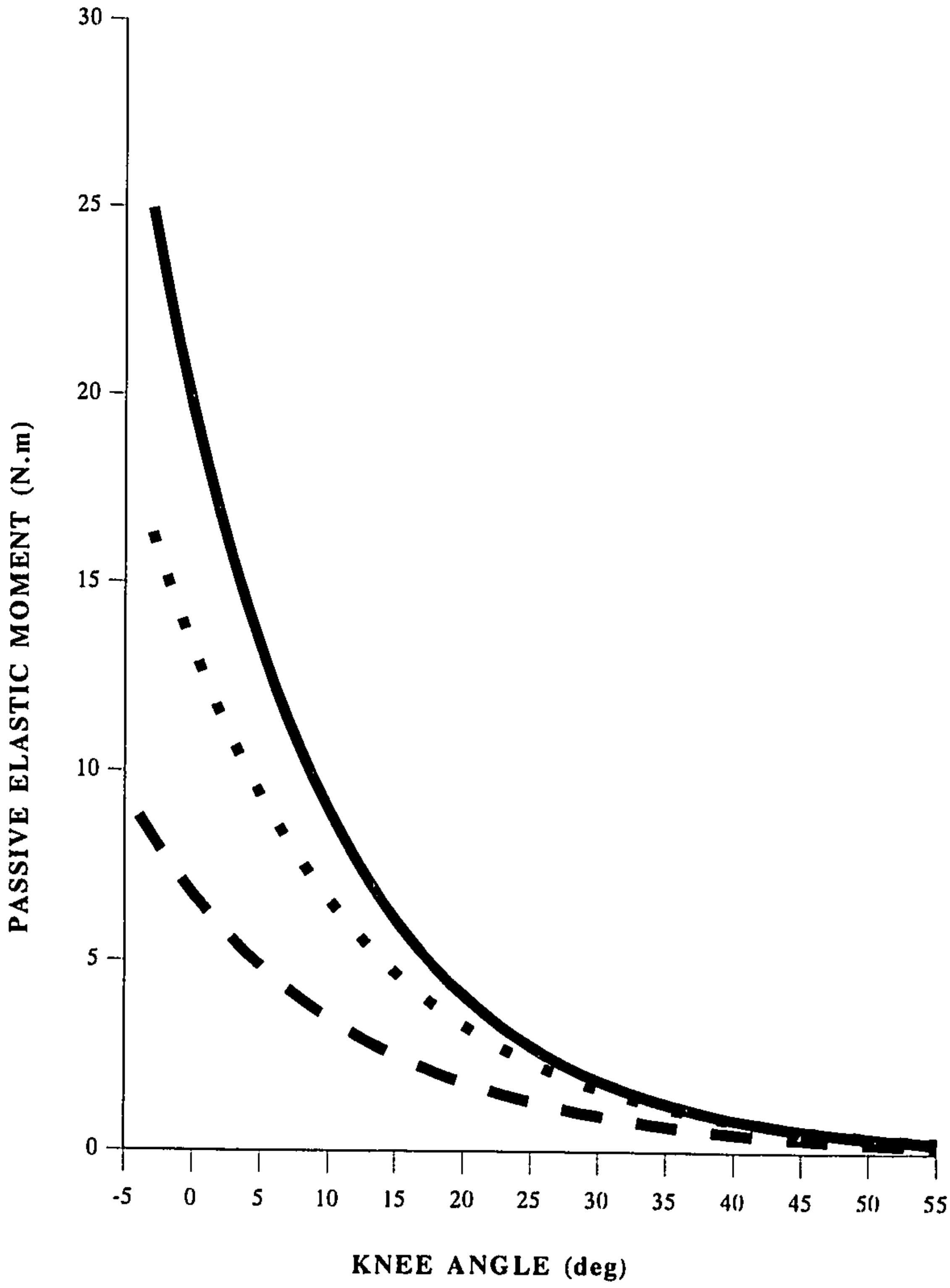

Figure 27. Range of the passive elastic moments obtained for the extension phase of knee joint motion. Solid curve is the maximum, dashed curve is the minimum, and dotted line is an intermediate curve. Each curve is the best exponential fit (Table 3).

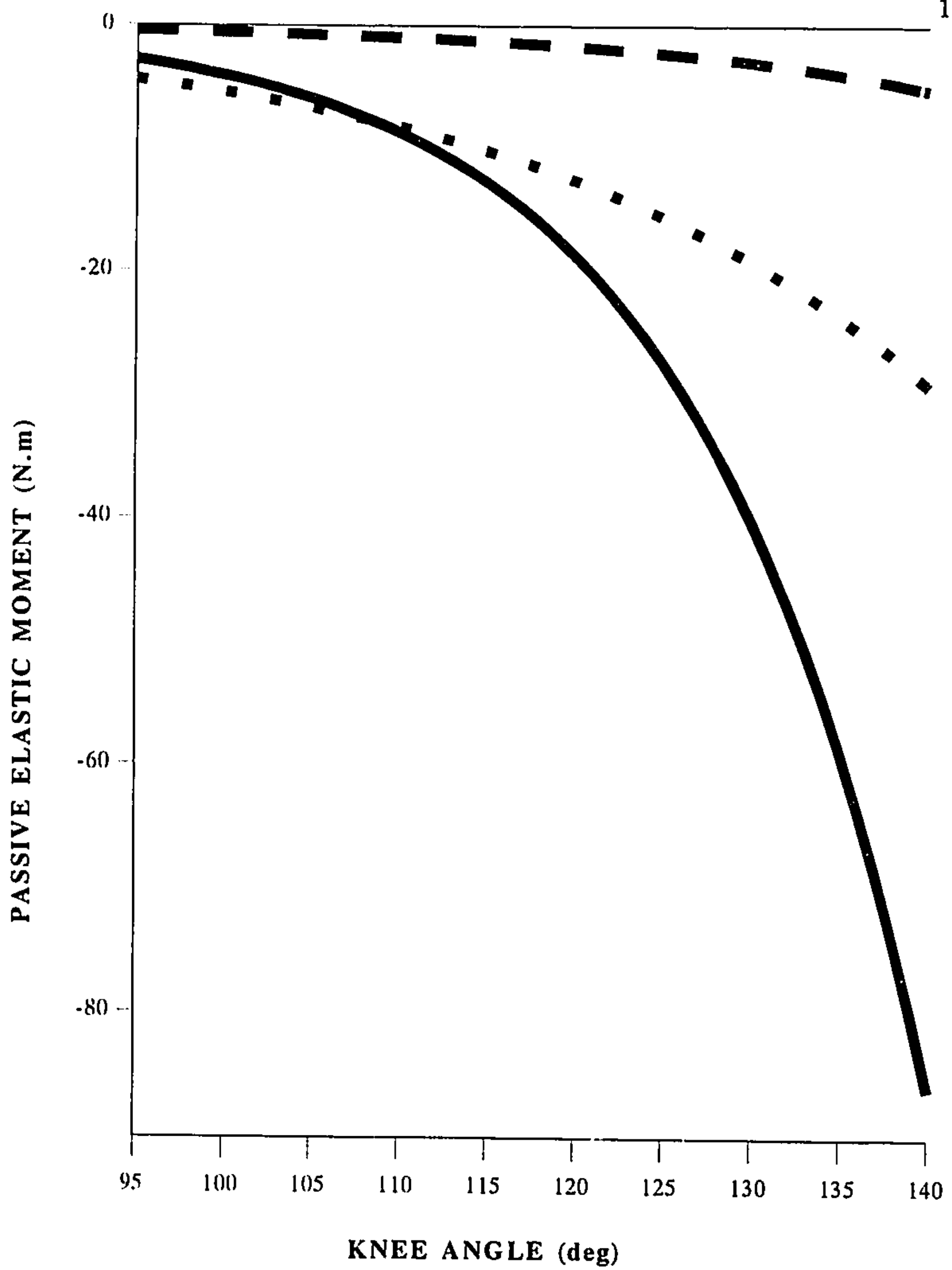

Figure 28. Range of the passive elastic moments obtained for the flexion phase of knee joint motion. Solid curve is the maximum, dashed curve is the minimum, and dotted line is an intermediate curve. Each curve is the best exponential fit (Table 4).

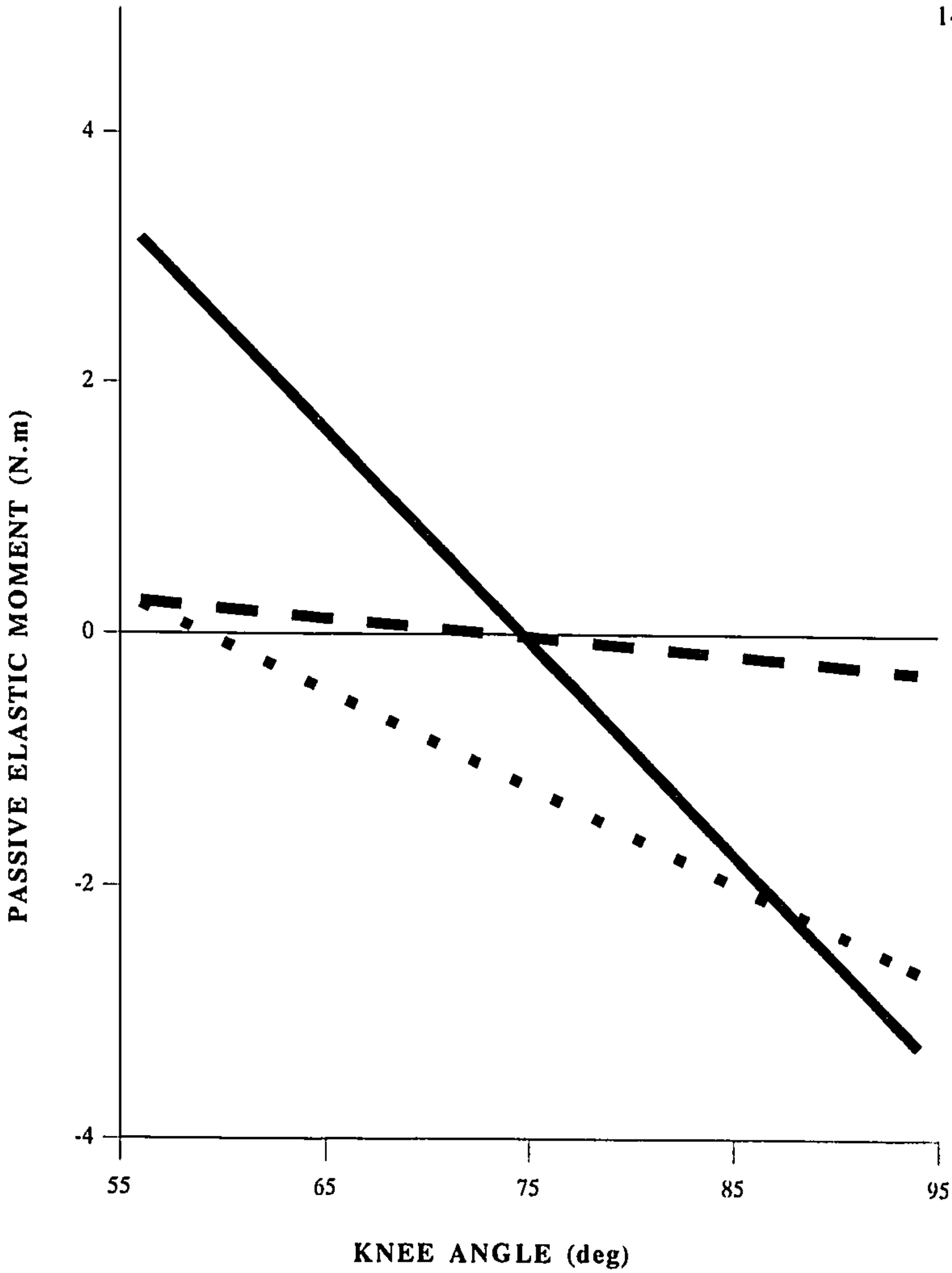

Figure 29. Range of the passive elastic moments obtained for the midrange phase of knee joint motion. Solid curve is the maximum, dashed curve is the minimum, and dotted line is an intermediate curve. Each curve is the best linear fit (Table 5).

Table 6. Average location of the soft joint stops and the equilibrium angle.

Statistic	θ_{SE}	θ_{SF}	θ_e
Mean (°)	11.4	123.3	64.5
CV(%)	41.4	1.6	13.4
Maximum (°)	18.9	127.8	81.7
Minimum (°)	2.3	121.0	47.1

extension, flexion, and midrange phases, respectively. A number of interesting observations are evident in these plots. The variability tended to increase as the joint limits were approached. This was especially evident in flexion (Figure 25) where at 140° the standard deviation envelope diverged. There existed considerable variation in the range of magnitudes of the passive moments. At 3° of hyperextension (i.e., -3°) the minimum moment obtained was 8.229 N·m (subject CH) while the maximum value observed was 24.956 N·m (AR). At 140° of flexion the range was even greater: the minimum value obtained was -5.212 N·m (subject DS) while the maximum value measured was -86.141 N·m (subject JF).

THE ANGULAR DAMPING COEFFICIENT

The following paragraphs describe the main results obtained for the viscous component, including determination of the mechanical constants of the SOA and validation results.

Calibration: load cell

The load cell was highly linear (r=0.999) with a root mean squared error

(RMSE) of 0.585 N and hysteresis of 0.930 % of full scale. Figure E3 (Appendix E) displays a plot of the calibration curve.

The moment of inertia of the SOA

Theoretically, the moment of inertia of the SOA (I_a) should be given by 4.100 d^2. The experimental data points fitted to a power curve resulted in the following equation:

$$I_a = 4.186 d^2 \tag{74}$$

where d is in metres. The power fit had an R^2 of 0.999 and the RMS error between the power fit and the experimental data points was 0.019 kg·m². Equation (74) was used in all subsequent calculations.

The damping coefficient of the SOA

The damping function of the SOA was a negative linear function of the suspension distance and was given by the regression equation (R^2=0.889):

$$C_a(d) = 0.298 - 0.004 d \tag{75}$$

where d is in centimetres. The RMS error between the experimental data points and the regression line was 0.016 $N \cdot m \cdot s \cdot rad^{-1}$.

Validation I: vertical mass-spring system (VMSS)

Table 7 presents the results of the VMSS analysis. Except for the 5.177 kg mass all of the calculated masses were very close to the actual mass. It is suspected that the relatively larger percent error (6.799 %) for the 5.177 kg mass was due to out-of-plane motion which is more likely with a smaller mass. The out-of-plane motion has the effect of increasing the time period which, from equation (71), causes an overestimate of the mass.

Table 7. Mean data for the analysis of the vertical mass-spring system. The spring stiffness was fixed at $K=1000\ \mathrm{N \cdot m^{-1}}$.

Actual Mass (kg) (m)	Calculated Mass (kg) (m_{cal})	Percent Difference (%)*	Number of Cycles
5.177	5.529	6.799	99
9.177	9.376	2.169	73
13.177	13.226	0.374	62
19.707	19.536	-0.869	48

* $\% \ Difference = \dfrac{(m_{cal} - m)}{m} * 100$

Validation II: determination of the moment of inertia of a solid object of known physical parameters

The predicted moments of inertia were all within < 3% of the known value (Table 8) with a total RMS error across all values of d of 0.010 $\mathrm{kg \cdot m^2}$. An important finding was also revealed during the testing. When the cylinder was attached to the distal leg support, a vertically adjustable horizontal bar was used to clamp the end of the cylinder in place. Upon testing, it was found that the predicted moments of inertia were up to 30% in error (Table 8). After a number of tests, the problem was discovered to be located at the interface between the horizontal bar and the top of the cylinder. As the cylinder oscillated, shearing occurred at this interface which altered the measured time period and the logarithmic decrement. The error was greater for smaller suspension distances since there was more angular motion for a given displacement. The data were then recollected without distally clamping the cylinder and the percentage error dramatically decreased as indicated in Table 8. Thus, for the subsequent human testing the vertically adjustable horizontal bar was not used.

Table 8. Results of the oscillation tests designed to predict the moment of inertia of a nylon cylinder of known physical parameters. K is fixed at 1000 $N \cdot m^{-1}$.

d (cm)	I_s ($kg \cdot m^2$)	$I_{s(cal)}$ ($kg \cdot m^2$) (no clamping)	% Difference* (no clamping)	% Difference* (clamping)
33.420	0.477	0.471	-1.206	30.000
42.620	0.477	0.489	2.461	23.000
51.820	0.477	0.489	2.514	13.000

$$^{*}\ \%\ Difference = \frac{(I_{s(cal)} - I_s)}{I_s} * 100$$

Testing the effects of the tightness of the oversling

Table 9 presents the results of the tests to determine the effects of the tightness of the oversling on the total damping coefficient. The damping coefficient of the apparatus was not removed since it was constant for all conditions. The results of the analysis of variance indicated that there were definite differences between some of the means (F-ratio=36.49). Post-hoc analysis revealed that N<L<M=T<VT.

Table 9. Mean and standard deviation of the total damping coefficient (in $N \cdot m \cdot s \cdot rad^{-1}$) at different levels of oversling tightness. K=1000 $N \cdot m^{-1}$, d=45.0 cm, θ=10°.

Fixation level	$C_t(10°)$	S.D.
None (N)	0.866	0.057
Loose (L)	0.990	0.053
Moderate (M)	1.146	0.034
Tight (T)	1.106	0.029
Very tight (VT)	1.243	0.024

Muscle activity

As with the elastic component most subjects had no difficulty remaining relaxed but there were a few who required more time to obtain the desired number of trials. Figures 30 and 31 display the raw EMG signals of the RF and LBF muscles along with the load cell output for a typical oscillation trial (subject GW) at θ=45° and 130°, respectively. One can see the minimal muscle activity and the smooth exponential decay of the oscillations. Voluntary contractions produced observable disturbances in the load cell output (Figure 32).

Initial damping

The data of four of the subjects were analyzed by calculating the time period between the first and second positive peaks and then calculating the mean percent difference between this value and the mean time period of all subsequent cycles. The results are presented in Table 10. It can be seen that the mean percent difference for knee angles 10°, 45°, 90°, and 110° was about 25 % while that for 130° was

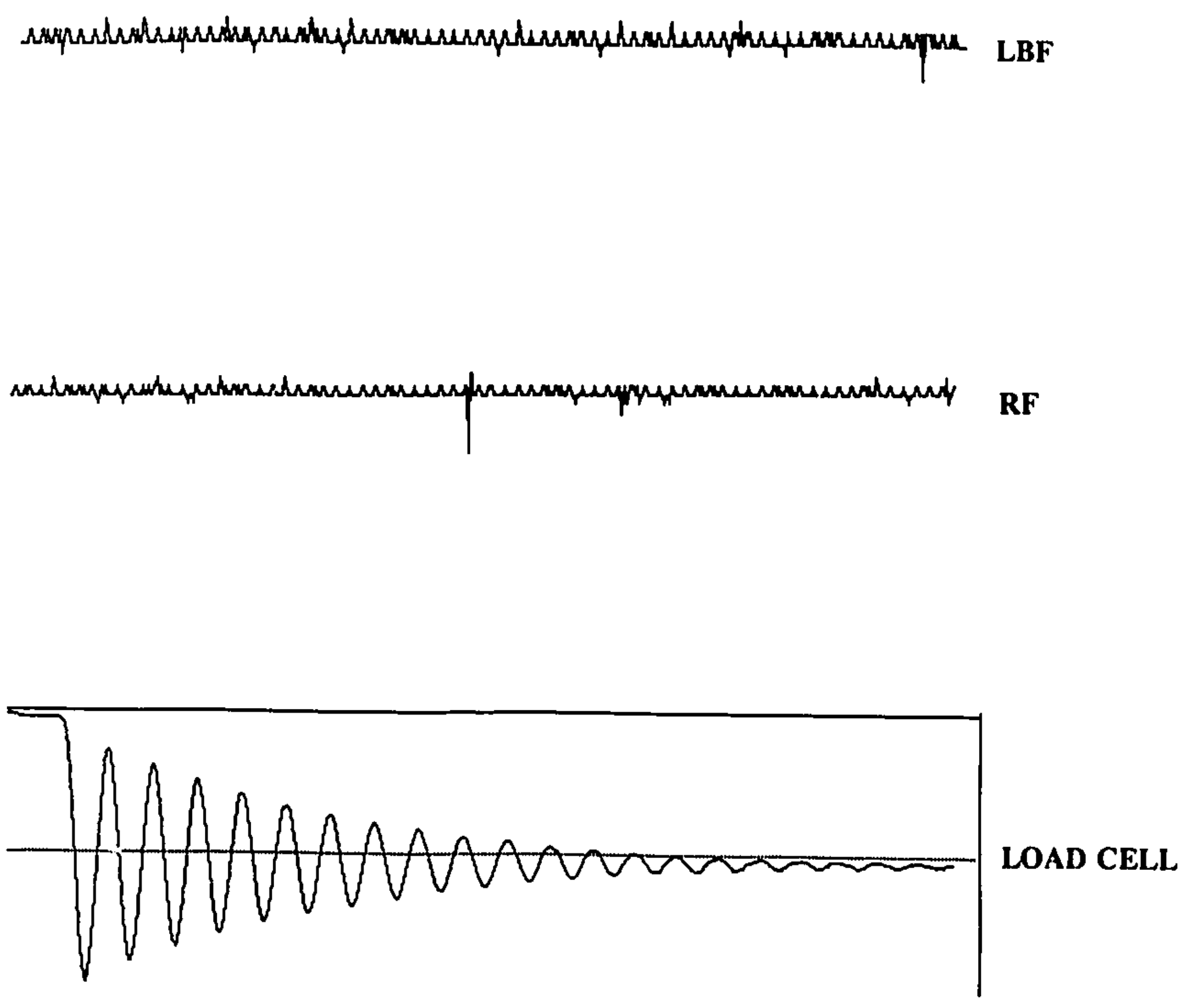

Figure 30. Raw EMG signals of the RF and LBF muscles during an oscillation trial at θ=45° for subject GW. Lower trace is the load cell signal.

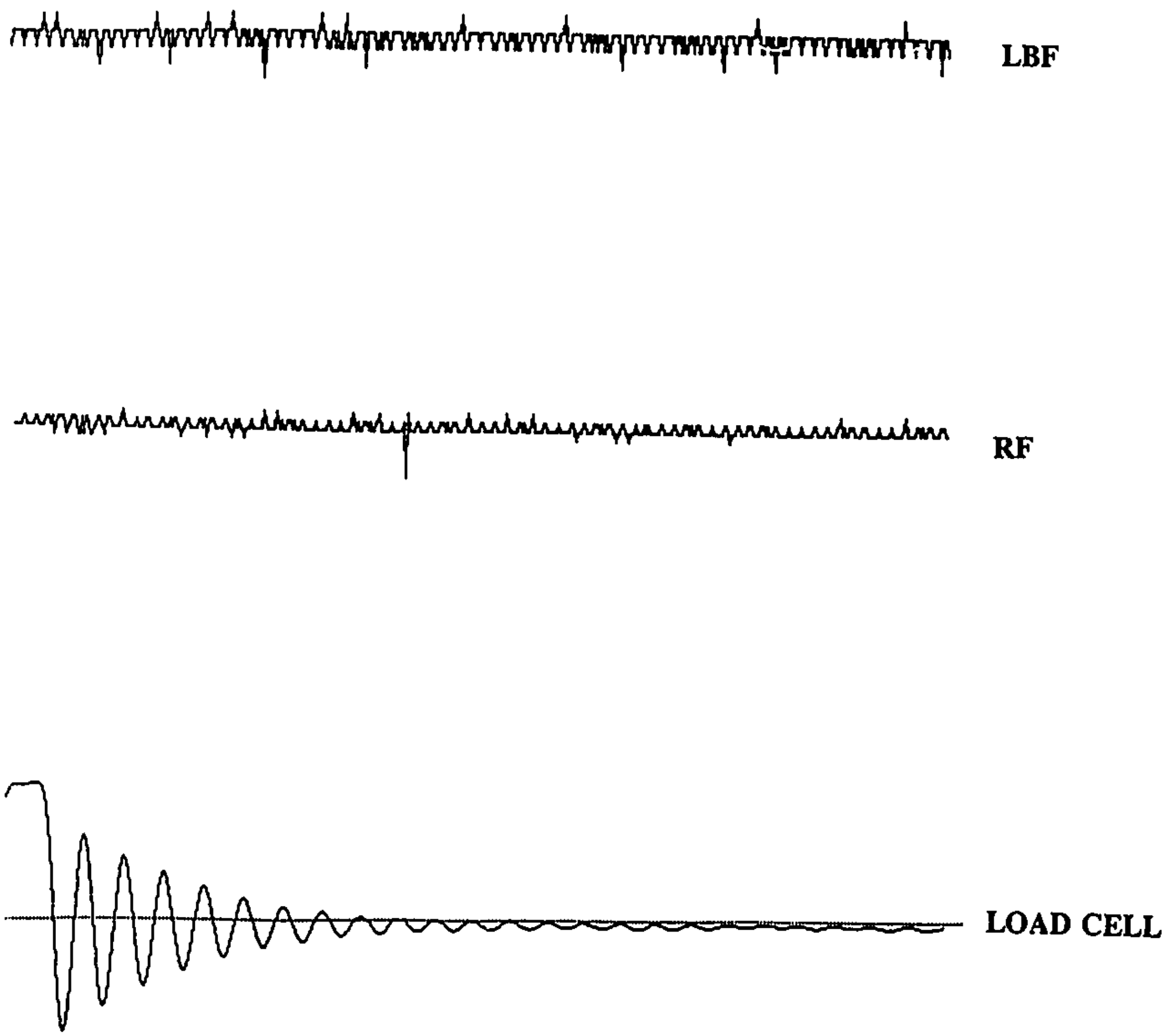

Figure 31. Raw EMG signals of the RF and LBF muscles during an oscillation trial at $\theta = 130°$ for subject GW. Lower trace is the load cell signal.

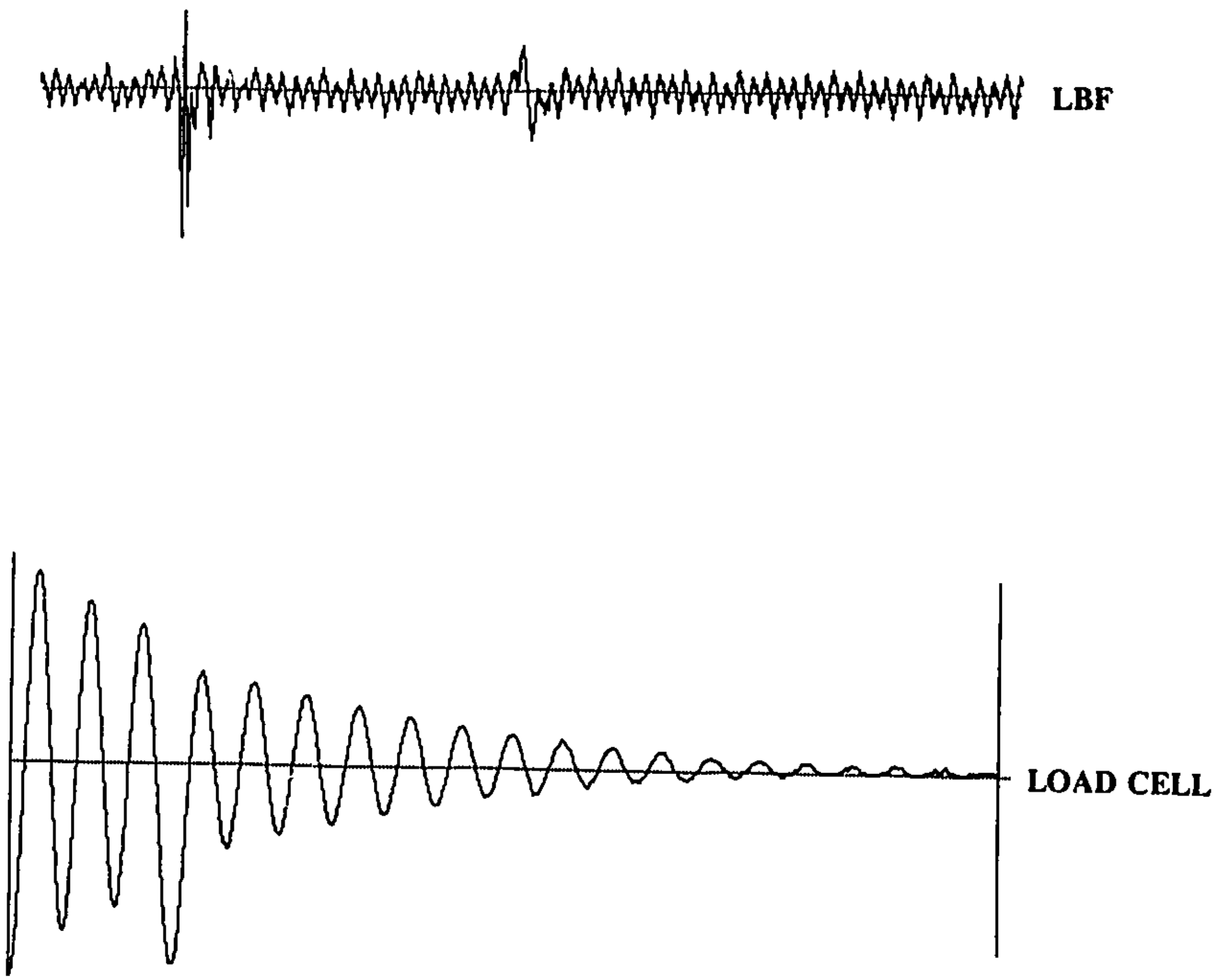

Figure 32. Effect of a small contraction of the LBF on the output of the load cell signal. θ=90°; subject JT.

significantly higher (43.808 %).

Angular damping coefficient of the knee joint

Since the damping coefficient was calculated at only five knee angles and the value measured at 130° of flexion was actually a member of another family of the damping functions (since the hip angle was different) it was decided not to fit the data to a curve due to the small number of data points. Table 11 presents the results of the small oscillation experiments for each subject at each of the five knee angles. Each value is the mean damping coefficient (in $N \cdot m \cdot s \cdot rad^{-1}$) over the five trials. Standard deviations were not included in this table since the variability of the parameters (τ and δ) which were used to calculate the damping (equation (58)) is addressed in the next section.

For a few subjects, usually at 10° or 110°, the moment of inertia as calculated by equation (60) was judged to be inaccurate based on current anthropometric literature. For these trials, instead of using equation (60), the moment of inertia was determined from the nonlinear regression equations of Yeadon and Morlock (1989).

From the results in Table 11 it can be seen that the variability was highest at the knee angle of 130°. On average, the damping coefficient reached a minimum at 90° of flexion, although some subjects (DS, RV, GK, and JC) reached a minimum at 45°. Figure 33 displays the mean damping function within the standard deviation envelope. The nonlinear, parabolic nature of the damping function is evident. It should be noted that the curves presented in Figure 33 are not mathematical curve fits but rather just smooth curves drawn through the data points using commercial graphics

Table 10. Percent differences between the initial time period and the mean time period of subsequent cycles for each of five knee angles.

	θ				
% Difference*	10°	45°	90°	110°	130°
Mean	27.170	26.940	22.677	24.106	43.808
S.D.	24.403	15.644	8.329	8.397	26.349
Maximum	115.242	71.616	45.726	41.794	101.446
Minimum	8.889	8.303	7.787	11.250	6.122
# of Cycles	202	202	195	175	97

* *% Difference* $= \frac{(\tau_1 - \tau)}{\tau} * 100$ where τ_1 is the time period for the initial cycle and τ is the mean time period of all subsequent cycles.

software (Harvard Graphics 3.0).

Variability of the oscillation parameters (τ and δ)

Tables 12 through 16 present the variability analysis for the oscillation parameters. Each table presents the mean coefficient of variation and other variability statistics for both types of variability of τ and δ at a specific knee angle. Also included, in the last two columns of each table, are the number of cycles analyzed and the correlation coefficient of the $\boldsymbol{ln(\phi)}$ versus time regression. At all knee angles the mean CV of the time period within trials was relatively constant at about 2-3%. The average CV of the time period across trials was <1% for all knee angles except 130° (1.201%). The variability in the logarithmic decrement was somewhat larger but still considered acceptable for an approximation technique. Within trials the mean CV of

Table 11. Average values of the angular damping coefficients of the human knee joint (in $N \cdot m \cdot s \cdot rad^{-1}$) at each of the five testing positions.

	θ				
Subject	**10°**	**45°**	**90°**	**110°**	**130°**
DS	0.919	0.666	0.741	0.894	1.379
JF	1.739	1.308	1.224	1.329	3.880
AR	1.823	1.191	0.653	0.800	0.855
BG	2.088	1.274	1.150	1.215	2.504
EM	1.104	1.071	1.041	1.554	2.463
RC	1.112	0.646	0.567	0.624	0.888
RV	1.242	0.719	0.796	0.892	2.233
JB	1.001	0.908	0.674	0.885	1.062
BC	0.800	0.700	0.629	0.747	1.367
JT	1.148	0.823	0.712	0.986	2.350
GK	1.364	1.099	1.182	1.235	2.151
GW	1.170	0.836	0.759	1.006	1.384
PP	1.066	0.942	0.745	0.987	1.630
CH	0.986	0.915	0.730	0.868	1.983
FH	1.440	1.265	1.104	1.398	1.687
JC	1.369	1.110	1.140	1.448	1.956
YF	1.306	0.997	0.917	1.318	1.538
MEAN	1.275	0.969	0.868	1.070	1.842
S.D.	0.341	0.219	0.222	0.273	0.742
CV(%)	26.745	22.601	25.576	25.514	40.282

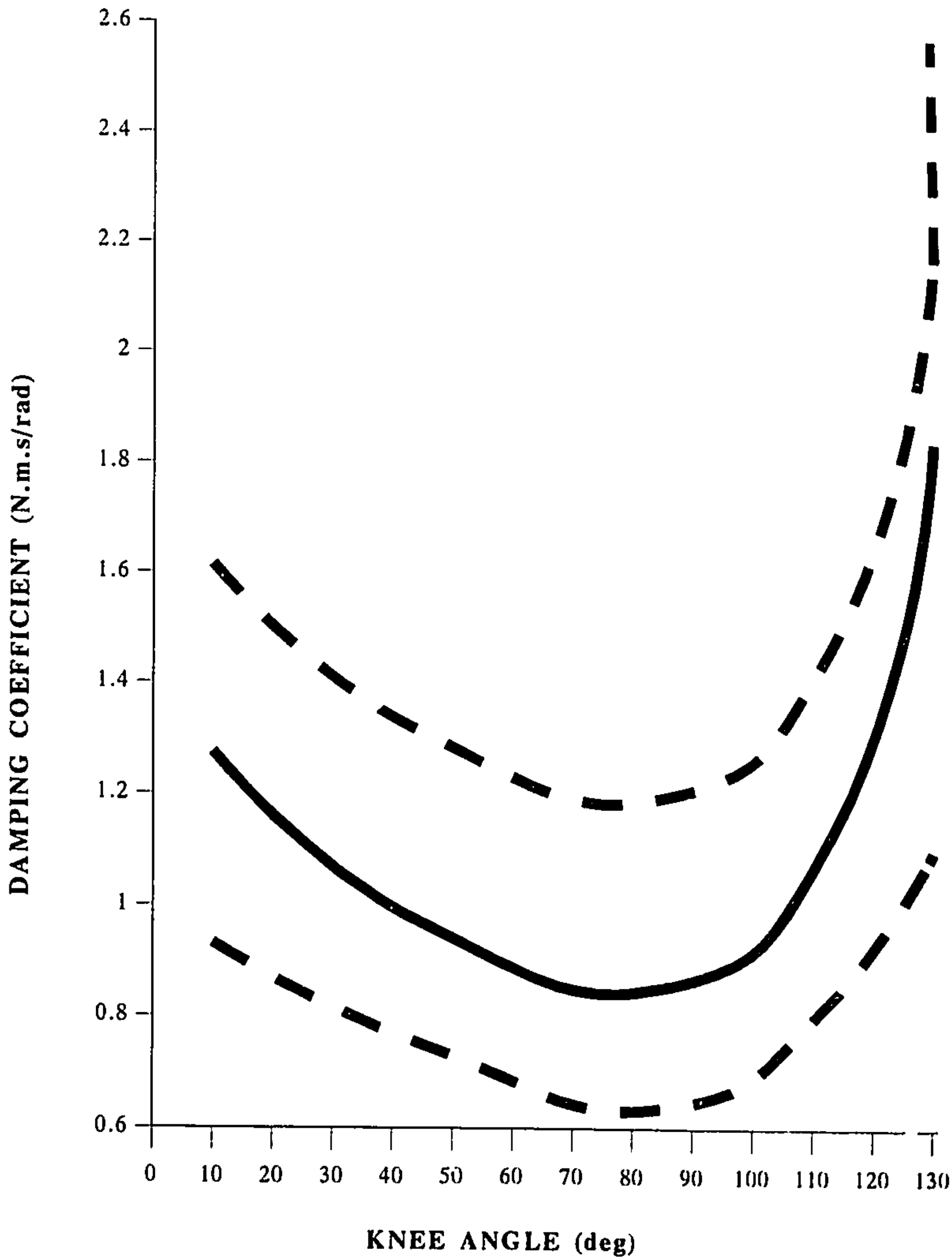

Figure 33. Variability in the angular damping coefficients as a function of knee angle. Solid line is the mean function while the upper and lower dotted lines are the ± 1 standard deviation envelope.

Table 12. The coefficient of variation (%) of τ and δ within and across trials at θ = 10°.

Statistic	τ - within	τ - across	δ - within	δ - across	Cycles	r
Mean	2.320	0.691	11.335	4.157	42.588	0.997
S.D.	1.070	0.402	3.570	3.455	10.100	0.001
CV(%)	46.118	58.197	31.498	83.116	24.285	0.141
Maximum	5.207	1.697	16.256	15.681	58.000	0.999
Minimum	0.695	0.118	5.047	1.636	21.000	0.994

Table 13. The coefficient of variation (%) of τ and δ within and across trials at θ = 45°.

Statistic	τ - within	τ - across	δ - within	δ - across	Cycles	r
Mean	2.316	0.705	13.370	3.778	48.941	0.996
S.D.	0.991	0.359	4.412	1.962	11.054	0.002
CV(%)	42.771	50.908	32.998	51.932	22.586	0.191
Maximum	4.570	1.382	19.013	7.279	66.000	0.999
Minimum	0.853	0.266	4.940	0.724	26.000	0.993

Table 14. The coefficient of variation (%) of τ and δ within and across trials at θ = 90°.

Statistic	τ - within	τ - across	δ - within	δ - across	Cycles	r
Mean	2.068	0.501	16.872	4.780	43.706	0.994
S.D.	0.819	0.348	5.249	2.442	9.961	0.003
CV(%)	39.616	69.550	31.113	51.081	22.791	0.342
Maximum	3.316	1.427	25.930	9.981	56.000	0.999
Minimum	0.838	0.089	7.813	0.768	26.000	0.987

Table 15. The coefficient of variation (%) of τ and δ within and across trials at $\theta = 110^{o}$.

Statistic	τ - within	τ - across	δ - within	δ - across	Cycles	r
Mean	2.650	0.610	16.313	4.288	39.471	0.994
S.D.	0.961	0.341	4.433	1.450	10.001	0.003
CV(%)	36.261	55.964	27.174	33.824	25.337	0.302
Maximum	4.112	1.459	23.454	6.856	52.000	0.999
Minimum	1.016	0.173	7.745	2.061	19.000	0.989

Table 16. The coefficient of variation (%) of τ and δ within and across trials at $\theta = 130^{o}$.

Statistic	τ - within	τ - across	δ - within	δ - across	Cycles	r
Mean	3.088	1.201	11.942	7.504	28.000	0.997
S.D.	1.240	0.706	2.725	5.409	8.937	0.002
CV(%)	40.144	58.805	22.819	72.084	31.919	0.158
Maximum	4.998	2.948	16.435	19.561	43.000	0.999
Minimum	1.041	0.337	7.991	1.988	14.000	0.993

δ ranged from about 11% to 17% over the five knee angles while across trials the values were approximately in the 4-8% range. The exponential decay model was valid as evidenced by the high **r** values.

Table 17 presents the results of the analysis of variance and post-hoc analysis on the data of Tables 12 through 16. A significant *F*-ratio indicated that there existed a knee angle effect. The post-hoc analysis indicated exactly where these differences were located.

Table 17. ANOVA and Newman-Keuls results for the oscillation parameter variability analysis.

Type of mean	F - ratio	Post-hoc analysis (α = 0.05)
τ - within	2.51*	90° ≠ 130°
τ - across	6.01*	10° = 45° = 90° = 110° ≠ 130°
δ - within	6.20*	10° = 45° = 130° ≠ 90° = 110°
δ - across	3.59*	10° = 45° = 90° = 110° ≠ 130°

* Significant at α = 0.05

For both τ-across and δ-across the variability was significantly higher at $\theta = 130°$ than at the other four knee angles. Within trials, only the variability of the time period at 90° was different from that at 130°; all other means were statistically equal. For the logarithmic decrement two clusters of means were statistically different: 10°, 45°, 130° and 90°, 110°.

STATISTICAL ANALYSIS

Overall, 24 separate regression analysis were run: normal and robust linear regression at seven different knee angles for the elastic component and five for the damping coefficient. The following sections present the prediction equations which were generated from this analysis.

Elastic component

Tables 18 and 19 present the prediction equations developed to predict the net passive elastic joint moment using normal MLR and robust regression, respectively. Each table also includes the R^2-statistic and the RMS error. At knee angles of 0°, 10°, 45°, 130°, and 140° between 72.5% and 84.4% of the variation in the passive moment could be accounted for by the anthropometric parameters. Predictability was not quite as good at knee angles of 90° and 110°, with only 48.2% to 51.1% of the variance being accounted for. The robust regression analysis increased all R^2 values and decreased all RMSE values. At knee angles of 0°, 10°, 45°, 130°, and 140° the robust equations allowed between 86.6% and 97.7% of the variation in the passive moments to be accounted for by the anthropometric parameters. At 90° and 110°, between 50.1% and 73.4% of the variance could be accounted for by the independent variables.

Stability of the regression coefficients

For the coefficients presented in Table 18, on average, the probability of any estimate of β_o being equal to zero was 3.414% (S.D.=3.415, range=0.2-10.3) while the chance of any of the other estimates ($\hat{\beta}_1$, $\hat{\beta}_2$, $\hat{\beta}_3$) being equal to zero was 3.360% (S.D.=1.71, range=1.90-6.70). For the coefficients in Table 19 the corresponding probabilities were 2.486% (S.D.=3.144, range=0.1-8.8) for β_o and 2.390% (S.D.=2.295, range=0.03-5.63) for the other estimates.

Angular damping coefficient

Overall, predictability was not quite as good as it was for the elastic component. Tables 20 and 21 present the normal and robust regression results. At 10° and 45° only 25.8% and 30.0%, respectively, of the variation in the damping coefficients could be accounted for by the anthropometric parameters. At knee angles of 90°, 110°, and 130° between 51.7% and 96.0% of the variation could be accounted for. The robust analysis significantly increased the R^2 values of a number of equations. Overall, 42.6% to 95.7% of the variation in the damping coefficients could be accounted for by the independent variables.

Stability of the regression coefficients

For the coefficients presented in Table 20, on average, the probability of any estimate of β_o being equal to zero was 3.920% (S.D.=5.417, range=0.100-12.100) while the chance of any of the other parameter estimates being equal to zero was 1.840% (S.D.=1.710, range=0.000-3.700). The corresponding values for Table 21 were 2.420% for β_o (S.D.=1.639, range=0.000-4.300) and 2.044% (S.D.=2.110, range=0.500-5.050) for the other betas'.

Table 18. Regression equations for predicting the net passive elastic joint moments from anthropometric parameters* at each of seven different knee angles. Passive moments are in N·m; W is in kg; all other measures are in cm.

REGRESSION EQUATION	R^2	RMSE (N·m)
$M_e(0°)$ = 13.278 - 0.684 * W + 1.936 * LTD + 0.015 * KB^3	0.725	2.637
$M_e(10°)$ = 15.929 - 0.462 * W + 0.162 E-01 * LTCSA + 0.105 E-01 * KB^3	0.844	1.383
$M_e(45°)$ = 9.416 + 0.370 * LTB - 1.422 * CD + 0.242 E-02 * KB^3	0.739	0.635
$M_e(90°)$ = 13.187 - 0.294 * CL - 0.412 E-04 * KC^3	0.482	0.917
$M_e(110°)$ = 32.746 - 0.135 * H - 1.147 * KB	0.511	1.880
$M_e(130°)$ = -34.551 - 0.600 * W + 1.571 * UTC - 0.144 E-01 * KB^3	0.828	4.054
$M_e(140°)$ = -96.208 - 6.816 * GFD + 5.303 * MC - 0.404 E-01 * KB^3	0.8[illegible]9	8.349

* Complete descriptions of these parameters are given in Appendix C. The ranges of the parameters over which the equations are valid are presented in Table D1 (Appendix D).

Table 19. Robust regression equations for predicting the net passive elastic joint moments from anthropometric parameters* at each of seven different knee angles. Passive moments are in N•m; W is in kg; all other measures are in cm.

ROBUST REGRESSION EQUATION	R^2	RMSE (N•m)
$M_e(0^\circ)=10.403 - 0.206 * W + 0.010 * KB^3$	0.866	1.553
$M_e(10^\circ)=25.086 - 2.625 * KD + 0.888\ E\text{-}02 * KB^3$	0.876	1.103
$M_e(45^\circ)=8.991 + 0.566 * GFD - 0.670 * LTC + 0.185\ E\text{-}01 * LTCSA$	0.944	0.292
$M_e(90^\circ)=13.527 - 0.299 * CL - 0.423\ E\text{-}04 * KC^3$	0.501	0.776
$M_e(110^\circ)=30.625 - 0.122 * H - 2.320 * KB + 0.308 * LTC$	0.734	1.212
$M_e(130^\circ)=-39.429 - 0.649 * MC + 0.125 * (KC * KB) - 0.377\ E\text{-}01 * KB^3$	0.977	1.951
$M_e(140^\circ)=-86.271 - 8.248 * GFD + 5.624 * MC - 0.402\ E\text{-}01 * KB^3$	0.950	4.365

* Complete descriptions of these parameters are given in Appendix C. The ranges of the parameters over which the equations are valid are presented in Table D1 (Appendix D).

Table 20. Regression equations for predicting the angular damping coefficients from anthropometric parameters* at each of five different knee angles. Damping coefficients are in N•m•s•rad^{-1}; W is in kg; all other dimensions are in cm.

REGRESSION EQUATION	R^2	RMSE (N•m•s /rad)
$C_k(10^\circ)=0.777 + 0.310\ E\text{-}03 * KB^3$	0.258	0.303
$C_k(45^\circ)=0.624 + 0.215\ E\text{-}03 * KB^3$	0.300	0.190
$C_k(90^\circ)=-0.569 + 0.101 * LTD$	0.624	0.141
$C_k(110^\circ)=0.319 + 0.128\ E\text{-}02 * LTCSA$	0.517	0.196
$C_k(130^\circ)=-4.451 + 0.255\ E\text{-}01 * W - 0.598 * MTD + 0.161 * (MTC+CC)$	0.960	0.166

* Complete descriptions of these parameters are given in Appendix C. The ranges of the parameters over which the equations are valid are presented in Table D1 (Appendix D).

Table 21. Robust regression equations for predicting the angular damping coefficients from anthropometric parameters* at each of five different knee angles. Damping coefficients are in N•m•s•rad^{-1}; W is in kg; all other measures are in cm.

ROBUST REGRESSION EQUATION	R^2	RMSE (N•m •s/rad)
$C_k(10°)=-2.916 + 0.347 * CD$	0.609	0.240
$C_k(45°)=3.202 - 0.416 * LTB + 0.539\ E\text{-}02 * LTCSA$	0.426	0.150
$C_k(90°)=-1.462 + 0.275 * KD + 0.152\ E\text{-}02 * LTCSA - 0.141\ E\text{-}02 * KC^2$	0.945	0.070
$C_k(110°)=0.950 - 0.222\ E\text{-}01 * W + 0.314\ E\text{-}02 * LTCSA$	0.622	0.163
$C_k(130°)=-4.298 + 0.339 * AB - 0.737 * MTD + 0.233 * (MTC + CC)$	0.957	0.134

* Complete descriptions of these parameters are given in Appendix C. The ranges of the parameters over which the equations are valid are presented in Table D1 (Appendix D).

CHAPTER V

DISCUSSION AND CONCLUSIONS

The biomechanical literature is decidedly lacking in a statistical database of the passive viscoelastic properties of the *in vivo* human knee joint during full range flexion-extension. The present investigation has to some degree filled this gap by determining the passive elastic moment and the angular damping coefficient of the knee joint of a specific subpopulation along with providing a set of regression equations which allows for the prediction of the passive properties at a number of different knee angles over a fairly wide range of subject anthropometry.

The following discussion is structured similarly to previous chapters. The first two main sections deal with the important results of the elastic and viscous components, respectively. The third section discusses the statistical results while the following section considers the significance of the experimental results through an example: the potential contribution of the passive tissues to the net joint moment during the swing phase of walking. The final section presents an overall summary and conclusions.

THE NET PASSIVE ELASTIC JOINT MOMENT

This section provides a detailed discussion of some of the important aspects of the results of the elastic component including muscle activity, curve fitting, and variability.

Muscle tone and myotatic reflex activity

Even though an individual is relaxed and no raw EMG signal is evident, a certain amount of tautness usually remains. This small amount of residual muscle contraction is referred to as muscle tone and results entirely from nerve impulses originating in the spinal cord (Guyton, 1986). Only when the posterior roots are cut or the subject is under anesthesia do the muscles become completely flaccid. Therefore, in reality there exists essentially two levels of base line passiveness: with and without muscle tone.

This phenomenon may have been illustrated in part by the results of Smith (1957) which were discussed in chapter II of this document (Figure 3). Measurements were made with the subjects under anesthesia prior to unrelated surgery. At 10° of hyperextension (i.e., θ = -10°) only 8.16 N•m was obtained while at full extension (0°) the moment was 2.27 N•m: significantly lower than any other literature values including all data in the present investigation. It must be kept in mind, however, that the data of Smith (1957) was not based on a reasonable sample size (n=3) and was therefore not proof that a larger sample would yield the same results.

It was also anticipated that myotatic reflex activity may be elicited by the motion and therefore contaminate the measurement. The higher the rate of change of length of the muscle the more the possibility of eliciting a strong dynamic stretch reflex (Guyton, 1986). Bierman and Ralston (1965) tested the effects of different rates of passive rotation on the EMG signal of the RF and LBF muscles of 16 subjects between the ages of 16 and 28 years. The leg was rotated at velocities of 0.837, 1.950, 3.072, and 4.189 rad•s^{-1} from 0° to 120° of flexion. Overall, no detectable EMG activity was present for all subjects although some required an initial training period to achieve relaxation. The angular velocities used by Bierman and Ralston (1965) study were between 3.5 and 18 times faster than the average velocity used in the present investigation (0.237 $rad \cdot s^{-1}$). As can be seen from Figures 19 and 20 (which are typical) the EMG activity is minimal and small contractions produce a clear disturbance in the strain gauge output. Due to the weaker static component of the myotatic reflex (Guyton, 1986), reflex activity is probably never totally eliminated but presumably represents a very small percentage of the resistive moment as compared to the actual elastic moment. Therefore one can be confident that the measurements made in the present investigation were essentially those of a completely relaxed yet alert subject and were basically passive in nature.

Angular velocity

The average angular velocity used in the present investigation was 0.237 $rad \cdot s^{-1}$; this value is well within the current accepted range (0.017 to 1.62 $rad \cdot s^{-1}$). From the potentiometer signals in Figures 19 and 20, it can be seen that the output was approximately linear until the joint limits were approached, after which point the velocity decreased to zero. Thus, for most of the movement the acceleration was close to zero. Although the leg negatively accelerated during the final phase, the absolute value was small enough that inertial moments were negligible. Therefore, it is unlikely that the measurements were contaminated with viscous or inertial components.

Curve fitting

Overall, the extension and flexion phases were very well modelled as simple exponential functions while the midrange phase was adequately described with a linear function. Although the individual curve fits were quite good, with some subjects considerable variation existed across the five trials. This was most pronounced during flexion (Table 4) where the coefficient of variation (CV) went as high as 82.979% (subject BG) for a_3. Conversely, for the same coefficient, four subjects (DS, GK, GW, CH) had a CV=0% (at three decimal places) across the five trials. Since the variability appeared to be subject specific it was hypothesized that the CV may correlate with various anthropometric parameters and/or the absolute magnitudes of the passive moments at the extremes of motion. A correlation analysis, however, dismissed this theory. The variation across trials with some subjects may have been due to positioning discrepancies. Although every attempt was made to maintain the subject in the same position between trials, a number of subjects required repositioning while some subjects became restless and may have shifted slightly causing a misalignment of the knee\HKA centres of rotation. Although apparently no data is available for the knee, Vrahas et al., (1990) found that for the hip joint misalignment of the centre of rotation caused up to a 25% (with respect to the maximum moment) change in the measured moment. Another potential source of variation was stress relaxation effects. The position of the knee joint in between trials was not controlled: some subjects flexed and extended the leg while others maintained a specific angle. To the authors knowledge no data is available for the knee joint, but it has been shown for the ankle and metacarpophalangeal joints that if the joint is fixed at a specific angle the moment will decline exponentially over time to a stable value due to the time dependent viscoelastic properties of the passive tissues. The degree of decline depends on the initial angle and the joint. Toft et al., (1989) found a 10% decline in moment after 30 seconds and a 23% decline after five minutes for the ankle in extreme dorsiflexion. Wright and Johns (1961) found a 35% decrease in moment after two minutes for the MCP joint. Thus the moment measured during a given trial will depend to some degree on the recent kinematic history of the joint. These two factors may have contributed to the high across trial variability observed for some subjects.

Comparison to the previous literature values

In general, the data of the present investigation was of lower magnitude compared to the results reported in previous studies. This was especially evident when comparing the NPEJM at full extension ($\theta=0°$) to the values reported in three of the small sample investigations. Hatze (1975a; n=1) measured 35 N•m at full extension while Mansour and Audu (1986; n=4) and Engin (1985; n=3) reported 60 N•m and 66 N•m, respectively. These moments were significantly higher (> 5 S.D.) than the mean value obtained in the present study (11.399 N•m) and even the maximum moment obtained (22.460 N•m). If it is assumed that there were no errors in the data collection process (i.e., transducer error, muscle activity, inertia, etc.) then two factors may explain the discrepancies. The first factor involves the length of the biarticular muscles. To directly compare the data from two studies the hip and ankle angles must be the same. Large hip angles (i.e., flexed) will lengthen the LBF, ST, and SM thereby potentially increasing (depending on the knee and ankle angles) their passive flexion moment capability while at the same time potentially decreasing the passive extension moment capability of the RF and SR. Regression equations generated by Hawkins and Hull (1990) indicate that the hamstrings are the longest when the knee is fully extended and the hip is at 120° of flexion. Similarly, dorsiflexion at the ankle will stretch the GA and potentially increase its passive flexion moment capability. The hip and ankle angles used in the Engin (1985) study were not stated explicitly but from the photographs and schematics it appears that they were the same as those used in the present study, i.e., $\theta_H=90°$ and $\theta_A=0°$. The data of Hatze (1975a) was stated to be independent of the length of the biarticular muscles since these effects were subtracted out. Thus the value of 35 N·m is probably a minimum value for that subject. Mansour and Audu (1986) collected data at a number of different hip and ankle angles. The value of 60 N·m at $\theta=0°$ was obtained while the hip was set at 12° and the ankle was in 10° of dorsiflexion. When the ankle was changed to 10° of plantarflexion the moment decreased to 40 N·m. According to the authors the moment in extension was independent of the hip angle for $0° < \theta_H < 20°$. Therefore, the flexion moment of 40 N·m was probably also a minimum value since an increase in hip angle and/or ankle angle will increase the magnitude of the passive flexion moment. These results lead to the conclusion that the second factor is the more important: The data of Engin (1985), Mansour and Audu (1986), and Hatze (1975a) were probably not representative of the population but were extreme cases (outliers). In comparing the results to some of the larger sample studies the results were more in line ($\leq \pm 2$ S.D.) with those observed presently. The data of Heerkins et al., (1985; n=29) was directly comparable to that of the present investigation since the same hip and ankle angles and approximately the same age range (20 to 33 years) were used. Between 10° and 110° the passive moments reported by Heerkins et al., (1985) were $< +2$ S.D. away from the mean values of the present study. Most of the passive moment data reported by Otahal (1971, n=26) were within ± 2 S.D. of the mean reported in this study. However, the hip joint was fixed at 0° and presumably if it was increased to 90° the flexion moments would be larger. Also, Otahal (1971) did not indicate the angle of the ankle joint. The only investigators to measure the passive moments at high flexion angles were Engin (1985) and Hatze (1975a). At 130° and 140° of flexion the mean values reported by Engin (1985) were comparable ($<$ 2 S.D. and $<$ 1 S.D. respectively) to those observed in this study while at 130° the data of Hatze (1975a) was $>$ 2 S.D. away from the mean reported here. As discussed previously, due to the anesthetized state of the subjects of Smith (1957), it was felt that these data were not directly comparable to the present results.

Magnitudes and variability of the measured passive elastic moments

From the results of the present investigation it is evident that the potential exists for both significant passive elastic moments and a large variability as the extremes of joint motion are approached. Researchers attempting to predict the force contribution or the mechanical work and power of individual muscles to a specific movement (e.g., Dowling, 1988; Pierrynowski, 1982) have traditionally assumed that the contribution of the passive tissues was insignificant. Based on the results of this study, depending on the subject and the knee angle this assumption may or may not be justified. In the midrange of joint motion it is safe to assume that the passive elastic moments are negligible for modelling purposes since all moments recorded in this study were < 5 N·m (for $55^{\circ}<\theta<95^{\circ}$). As the mechanical limits were approached the passive moments increased dramatically; however, for some subjects, although the increase was very rapid, the absolute magnitudes finally reached were relatively low. For example, subject CH exhibited only 6.756 N·m at full extension and -6.398 N·m at 140°. Depending on the movement being modelled some investigators may take these values to be negligible. Conversely, subject JF exhibited 22.460 N·m at 0° and -86.141 N·m at 140°. These values are certainly not negligible, especially for movements which require relatively small net joint moments such as during the swing phase of walking, and their omission may cause significant errors in the force or work predictions of a model (depending on the models' purpose).

Figures 24 and 25 indicate that the variability increases as the extremes of joint motion are reached. In the case of flexion, the standard deviation envelope actually diverges. Part of this may be due to the fact that with certain measurements the standard deviation increases (linearly or nonlinearly) as the mean increases (Pheasant, 1986). However, the increase in variability at the joint limits was probably also due to the fact that in the midrange of joint motion the tissues were not strained to a significant degree and thus the joint behaved similarly across subjects; but as the joint entered into the terminal phases the tissue strain increased and the inter-individual differences in stiffness became more apparent.

There are a number of reasons for the large degree of variability across subjects. The primary factor was the anthropometry of the subjects. As indicated in Tables 18 and 19, depending on the knee angle, various anthropometric dimensions could account for 48% to 98% of the variation in the passive elastic moments. However, the size of the subject did not always correlate with the magnitude of the passive elastic moments. For example, subject AR (mass=62.8 kg; knee breadth= 11.2 cm; midthigh circumference=50.0 cm; calf circumference=35.5 cm) exhibited 19.720 N•m at $\theta=0^{\circ}$ while the much larger subject EM (mass=98.1 kg; knee breadth=12.9 cm; midthigh circumference=68.5 cm; calf circumference=42.0 cm) displayed only 12.417 N•m at full extension. Therefore, not only was the absolute size of the subject important, but also the constitutive behaviour of the individual tissues which were creating the passive elastic moment. The constitutive behaviour of a tissue will be partly a function of the subjects exercise/sports history. Subject AR indicated in one of the questionnaires in Appendix A that his hamstrings were extremely tight. A number of examples illustrate the importance of inter-individual differences and the influence of a subjects athletic\exercise history. The two largest subjects, EM and JF (mass=109.0 kg; knee breadth=14.8 cm; midthigh circumference=64.5 cm; calf circumference=45.5 cm), would be expected to display similar magnitudes of the passive moments. However, inspection of the data indicates otherwise. At full extension subject JF displayed almost twice as much passive elastic resistance as subject EM (22.460 N$\cdot$m versus 12.417 N$\cdot$m). The discrepancy was even more pronounced at 140° of flexion. Subject JF exhibited -86.141 N$\cdot$m while subject EM exhibited only -15.020 N$\cdot$m. Inspection of the responses in the questionnaires and discussion with the subjects revealed that subject JF had been quite sedentary in the past year while subject EM was a competitive powerlifter and was training six days per week for the past three years. Part of subject EMs training included performing full squats with up to about 180 kg. Given this information it seems logical that the passive resistive moments would be low at high flexion angles for this subject since deep squatting with this amount of weight would render the tissues more compliant over time. The comparison between subjects JF and EM also leads to another point. Initially it was hypothesized that apposition of the posterior calf and thigh would cause a significant portion of the NPEJM at the limits of flexion and thus subjects with large calf and thigh circumferences would exhibit higher moments in flexion. However, the results of JF and EM seem to contradict this and indicate that the moments are mostly due to the stiffness of the tissues surrounding the knee. Subject CH displayed very low moments (<7 N$\cdot$m from 0° to 140°) and although he was one of the smallest subjects he also participated in martial arts which incorporates extensive flexibility training. Toft et al., (1989) has reported that a regimen of stretching lowers the magnitude of the passive elastic moment in the ankle at full dorsiflexion.

The soft joint stops

The position of the soft stops are sensitive to the criteria used to determine them. However, regardless of the criteria, the soft stops will be a function of the relative difference between the midrange stiffness and either the terminal flexion or extension stiffness.

Although the variability in the magnitudes of the NPEJM was higher in flexion than in extension (Figures 24 and 25), the reverse was true with respect to the soft stops. In extension the mean location was 11.4° and the coefficient of variation was 41.4%. In flexion the mean soft stop was located at 123.3° with very little variation (CV=1.6%). Based on the definition used in this study the results indicate that for this sample of subjects the stiffness of the knee was more variable in extension than in flexion. As indicated previously the hamstrings are longest when the knee is extended and the hip is at 120° (Hawkins and Hull ,1990). Therefore, with the hip at 90° as in this study the hamstrings were approaching their maximum length and thus inter-individual differences in hamstring stiffness may have been more resolved. It should also be noted that the soft stop in extension may be due in part to the onset of force in the ACL (if it has a moment arm) since recent cadaver work has indicated that the ACL force rises rapidly at 10° (Markolf et al., 1990).

Soft stops may be used as rough guidelines for modellers deciding whether or not (or at which angles) to consider passive sources. If the movement being modelled is constrained to joint angles in between the soft stops then one may be justified in disregarding passive contributions. If, on the other hand, the movement requires joint angles which are beyond the soft stop locations the investigator may consider including passive sources.

Equilibrium angle

The mean equilibrium angle was found to be 64.5° (CV=13.4%). Interestingly, Heerkins et al., (1985) found almost exactly the same value and about the same level of variability (64.4°, CV=9.5%). The equilibrium angle is the knee angle at which the passive extension moments balance the passive flexion moments. It is not known whether this position has any clinical significance (Heerkins et al.,1985) but it may have potential as a predictor of injury.

Experimental difficulties

One of the drawbacks of a horizontal apparatus was that the subject was required to lie on his side which required that he maintain his pelvis approximately perpendicular to the top of the subject table. It was observed that if the subject was unable to do so, and the pelvis rotated slightly, a moment due to the shearing of the lateral aspect of the hip against the table would be transferred down to the knee. A number of subjects tended to have this problem and therefore repositioning was required after each trial.

THE ANGULAR DAMPING COEFFICIENT

The main results of the experiments on the damping properties of the knee will be discussed in the subsequent sections.

Muscle activity and myotatic reflex activity

As with the elastic component muscle activity was not a major problem (Figures 30 and 31). However, with the small oscillation technique an additional problem was anticipated. Due to the cyclic nature of the technique and the relatively higher frequency (as compared to the HKA) it was expected that stretch (myotatic) reflex activity may manifest itself as momentarily increased damping at the beginning of the oscillation due to the sudden change in muscle length. This problem was pointed out previously by Hatze (1975b), Hayes and Hatze (1977), and Engin (1984). They found that the damping was much higher during the first cycle compared to subsequent cycles. The same phenomenon was observed in this study as evidenced from the results in Table 10.

Validation tests

The results of the validation tests indicated that the SOA and associated hardware were very accurate and were able to obtain masses and moments of inertia of solid objects with an error not exceeding 3%. This level of accuracy was also reported by Peyton (1986) and Stijnen et al., (1983). However, the error is expected to increase with the introduction of a human segment due to non-rigidity and errors in the measured passive elastic moment.

Oversling tightness

From the results presented in Table 9 it is evident that a potential problem exists with the oversling. During pilot testing (with $\theta=10^{\circ}$) it could easily be observed that if the oversling was not present or too loose most of the damping was occurring at the hip and by compression of the proximal aspect of the posterior compartment on the seat. This situation arose because in this configuration ($\theta=10^{\circ}$ and $\theta_{11}=90^{\circ}$) the knee joint was the stiffest component in the system and, therefore, the more compliant sites responded first. The problem was not as apparent when testing the knee in the other four positions. On the other hand, if the oversling was too tight it squeezed the quadriceps tendon and increased the damping. Before the actual data collection a significant amount of time was taken to ensure that the oversling was optimally secured. The oversling was tightened incrementally just up to the point where motion at the knee predominated over movement at other sites. Therefore, it is expected that in the present experiment the oversling had a minimal influence on the measured damping coefficients.

The angular damping coefficient of the knee joint

The results of the present study (Table 11) are in general slightly lower but comparable to those reported by Hatze (1975a), although it is not clear which hip and ankle angles Hatze (1975a) used. For all knee angles except 90° and 110°, the damping coefficients presented by Hatze (1975a) were < ±2 S.D. away from the mean value obtained in the present investigation. At 90° and 110° the data of Hatze (1975a) was < 3 S.D. and > 3 S.D. respectively away from the mean reported here.

Although the average damping function was approximately parabolic in nature, a number of subjects displayed somewhat different trends. For eight of the subjects (AR, CH, FH, JB, PP, YF, BC, and EM) the damping coefficient was approximately a negative linear function of knee angle from 10° to 90°. Beyond 90°, the damping coefficient increased either linearly or nonlinearly to 130°.

The average parabolic nature of the damping function (Figure 33) was probably the result of two factors. First, as the extremes of joint motion were approached structures such as ligaments and the joint capsule were added and the damping was correspondingly increased. However, the increase in damping may also have been due to the fact that the viscosity is a function of the length of a tissue and therefore the properties of the ground substance change as the length of the tissue in which it resides changes.

The correlation between the size of the subject and the damping coefficient was not as strong compared to the elastic component (Tables 20 and 21). Similar to the elastic component, there were particular subjects who exhibited trends opposite to the general pattern. Subject AR (small subject, also an extreme case for the elastic component) displayed a very high damping coefficient at 10° after which point it rapidly decreased. Subject RC (mass=59.4 kg; knee breadth=10.1 cm; midthigh circumference=47.5 cm; calf circumference=33.0 cm) also had a relatively high damping coefficient at 10°. Conversely, subject EM (larger) displayed relatively low damping at $\theta=10^{\circ}$.

Overall, the variability (CV) in the angular damping coefficient was about the same ($\sim 25\%$) at all knee angles except 130° where $CV \approx 40\%$. The increase in variability as the flexion limits were approached may have been due to the fact that the viscous properties of the tissues were more apparent at high tissue strains and close packing of the joint.

Since the small oscillation technique is a linear approximation, the values of the damping coefficients presented in Table 11 probably represent the upper limits since at higher velocities the viscosity of the passive tissues decreases due to the non-Newtonian (thixotropic) nature of biological tissues and fluids (Fung, 1981). It is not known, however, at what value of angular velocity of the knee joint the viscosity would begin to behave nonlinearly; and even if a value of shearing rate was determined for a number of different tissues *in vitro*, these values would have to be translated into an angular velocity of the whole joint.

Comparison between the viscous and elastic components

A correlation analysis of the passive elastic moments versus the damping coefficient at each knee angle was performed. Interestingly, except for 130°, the correlations were not very high: r=0.552 (θ=10°); r=0.338 (θ=45°); r=-0.339 (θ=90°); r=-0.518 (θ=110°); and r=0.754 (θ=130°). Therefore, a maximum of 57% of the variance in one component could be accounted for by the other component. A high elastic moment does not necessarily indicate a high damping coefficient (and vice versa); in fact at 90° and 110° a negative correlation existed. These correlations indicate that possibly the damping properties are dependent on factors other than the size of the subject.

In comparing the angle-matched variabilities (CV) of the viscous and elastic components, an interesting trend appears. At 10° the variability in the elastic moment was about 50% while that of the damping was about 26%. Similarly for the other four knee angles: At 45° CV(elastic)=104%, CV(viscous)=23%; at 90° CV(elastic) =62%, CV(viscous)=25%; at 110° CV(elastic)=59%, CV(viscous)=25%; at 130° CV(elastic)=82%, CV(viscous)=40%. These results would tend to indicate that either the sample size was not large enough or perhaps the angular damping coefficient of the knee joint is an inherently less variable biomechanical parameter.

In comparing the magnitudes of the passive viscous and elastic moments it can be seen that, depending on the angular velocity and the knee angle, either the elastic component or the viscous component could predominate. For example, At 10° and with the leg rotating at an angular velocity of 5 rad•s^{-1}, subject JF would exhibit 15.59 N•m of elastic resistance and 8.695 N•m of viscous moment whereas subject BG would exhibit 6.102 N•m of passive elastic resistance and 10. 44 N•m of viscous resistance. In the literature, for the MCP joint, the elastic stiffness was found to predominate (Wright and Johns, 1960, 1961). The relative contributions of the viscous and elastic components during the late swing phase of walking will be discussed in a subsequent section.

Variability of the oscillation parameters (τ and δ)

One of the basic assumptions of the small oscillation technique is that the value of the logarithmic decrement (δ) is the same throughout the oscillation. This constancy of δ represents an ideal exponentially decaying system. Since the small oscillation technique was a linear approximation some level of error should be expected. This error is represented in the δ-*within* column of Tables 12 through 16. This error is a combination of inherent approximation error and measurement error. The error level (11%-17%) is considered acceptable for an approximation technique.

Experimental difficulties

For four subjects, at the knee angles of 10° and/or 110° , the moment of inertia as calculated by equation (60) was judged to be inaccurate based on the current anthropometric literature. Although it is known that the current anthropometric literature also includes error, the calculated values were unrealistic (i.e., 0.1 $kg \cdot m^2$ or 0.8 $kg \cdot m^2$). For these trials, instead of using equation (60) the moment of inertia was calculated using the nonlinear regression equations of Yeadon and Morlock (1989). A number of factors may explain the observed discrepancies. First, with the subject positioned in the small oscillation apparatus it often took up to 20 minutes before actual data collection began due to sling/oversling adjustments and other preliminaries. Therefore, the joint was effectively fixed at the particular joint angle (in this case 10° and 110°) for up to 20 minutes. During this time period the strained tissues underwent stress relaxation. Toft et al., (1989) found a ~25% reduction in moment after five minutes for the ankle joint while Wright and Johns (1961) observed a 35% reduction in moment at flexion of the MCP joint after two minutes. Since the elastic data was collected over a shorter period of time, the elastic stiffness value which was input into the small oscillation equations may not have been exactly the same value as that which was present during the oscillation testing. It is not surprising that this effect was observed at 10° and 110°, and not at 45° or 90°, since stress relaxation effects are more pronounced at extreme joint angles (Toft et al., 1989). Another factor which may have contributed to the discrepancy was the fact that for most subjects, due to equipment availability, the viscous and elastic components were tested up to 4.1 months (S.D.=0.55 months) apart. Since many subjects were active in exercise and sports, the constitutive properties of the tissues may have changed over the time period between sessions (Toft et al., 1989). Finally, for many subjects either the small oscillation data or the elastic data was collected in the early morning

(~7 AM) while the other component was tested in the late evening (on another day). Therefore, diurnal variations may have had some influence.

Since the small oscillation technique is also used as a method of determining the moment of inertia (Hatze, 1975b; Peyton, 1986; Stijnen et al., 1983) investigators should be aware of the sensitivity of the technique to the elastic stiffness and take the necessary precautions. Hatze (1975b) provides a mathematical criterion which can be used as a guide to find the optimal testing angle if the elastic moment function is not available.

As mentioned briefly in a previous section, due to positioning difficulties, the testing at 130° required changing the hip angle to 130°. The hamstrings are normally at their longest when the hip is flexed to 120° and the knee is fully extended (Hawkins and Hull, 1990). In this configuration the hip is highly flexed but this is somewhat offset by the flexed knee. Therefore, although the effects of the length of the biarticular muscles on the damping coefficient are not quite as clear as their effects on the elastic component, it is expected that the increased hip angle will increase the damping to some degree but since the knee is also highly flexed the effect may not be large. Therefore, the data points reported for $\vartheta = 130°$ are probably upper limits and are, strictly speaking, members of another family of the damping function.

STATISTICAL ANALYSIS

From Tables 18 through 21 it can be seen that the robust regression (RR) procedure significantly increased the R^2-statistic at almost all knee angles. For the elastic component, at full extension the RR significantly reduced the influence of outliers by assigning a zero weight to three subjects (AR, EM, and BG). At 130° seven subjects (YF, RV, JC, DS, GK, FH, and CH) were assigned a zero weight. For the damping coefficient, at 10° six subjects were zero weighted (AR,EM, JC, DS, FH, and GW). At 90° seven subjects were assigned a zero weight (BG, YF, DS, GW, BC, PP, and CH). The RR procedure not only reduced the influence of obvious outliers but also those data points which would probably not have been chosen if an informal inspection-based procedure had been used. It should also be noted that different subjects were outliers at different knee angles.

From Tables 18 and 19 (elastic component) it can be seen that predictability was not as good at 90° and 110° as at the other angles. Therefore, the anthropometric parameters were not sufficient predictors in the midrange and early flexion phase of joint motion. This may be due to the fact that since the tissues are not strained significantly at these angles the effects of anthropometry were reduced or were not detectable with the current sample size.

Overall, the damping coefficient was not as well predicted (compared to the elastic component) except at 90° and 130°. It appears that at some knee angles anthropometric parameters were not useful in predicting the damping properties. It may be that cross-sectional area is not as important as intrinsic rheological properties of the ground substance and synovial fluid.

It should be noted that larger R^2 values than those indicated in Tables 18 through 21 were obtained with the initial regression runs but had to be reduced to keep the coefficients stable.

It was expected that the normalized flexibility parameter, Trunk Forward Flexion (TF(NORM)) would be a significant predictor. However, it turned out that this parameter did not even make the first level of variable selection criteria ($r > 0.412$). In fact, the normalization procedure (equation (C1) in Appendix C) did not improve the correlation for the elastic component and actually reduced the correlation (from 0.271 to 0.199) for the damping component. The discrepancies may be due to the fact performance in the Trunk Forward Flexion is dependent on other factors such as lumbar flexibility, motivation, time of day, etc.

Improvements in the statistical analysis

For researchers to incorporate the data of the present investigation into their model the anthropometric data of their specific subject(s) would have to be input into the regression equations in Tables 19 and 21. The data points for each component (seven for the elastic and five for the damping) would then have to be fit to a mathematical function. If the knee angle were incorporated into the regression equations they would be more easily implemented into a biomechanical model. Incorporation of the knee angle as an independent variable may also increase the predictability of some of the equations. For angles in the flexion and extension phases the natural logarithm of the knee angle would be used ($ln[\theta]$) and for angles in the midrange phase, θ would be the predictor. Other useful predictors may be body fat content and, for theoretical purposes, possibly some invasive biochemical parameters.

THE POTENTIAL CONTRIBUTION OF THE PASSIVE TISSUES TO THE NET JOINT MOMENT DURING THE SWING PHASE OF WALKING

To judge the significance of the present experimental results, the data were applied to the swing phase of walking. In particular, the late swing phase (reach) was analyzed. During this portion of the movement, which is from about 72% to 100% of the stride period, the knee extends from about 65° to full extension while a flexor moment slows down the leg prior to impending heel contact. This movement was chosen for a number of reasons. First, there exist many studies in the literature which focus on this activity (Cavanagh and Gregor, 1975; Davy and Audu, 1987; Pierrynowski, 1982). Also, it was felt that the conditions during the swing phase of walking are close to those of the present experiment in the sense that the knee was unloaded and the net moments were relatively low. The angular velocities are also quite low which makes application of the linear damping model more appropriate.

The gait data included in Winter (1988) was used for the analysis. This data is normalized with respect to bodymass so it was easy to apply to any subject. Two subjects from the present study were analyzed: one who displayed large passive moments in extension (JF) and one who exhibited small moments (CH). The predicted net moment for each subject was determined by multiplying his bodymass by the normalized values given in Winter (1988). The curve fits given in Tables 3 and 5 were used for the elastic moments. The damping coefficients for subject JF (Table 11, excluding the data point for 130°) were fitted to a quadratic function (Spiegel, 1975) while the coefficients for subject CH (for 10°, 45°, and 90°) were fitted to a linear function. The damping coefficient was multiplied by the angular velocity (also taken from Winter (1988)) as in equation (3) to obtain the viscous moment. Since the hip was at 90° in the present study while in walking it is around 10-20°, the elastic moment data were scaled down by multiplying by 0.50 (Heerkins et al., 1985; Mansour and Audu, 1986). Since the effects of the biarticular muscles on the viscous component were not known the present data were not scaled. The effects of the ankle joint were not considered since, except for the early portion of the movement when the foot is slightly plantarflexed, the ankle is close to the neutral position.

The results of the analysis are presented in Figures 34 and 35. It is evident that the passive moments may significantly contribute to the net joint moment. For example, at 90% of stride, when the knee was at about 17°, for subject JF the total passive moment was 85% of the net joint moment while for subject CH the same value was 54%. Just before heel contact the total passive moment exhibited by subject JF was 45% of the net joint moment while the same value for subject CH was 19%.

Since the hamstrings are active (as evidenced by EMG, Winter, 1988) during the late swing phase it has been hypothesized that the function of the hamstrings is to produce the flexor moment which decelerates the leg. However, it can be seen that a significant portion of the net moment can be satisfied passively.

It must be kept in mind, however, that comparison of two different sources will involve some error. The subject JF, for example, may have been outside of the range (in terms of size) of the sample used by Winter (1988). Also, even if the subject displayed passive moments which were theoretically higher than the average

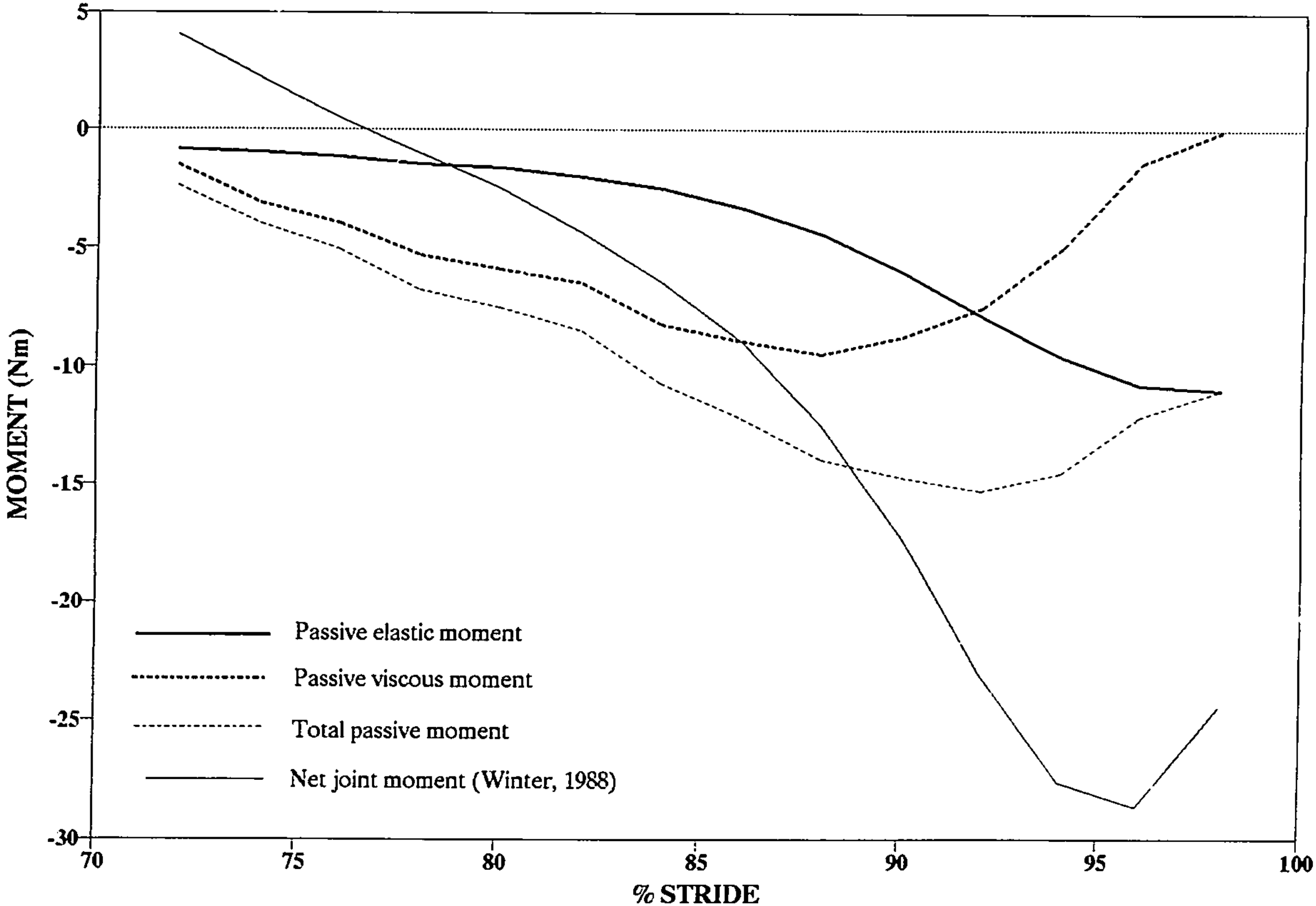

Figure 34. The potential contribution of the passive tissues to the net joint moment during the late swing phase of gait. Subject JF.

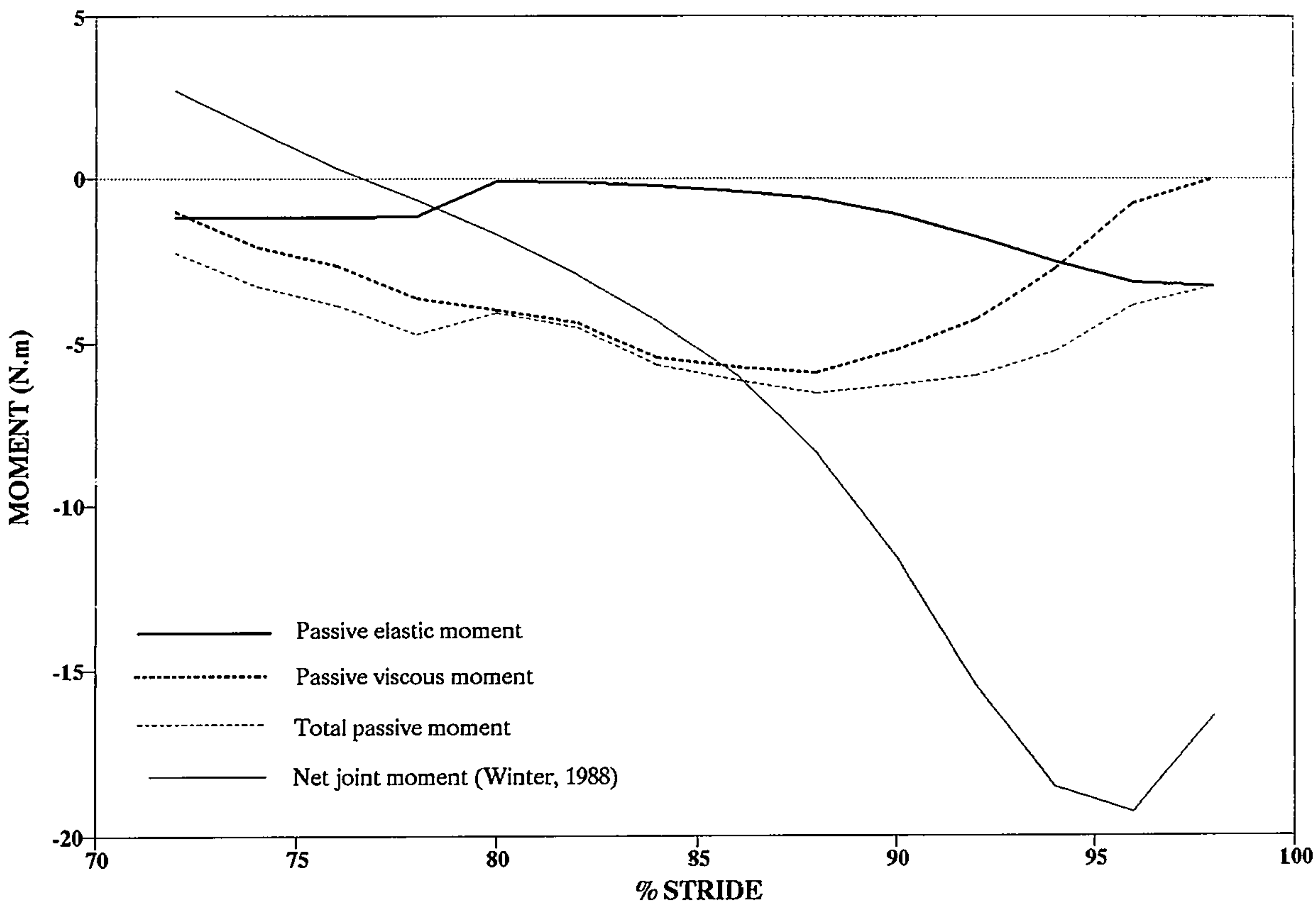

Figure 35. The potential contribution of the passive tissues to the net joint moment during the late swing phase of gait. Subject CH

net moment for walking (which was the case in Mansour and Audu (1986)), it is unlikely that the CNS would turn off the muscles completely since the joint must be stabilized for the impending heel contact. Van Ingen Schenau, Bobbert, and Rozendal (1987) and Van Soest, Schwab, Bobbert, and Van Ingen Schenau (1993) have indicated that the human system is designed so that muscle activity protects the passive structures from excessive loading (anatomical constraint). Therefore, more work is needed to determine the role played by the passive tissues in specific movements. It was also observed that early in the movement (around 70%-75% of stride) the passive moments oppose the net joint moment and the muscles would have to overcome this resistance

CONCLUSIONS AND RECOMMENDATIONS

In conclusion, the results of the present investigation reveal that the moments produced by the passive tissues may be significant depending on the subject and the joint angle. Modellers attempting to predict individual muscle forces or powers may be wise to consider the passive moments, especially when analyzing a movement at the extremes of joint motion or relatively fast movements.

Since the passive moments about the knee are dependent on a number of parameters including the population (age, gender, pathology, etc.) the lengths of the biarticular muscles, and the degree of loading of the knee, it is recommended that further research be done to obtain data in order to fill these gaps.

REFERENCES

Abrahams, M. (1967). Mechanical behaviour of tendon *in vitro*. Medical and Biological Engineering, 5, 433-443.

Adams, M.A., Dolan, P., and Hutton, W.C. (1987). Diurnal variations in the stresses on the lumbar spine. Spine, 12(2), 130-137.

An, K.N., Kaufman, K.R., and Chao, E.Y.S. (1989). Physiological considerations of muscle force through the elbow joint. Journal of Biomechanics, 22(11/12), 1249-1256.

Analog Devices. (1988). Linear products databook (11-45 - 11-52). Toronto: Analog Devices, Inc.

Andriacchi, T.P., Mikosz, R.P., Hampton, S.J., and Galante, J.O. (1983). Model studies of the stiffness characteristics of the human knee joint. Journal of Biomechanics, 16(1), 23-29.

Audu, M.L., and Davy, D.T. (1985). The influence of muscle model complexity in musculoskeletal motion modelling. Journal of Biomechanical Engineering, 107, 147-157.

Barter, J.T., Emanuel, I., and Truett, B. (1957). A statistical evaluation of joint range data (WADC-TR-57-311). Ohio: Wright-Patterson Airforce Base.

Bartz, J.A. (1972). Development and validation of a computer simulation of a crash victim in three dimensions. Proceedings of the 16th Stapp Car Crash Conference, 105-127.

Beckwith, T.G., and Marangoni, R.D. (1990). Mechanical measurements (4th ed.). New York: Addison-Wesley Publishing Company.

Berme, N., Engin, A.E., and Correia da Silva, K.M. (Eds.). (1985). Biomechanics of normal and pathological human articulating joints. Dordrecht: Martinus Nijhoff Publishers.

Beyer, W.H. (1984). CRC standard mathematical tables (27th ed.). Florida: CRC Press.

Bierman, W., and Ralston, H.J. (1965). Electromyographic study during passive and active flexion and extension of the knee of the normal human subject. Archives of Physical Medicine and Rehabilitation, 46, 71-75.

Binkley, J. (1989). Overview of ligament and tendon structure and mechanics: implications for clinical practice. Physiotherapy Canada, 41(1), 24-30.

Blacharski, P.A., Somerset, J.H., and Murray, D.G. (1975). A three dimensional study of the kinematics of the human knee. Journal of Biomechanics, 8, 375-384.

Blankevoort, L., Huiskes, R., and de Lange, A. (1988). The envelope of passive knee joint motion. Journal of Biomechanics, 21(9), 705-720.

Boon, K.L., Hof, A.L., and Wallinga-de Jonge, W. (1973). The mechanical behaviour of the passive arm. In S. Cerquiglini et al., (Eds.), Biomechanics III: Medicine and sport (Vol. 8, pp. 243-248). New York: Basel, Karger.

Brantigan, O.C., and Voshell, A.F. (1941). The mechanics of the ligaments and menisci of the knee joint. Journal of Bone and Joint Surgery, 23A, 44-66.

Braune, W., and Fischer, O. (1889). The center of gravity of the human body as related to the German infantrymen (ATI 138). U.S.: National Technical Information (NTI) Office.

Bresler, B., and Frankel, J.P. (1950). The forces and moments in the leg during level walking. Transactions of the American Society of Mechanical Engineers, 72, 27-36.

Butler, D.L., Noyes, F.R., and Grood, E.S. (1980). Ligamentous restraint to anterior-posterior drawer in the human knee. Journal of Bone and Joint Surgery, 62A, 259-270.

Canada Fitness Survey (1982). Canada's Fitness: Preliminary Findings of the 1981 Survey. Ottawa: Canada Fitness Survey.

Canadian Standardized Test of Fitness (1987). Canadian Standardized Test of Fitness: Operations Manual (FAS7378, 3rd ed.). Ottawa: Government of Canada, Fitness and Amateur Sport.

Carlstedt, C.A., Madsen, K., and Wredmark, T. (1986a). The influence of indomethacin on collagen synthesis during tendon healing in the rabbit. Prostaglandins, 32, 353-358.

Carlstedt, C.A., Madsen, K., and Wredmark, T. (1986b). The influence of indomethacin on tendon healing. A biomechanical and biochemical study. Archives of Orthopaedic and Trauma Surgery, 105, 332-336.

Cavanagh, P.R., and Gregor, R.J. (1975). Knee joint torque during the swing phase of normal treadmill walking. Journal of Biomechanics, 8, 337-344.

Chandler, R.F., Clauser, C.E., McConville, J.T., Reynolds, H.M., and Young, J.W. (1975). Investigation of the inertial properties of the human body (Contract No. DOT HS-801-430). Washington, D.C.: U.S. department of Transportation, National Highway Traffic Safety Administration.

Chandler, G.N., Wright, V., and Hartfall, S.J. (1958). Intra-articular therapy in rheumatoid arthritis, comparison of Hydrocortisone Tertiary Butyl Acetate and Hydrocortisone Acetate. Lancet, 2, 659.

Cichowski, W.G. (1968). A third generation test dummy "sophisticated sam". Proceedings of the General Motors Automotive Safety Seminar. Michigan: GM Proving Ground.

Clauser, C.E., McConville, J.T., and Young, J.W. (1969). Weight, volume, and center of mass of segments of the human body (Report No. AMRL-TR-69-70). Ohio: Wright-Patterson Airforce Base, Aerospace Medical Research Laboratory.

Crowninshield, R., Pope, M.H., Johnson, R., and Miller, R. (1976). The impedance of the human knee. Journal of Biomechanics, 9, 529-535.

Davy, D.T., and Audu, M.L. (1987). A dynamic optimization technique for predicting muscle forces in the swing phase of gait. Journal of Biomechanics, 20(2), 187-201.

De Avila, G.A., O'Connor, B.L., Visco, D.M., and Sisk, T.D. (1989). The mechanoreceptor innervation of the fibular collateral ligament. Journal of Anatomy, 162, 1-7.

Delagi, E.F., Perotto, A., Iazzetti, J., and Morrison, D. (1975). Anatomic guide for the electromyographer: The Limbs. Illinois: Charles C. Thomas Publisher.

Dempster, W.T. (1955). Space requirements of the seated operator (WADC-TR-55-159). Ohio: Aerospace Medical Research Laboratory.

Diamant, J., Keller, A., Baer, E., Litt, M., and Arridge, R.G.C. (1972). Collagen: ultrastructure and its relations to mechanical properties as a function of aging. Proceedings of the Royal Society London (Biology), 180, 293-315.

Dowling, J.J. (1987). The prediction of force in individual muscles crossing the human elbow joint. Unpublished doctoral dissertation, University of Waterloo, Waterloo, Ontario.

Dowling, J.J. (1988). Comparison of muscular and segmental work estimates during dynamic elbow movements. Proceedings of the Fifth Biennial Conference and Symposium of the Canadian Society for Biomechanics (pp. 56-57), C.E. Cotton, M. Lamontagne, D.G.E. Robertson, and J.P. Stothart (Eds.), University of Ottawa, Canada.

Edwards, R.G., Lafferty, J.F., and Lange, K.O. (1970). Ligament strain in the human knee joint. Journal of Basic Engineering, March.

Elliot, D.H. (1965). Structure and function of mammalian tendon. Biological Reviews, 40, 392.

Engin, A.E. (1984). On the damping properties of the shoulder complex. Journal of Biomechanical Engineering, 106, 360-363.

Engin, A.E. (1985). Passive and active resistive force characteristics in major human joints. In N. Berme, A.E. Engin, and K.M. Correia da Silva (Eds.). Biomechanics of normal and pathological human articulating joints (pp. 137-164). Dordrecht: Martinus Nijhoff Publishers.

Engin, A.E., Akkas, N., and Kaleps, I. (1980). Passive resistive force and moments in human elbow joint. In V.C. Mow (Ed.), 1980 Advances in Bioengineering (pp. 229-232). New York: American Society of Mechanical Engineers.

Engin, A.E., and Chen, S.-M. (1986). Statistical database for the biomechanical properties of the human shoulder complex - II: Passive resistive properties beyond the shoulder complex sinus. Journal of Biomechanical Engineering, 108, 222-227.

Engin, A.E., and Peindl, R.D. (1980). Two devices developed for kinematic and force data collection in biomechanics - application to the human shoulder complex. In J.E. Stoneking (Ed.), Developments in theoretical and applied mechanics (Vol. 10, pp. 35-50). The University of Tennessee Press.

Engin, A.E., and Peindl, R.D. (1987). Passive resistive motion properties of the human shoulder complex. In B. Jonsson (Ed.), Biomechanics X-B (pp. 1071-1076). Illinois: Human Kinetics Publishers.

Fischer, G.M. (1973). Comparison of collagen dynamics in different tissues under the influence of Estradiol. Endocrinology, 93, 1216-1218.

Fleck, J.T., Butler, F.E., and Vogel, S.L. (1975). An improved three dimensional computer simulation of vehicle crash victims (Contract No. DOT-HS-053-2-485). Washington: U.S. Department of Transportation, National Highway Traffic Safety Administration.

Foster, J.K., Kortge, J.O., and Wolanin, M.J. (1977). Hybrid III - A biomechanically based crash test dummy. Proceedings of the 21st Stapp Car Crash Conference , 973-1014.

Fowles, G.R. (1986). Analytical mechanics (4th ed.). Philadelphia: Saunders College Publishing.

France, E.P., Daniels, A.U., Golbe, E.M., and Dunn, H.K. (1983). Simultaneous quantitation of knee ligament forces. Journal of Biomechanics, 16(8), 553-564.

Frankel, V.H., Burstein, A.H., and Brooks, D.B. (1971). Biomechanics of internal derangement of the knee. Pathomechanics as determined by analysis of the instant centers of motion. Journal of Bone and Joint Surgery, 53A, 945-962.

Fukubayashi, T., and Kurosawa, H. (1980). The contact area and pressure distribution pattern of the knee. Acta Orthopaedica Scandinavica, 51, 871-879.

Fung, Y.C. (1967). The elasticity of soft tissues in simple elongation. American Journal of Physiology, 213, 1532-1544.

Fung, Y.C. (1977). A first course in continuum mechanics (2nd ed.). New Jersey: Prentice Hall.

Fung, Y.C. (1981). Biomechanics: mechanical properties of living tissues. New York: Springer-Verlag.

Gardner, D.L. (1978). Ageing of articular cartilage. In J.C. Brocklehurst (Ed.), Textbook of geriatric medicine and gerontology (pp. 524). Edinburgh: Churchill Livingstone.

Giles, R.V.G. (1977). Fluid mechanics and hydraulics (2nd ed.). New York: McGraw-Hill.

Giordano, F.R., and Weir, M.D. (1985). A first course in mathematical modelling. California: Brooks/Cole Publishing Company.

Glantz, S.A. (1974). A constitutive equation for the passive properties of muscle. Journal of Biomechanics, 7, 137-145.

Goldberg, A.L., et al., (1975). Mechanism of work-induced hypertrophy of skeletal muscle. Medicine and Science in Sports, 7, 185.

Goldstein, H. (1981). Classical mechanics (2nd ed., pp. 243-274). California: Addison-Wesley.

Grabiner, M.D. (1989). The knee joint. In P.J. Rasch (Ed.), Kinesiology and applied anatomy (7th ed., pp 208-226). Philadelphia: Lea and Febiger.

Greiling, H., and Bauman, G. (1973). Age dependent changes of nonsulphated disaccharide in the proteoglycans of knee joint cartilage. In H.G. Vogel (Ed.), Connective tissues and ageing (pp. 160). Amsterdam: Excerpta Medica.

Guyton, A.C. (1986). Textbook of medical physiology (7th ed.). Philadelphia: W.B.S. Saunders Company.

Hama, H., Yamamuro, T., and Takeda, T. (1976). Experimental studies on connective tissue of the capsular ligament. Acta Orthopaedica Scandinavica, 47, 473-479.

Hatze, H. (1975a). A control model of skeletal muscle and its application to a time optimal biomotion. Unpublished doctoral dissertation, University of South Africa, South Africa.

Hatze, H. (1975b). A new method for the simultaneous measurement of the moment of inertia, the damping coefficient, and the location of the center of mass of a body segment *in situ*. European Journal of Applied Physiology, 34, 217-226.

Hatze, H. (1976). The complete optimization of a human motion. Mathematical Biosciences, 28, 99-135.

Haut, R.C., and Littel, R.W.A. (1972). A constitutive equation for collagen fibers. Journal of Biomechanics, 5, 523-530.

Hawkins, D., and Hull, M.L. (1990). A method for determining lower extremity muscle-tendon lengths during flexion/extension movements. Journal of Biomechanics, 23(5), 487-494.

Hayes, K.C. (1972). Jendrassik manoeuvre facilitation and fractionated patellar reflex times. Journal of Applied Physiology, 32, 290-295.

Hayes, K.C. (1976). The tonic neck reflex influence on tendon and Hoffmann reflexes in man. Electromyography and Clinical Neurophysiology, 16, 251-261.

Hayes, K.C., and Hatze, H. (1977). Passive visco-elastic properties of the structures spanning the human elbow joint. European Journal of Applied Physiology, 37, 265-274.

Heerkins, Y.F., Woittiez, R.D., Huijing, P.A., Van Ingen Schenau, G.J., and Rozendal, R.H. (1987). Passive knee resistance as a function of actual muscle length. In B. Jonsson (Ed.), Biomechanics X-B (pp. 985-988). Illinois: Human Kinetics Publishers.

Heerkins, Y.F., Woittiez, R.D., Huijing, P.A., Van Ingen Schenau, G.J., Rozendal, R.H., and Huson, A. (1985). Interindividual differences in the passive resistance of the human knee. Human Movement Science, 4, 167-188.

Herron, R.E., Cuzzi, J.R., Goulet, D.V., and Hugg, J.E. (1974). Experimental determination of mechanical features of adults and children (Report No. DOT-HS-231-2-397). Washington, D.C.: U.S. Department of Transportation.

Herzog, W. (1985). Individual muscle force prediction in athletic movements. Unpublished doctoral dissertation, University of Iowa.

Hinrichs, R.N. (1985). Regression equations to predict segmental moments of inertia from anthropometric measurements: An extension of the data of Chandler et al., (1975). Journal of Biomechanics, 18(8), 621-624.

Hof, A.L., and Van Den Berg, J.W. (1981). EMG to force processing II: Estimation of parameters of the Hill muscle model for the human triceps surae by means of a calfergometer. Journal of Biomechanics, 14(11), 759-770.

Huiskes, R., Van Dijk, R., de Lange, A., Woltring, H.J., and Van Rens, Th.J.G. (1985). Kinematics of the human knee joint. In N. Berme, A.E. Engin, and K.M. Correia da Silva (Eds.), Biomechanics of normal and pathological human articulating joints (pp. 165-187). Dordrecht: Martinus Nijhoff Publishers.

Jackson, D.S., and Bentley, J.P. (1968). Collagen-glycosaminoglycan interactions. In G.A. Ramachandran (Ed.), Treatise on collagen. London: Academic Press.

Jans, H.W.J., Dortmans, L.J.M.G., Sauren, A.A.H.J., and Huson, A. (1988). An experimental approach to evaluate the dynamic behaviour of the human knee. Journal of Biomechanical Engineering, 110, 69-73.

Jebens, E.H., and Monk-Jones, M.E. (1959). On the viscosity and PH of synovial fluid and the PH of blood. Journal of Bone and Joint Surgery, 41B, 388.

Johansson, H. (1991). Role of knee ligaments in proprioception and regulation of muscle stiffness. Journal of Electromyography and Kinesiology, 1(3), 158-179.

Johns, R.J., and Wright, V. (1962). Relative importance of various tissues in joint stiffness. Journal of Applied Physiology, 17(1), 824-828.

Kabo, J.M., Goldsmith, W., and Nystrom, M. (1982). Stretch characteristics of whole muscle. Journal of Biomechanical Engineering , 104, 253.

Kahn, P.B. (1990). Mathematical methods for scientists and engineers. Linear and Nonlinear Systems. New York: John Wiley and Sons.

Kearney, R.E., and Hunter, I.W. (1990). Systems identification of human joint dynamics. Critical Reviews in Biomedical Engineering, 18(1), 55-87.

Kear, M., and Smith, R.N. (1975). A method for recording tendon strain in sheep during locomotion. Acta Orthopaedica Scandinavica, 46, 896-905.

Kennedy, J.C., Hawkins, R.J., Willis, R.B., and Danylchuk, K.D. (1976). Tension studies of human knee ligaments. Journal of Bone and Joint Surgery, 58A(3), 350-355.

King, R.G. (1966). Rheologica Acta, 5, 41-44.

Lamontagne, M., Bradley, D.C., and Lemaire, E.D. (1989). Data acquisition and analysis system on microcomputer for biomechanical studies. Proceedings of the XII International Congress of Biomechanics (pp. 239). California, UCLA.

Larsson, L., Frimby, G., and Karlsson, J. (1979). Muscle strength and speed of movement in relation to age and muscle morphology. Journal of Applied Physiology, 46, 451.

Laubach, L.L. (1969). Body composition in relation to muscle strength and range of motion. Journal of Sports Medicine and Physical Fitness, 9(5), 89-97.

Linn, F.C. (1968). Lubrication of animal joints II - the mechanism. Journal of Biomechanics, 1, 193-205.

Loeffler, L., and Sagawa, K. (1975). A one dimensional viscoelastic model of cat heart muscle studied by small length perturbations during isometric contraction. Circulation Research, 36, 498-512.

Luo, Z., and Goldsmith, W. (1991). Reaction of a human head/neck/torso system to shock. Journal of Biomechanics, 24(7), 499-510.

Manschot, J.F.M., and Brakkee, A.J.M. (1986a). The measurement and modelling of the mechanical properties of human skin *in vivo* - I. The measurement. Journal of Biomechanics, 19(7), 511-515.

Manschot, J.F.M., and Brakkee, A.J.M. (1986b). The measurement and modelling of the mechanical properties of human skin *in vivo* - II. The model. Journal of Biomechanics, 19(7), 517-521.

Mansour, J.M., and Audu, M.L. (1986). The passive elastic moment at the knee and its influence on human gait. Journal of Biomechanics, 19(5), 369-373.

Markolf, K.L., Gorek, J.F., Kabo, J.M., Shapiro, M.S., and Finerman, G.A.M. (1990). New insights into load bearing functions of the anterior cruciate ligament. In V.C. Mow, A. Ratcliffe, and S.L-Y. Woo (Eds.), Biomechanics of diarthrodial joints (Vol. 1, pp. 155-175). New York: Springer-Verlag.

Markolf, K.L., Mensch, J.S., and Amstutz, H.C. (1976). Stiffness and laxity of the knee. The contributions of the supporting structures. Journal of Bone and Joint Surgery, 58A(5), 583-593.

Marsden, C.D., Merton, P.A., and Morton, H.B. (1972). Changes in loop gain with force in human muscle servo. Journal of Physiology (London), 222, 32P-42P.

Massey, B.S. (1979). Mechanics of Fluids (4th ed.). New York: Van Nostrand.

Matthews, M.B., and Glagov, S. (1966). Acid mucopoly- saccharide patterns in ageing human cartilage. Journal of Clinical Investigation, 45, 1103.

McCutchen, C.W. (1962). The frictional properties of animal joints. Wear, 5, 1-17.

McHenry, R.R. (1963). Analysis of the dynamics of automobile-passenger restraint systems. Proceedings of the 7th Stapp Car Crash Conference, 207-249.

Measurements Group Education Division (1983). Student manual for strain gage technology. Raleigh: Micro Measurements Division.

Mendenhall, W. (1983). Introduction to probability and statistics (6th ed.). Boston: Duxbury Press.

Miller, D.I., and Nelson, R.C. (1973). Biomechanics of sport: A Research approach. Philadelphia: Lea and Febiger.

Mills, O.S., and Hull, M.L. (1991a). Apparatus to obtain rotational flexibility of the human knee under moment loads *in vivo*. Journal of Biomechanics, 24(6), 351-369.

Mills, O.S., and Hull, M.L. (1991b). Rotational flexibility of the human knee due to varus/valgus and axial moments *in vivo*. Journal of Biomechanics, 24(8), 673-690.

Moffatt, C.A., Harris, E.H., and Haslam, E.T. (1969). An experimental and analytic study of the dynamic properties of the human leg. Journal of Biomechanics, 2, 373-387.

Morrison, J.B. (1970). The mechanics of the knee joint in relation to normal walking. Journal of Biomechanics, 3, 51-61.

Mow, V.C., Ratcliffe, A., and Woo, S.L-Y. (Eds.). (1990). Biomechanics of diarthrodial joints (Vols. 1-2). New York: Springer-Verlag.

Nash, W.A. (1977). Strength of materials (2nd ed.). New York: McGraw-Hill Book Company.

Nashold, B.S. (1966). An electronic method of measuring and recording resistance to passive muscle stretch. Journal of Neurosurgery, 24 (Suppl.), 310-314.

Nordin, M., and Frankel, V.H. (1989). Basic biomechanics of the musculoskeletal system (2nd ed.). Philadelphia: Lea and Febiger.

Noyes, F.R. (1977). Functional properties of knee ligaments and alterations induced by immobilization. Clinical Orthopaedics, 123, 210.

Number Cruncher Statistical System (1987). Number cruncher statistical system: users manual. Kaysville, Utah.

Obergefell, L.A., Avula, X.J.R., and Kaleps, I. (1988). Calculation of stopping torques for limbs subjected to aerodynamic loads. In R.L. Spiker and B.R. Simon (Eds.), Computational methods in bioengineering (pp. 169-176). New York: American Society of Mechanical Engineers.

O'Connor, J.J., and Zavatsky, A. (1990). Kinematics and mechanics of the cruciate ligaments of the knee. In V.C. Mow, A. Ratcliffe, and S.L-Y. Woo (Eds.), Biomechanics of diarthrodial joints (Vol. 2, pp. 197-241). New York: Springer-Verlag.

Otahal, S. (1971). A method of measuring some kinetic properties of voluntary muscle activity. In J. Vredenbrecht and J. Wartenweiler (Eds.), Medicine and sport: Biomechanics II (pp. 181-184). New York: Karger, Basel.

Padgaonkar, A.J., Krieger, K.W., and King, A.I. (1977). A three dimensional mathematical simulation of pedestrian-vehicle impact with experimental verification. Journal of Biomechanical Engineering, 116-123.

Peyton, A.J. (1986). Determination of the moment of inertia of limb segments by a simple method. Journal of Biomechanics, 19(5), 405-410.

Pheasant, S. (1986). Bodyspace. Anthropometry, ergonomics, and design (pp. 34-35). Philadelphia: Taylor and Francis.

Pierrynowski, M.R. (1982). A physiological model for the solution of individual muscle forces during normal human walking. Unpublished doctoral dissertation. Simon Fraser University, Vancouver, British Columbia.

Piez, K.A. (1968). Cross-linking of collagen and elastin. Annual Review of Biochemistry, 37, 574.

Piziali, R.L., Rastegar, J., Nagel, D.A., and Schurman, D.J. (1980). The contribution of the cruciate ligaments to the load-displacement characteristics of the human knee. Journal of Biomechanical Engineering, 102, 277-283.

Pope, M.H., Crowninshield, R., Miller, R., and Johnson, R. (1976). The static and dynamic behaviour of the human knee *in vivo*. Journal of Biomechanics, 9, 449-452.

Prasad, P., and Chou, C.C. (1989). A review of mathematical occupant simulation models. In T.B. Khalil and A.I. King (Eds.), Crashworthiness and occupant protection in transportation systems (pp. 95-112). New York: American Society of Mechanical Engineers.

Quinn, T.P., Mote Jr., C.D., and Skinner, H.B. (1991). The effect of ankle constraint on the torsional laxity of the knee during internal-external rotation of the foot. Journal of Biomechanics, 24(7), 511-525.

Renaudeaux, J.P. (1985). Lubrication of joints. In N. Berme, A.E. Engin, and K.M. Correia da Silva (Eds.), Biomechanics of normal and pathological human articulating joints (pp. 215-237). Dordrecht: Martinus Nijhoff Publishers.

Ribitsch, V.O. (1990). Viscoelastic behaviour of synovial fluids and artificial replacements. In V.C. Mow, A. Ratcliffe, and S.L-Y. Woo (Eds.), Biomechanics of diarthrodial joints (Vol. 2, pp. 287-304). New York: Springer-Verlag.

Ross, S.L. (1964). Differential equations. New York: Blaisdell Publishing Company.

Rousseeuw, P.J., and Leroy, A.M. (1987). Robust regression and outlier detection. New York: Wiley.

Segal, D.J. (1971). Revised computer simulation of the automobile crash victim (Report No. VJ-2759-V-2). Cornell Aeronautical Laboratory.

Segal, D.J., and McHenry, R.R. (1967). Computer simulation of automobile crash victim - revision (Report No. VJ-2492-V-1). Cornell Aeronautical Laboratory.

Seireg, A., and Arvikar, R.J. (1975). The prediction of muscular load sharing and joint forces in the lower extremities during walking. Journal of Biomechanics, 8, 89-102.

Siegler, S., Moskowitz, G.D., and Freedman, W. (1984). Passive and active components of the internal moment developed about the ankle joint during human ambulation. Journal of Biomechanics, 17(9), 647-652.

Sinkjaer, T., and Hayashi, R. (1989). Regulation of wrist stiffness by the stretch reflex. Journal of Biomechanics, 22(11/12), 1133-1140.

Smith, J.W. (1957). Observations on the postural mechanism of the human knee joint. Journal of Anatomy (London), 91, 236-260.

Spence, A.P. (1982). Basic human anatomy. California: The Benjamin/Cummings Publishing Company.

Spiegel, M.R. (1975). Theory and problems of probability and statistics. New York: McGraw-Hill Book Company.

Spoor, C.W., Van Leeuwen, J.L., Meskers, C.G.M., Titulaer, A.F., and Huson, A. (1990). Estimation of instantaneous moment arms of lower-leg muscles. Journal of Biomechanics, 23(12), 1247-1259.

Stijnen, V.V., Willems, E.J., Spaepen, A.J., Peeraer, L., and Van Leemputte, M. (1983). A modified release method for measuring the moment of inertia of the limbs. In H. Matsui, and K. Kobayashi (Eds.), Biomechanics VIII-B (pp. 1138-1143). Illinois: Human Kinetics Publishers.

Stryer, L. (1981). Biochemistry (2nd ed.). New York: W.H. Freeman and Company.

Such, C.H. (1971). Study of stiffness of the human knee joint. Unpublished master's thesis, University of Leeds, U.K.

Such, C.H., Unsworth, A., Wright, V., and Dowson, D. (1975). Quantitative study of stiffness in the knee joint. Annals of the Rheumatic Diseases, 34, 286-291.

Thompson, D.T. (1978). A study of joint stiffness. Unpublished doctoral dissertation, University of Leeds, U.K.

Thompson, D.T., Wright, V., and Dowson, D. (1978). A new form of knee arthrograph for the study of stiffness. Engineering in Medicine, 7(2), 84-92.

Thomson, W.T. (1988). Theory of vibration with applications (3rd ed.). New Jersey: Prentice Hall.

Tierny, J.A. (1979). Differential equations. Boston: Allyn and Bacon, Inc.

Tipton, C.M., James, S.L., Mergner, W., and Tcheng, T. (1970). Influence of exercise on strength of medial collateral ligaments of dogs. American Journal of Physiology, 218, 894.

Toft, E., Sinkjaer, T., Kalund, S., and Espersen, G.T. (1989). Biomechanical properties of the human ankle in relation to passive stretch. Journal of Biomechanics, 22(11/12), 1129-1132.

Unsworth, A., Dowson, D., and Wright, V. (1975). The frictional behaviour of human synovial joints - Part I: Natural joints. Journal of Lubrication Technology, 97(3), 369-376.

Van Ingen Schenau, G.J., Bobbert, M.F., and Rozendal, R.H. (1987). The unique action of bi-articular muscles in complex movements. Journal of Anatomy, 155, 1-5.

Van Soest, A.J., Schwab, A.L., Bobbert, M.F., and Van Ingen Schenau, G.J. (1993). The influence of the biarticularity of the gastrocnemius muscle on vertical jumping achievement. Journal of Biomechanics, 26(1), 1-8.

Viano, D.C., Culver, C.C., Haut, R.C., Melvin, J.W., Bender, M., Culver, R.H., and Levine, R.S. (1978). Bolster impacts of the knee and tibia of human cadavers and anthropomorphic dummy. Proceedings of the 22nd Stapp Car Crash Conference, 401-428.

Viidik, A. (1966). Biomechanics and functional adaptation of tendons and joint ligaments. In F.G. Evans (Ed.). Studies on the anatomy and function of bones and joints (pp. 17-39). Berlin: Springer-Verlag.

Viidik, A. (1972). Simultaneous mechanical and light microscopic studies of collagen fibers. Z Anat Entwicki Gesch, 136, 204-212.

Viidik, A. (1973). Functional properties of collagenous tissues. International Review of Connective Tissue Research, 6, 127-215.

Viidik, A. (1978). Biomechanical behaviour of soft connective tissues. Proceedings of the NATO Advanced Study Institute on Progress in Biomechanics (pp. 75-114).

Viidik, A. (1980). Mechanical properties of parallel fibered collagenous tissues. In A. Viidik and J. Vuust (Eds.). Biology of collagen (pp. 237-255). London: Academic Press.

Viidik, A., Danielsen, C.C., and Oxlund, H. (1982). Fourth International Congress of Biorheology Symposium on Mechanical Properties of Living Tissues: On fundamental and phenomenological models, structure and mechanical properties of collagen, elastin, and glycosaminoglycan complexes. Biorheology, 19, 437.

Vogel, H.C. (1977). Mechanical and chemical properties of various connective tissue organs in rats as influenced by non-steroidal antirheumatic drugs. Connective Tissue Research, 5, 91.

Vogel, H.C. (1978). Influence of maturation and age on mechanical and biochemical parameters of connective tissue of various organs in the rat. Connective Tissue Research, 6, 161.

Vrahas, M.S., Brand, R.A., Brown, T.D., and Andrews, J.G. (1990). Contribution of passive tissues to the intersegmental moments at the hip. Journal of Biomechanics, 23(4), 357-362.

Webb Associates (1978). Anthropometric source book: Vol. 1 (NASA ref. No. 1024). National Aeronautics and Space Administration.

Weiss, P.L., Kearney, R.E., and Hunter, I.W. (1986). Position dependence of ankle joint dynamics - I: Passive Mechanics. Journal of Biomechanics, 19(9), 727-735.

Wells, D.A. (1967). Lagrangian dynamics (pp. 203-233). New York: McGraw-Hill Book Company.

Welsh, R.P. (1980). Knee joint structure and function. Clinical Orthopaedics and Related Research, 147, 7-14.

Winter, D.A. (1988). The biomechanics and motor control of human gait. Waterloo: University of Waterloo Press.

Winter, D.A. (1990). Biomechanics and motor control of human movement (2nd ed.). New York: Wiley Interscience.

Wismans, J., Griffioen, J.A., and Nieboer, J. (1988). Use of MADYMO in general impact biomechanics. In R.L. Spiker and B.R. Simon (Eds.), Computational methods in bioengineering (pp. 177-184). New York: American Society of Mechanical Engineers.

Woittiez, R.D., Huijing, P.A., Boom, H.B.K., and Rozendal, R.H. (1984). A three dimensional muscle model: a quantified relation between form and function of skeletal muscle. Journal of Morphology, 182, 95-113.

Woo, S.L.Y., Gomez, M.A., Amiel, D., Ritter, M.A., Gelberman, R.H., and Akeson, W.H. (1981). The effects of exercise on biomechanical and biochemical properties of swine digital flexor tendons. Journal of Biomechanical Engineering, 103, 51.

Woo, S.L.Y., Gomez, M.K., Woo, Y.K., and Akeson, W.H. (1982). Mechanical properties of tendons and ligaments. Biorheology, 19, 397-408.

Woo, S.L.Y., Ritter, M.A., Amiel, D., Sanders, T.M., Gomez, M.A., Kuei, S.C., Garfin, S.R., and Akeson, W.H. (1980). The biomechanical and biochemical properties of swine tendons. Long term effects of exercise on the digital extensors. Connective Tissue Research, 7, 177-183.

Wright, V. (1959). Some observations on diurnal variation of grip. Clinical Science, 18, 17-23.

Wright, V., and Johns, R.J. (1960). Observations on the measurement of joint stiffness. Arthritis and Rheumatism, 3, 328-340.

Wright, V., and Johns, R.J. (1961). Quantitative and qualitative analysis of joint stiffness in normal subjects and in patients with connective tissue diseases. Annals of the Rheumatic Diseases, 20, 36-46.

Yamada, H. (1970). In F.G. Evans (Ed.). Strength of biological materials. Baltimore: Williams and Wilkins.

Yeadon, M.R., and Morlock, M. (1989). The appropriate use of regression equations for the estimation of segmental inertia parameters. Journal of Biomechanics, 22(6/7), 683-689.

Yoon, Y.S., and Mansour, J.M. (1982). The passive elastic moment at the hip. Journal of Biomechanics, 12(12), 905-910.

Zajac, F.E. (1989). Muscle and tendon: properties, models, scaling, and application to biomechanics and motor control. Critical Reviews in Biomedical Engineering, 17(4), 359-411.

APPENDIX A

CONSENT AND SUBJECT INFORMATION FORMS

Faculty of Health Sciences
School of Human Kinetics
Department of Kinanthropology

Consent to a Biomechanical Investigation to Determine the Viscoelastic Properties of the Human Knee Joint

Principal Investigator: Steven R. McFaull
Advisor: Dr. Mario Lamontagne

Name of volunteer:____

Date:____

I UNDERSTAND the terms of my participation in this study including the procedures to be used and the possible risks involved, and I agree to participate as a volunteer.

I AM FREE TO WITHDRAW this consent and to discontinue my participation at any time without penalty or discrimination.

MY PRIVACY will be protected in the following manner:

All research data obtained about me during the course of this study will be kept confidential and accessible only to the principal investigator and assistants on the project.

Should the study be published, my identity will not be released.

Information about the study:

The purpose of the study is to measure the viscosity and elasticity of the inactive knee joint for a sample of healthy male subjects using specially designed aparatii.

Two sessions totalling approximately 5 hours will be required to obtain the desired data.

Discomforts and inconveniences expected include: EMG electrodes placed on the skin; the knee joint being slightly forced into flexion and extension; and lying in a 20° decline position.

The procedure is briefly reviewed on the following page.

Signature of volunteer and date:_________________________________

Witness:____

PROCEDURE

The experiment consists of three components. First, an anthropometric session of approximately 20 minutes will be required to obtain various measurements of the knee, thigh, and calf as well as a flexibility test (Trunk Forward Flexion).

Determination of the elasticity of the knee will require only one session. You will lie on a padded table on your right side with your leg securely fastened to a rotating manipulandum which will measure moment and angle. Your torso will be oriented at 90° with respect to the thigh while the ankle will be taped at 90° relative to the calf i.e., $(\theta_H, \theta_A)=(90°,0°)$. The experimenter will rotate your leg throughout the whole range of knee joint motion in both directions. The experimenter will also force slowly your leg into the extreme flexion and extension positions. This will be repeated for five successful trials. You will be asked to keep your muscles as relaxed as possible during these trials. To make sure that your muscles are inactive the surface electromyogram (EMG) of various muscles on your thigh and calf will be monitored. This requires preparing the skin by rubbing it with alcohol, shaving a small area, and rubbing with electrolyte paste and then applying the surface electrodes.

The viscosity requires somewhat more time (3-4 hours) since five knee joint angles will be tested. You will be required to sit and be secured in the apparatus which will be configured either at an incline of 80° or 45°, flat, or at a decline (head below knees) of 20° depending on the knee joint angle being tested. Your ankle will be taped at 90° and secured into a clamp fixture which is attached to a spring-load cell assembly. Again, you will be required to keep your muscles relaxed which will be monitored with EMG as described above. Your leg will then be slightly displaced from the resting (horizontal) position and allowed to oscillate for 10 seconds. This will be repeated for five successful trials.

In signing this consent form you acknowledge that you have read and understood the above statements. You enter the biomechanical investigation willingly and you may withdraw **AT ANY TIME** without penalty or discrimination.

Signature of volunteer and date:____________________________________

Witness:____

Sports/Exercise History Information

Name:____

Date:______________________________

1. Which sports activities do you currently participate in? Indicate the frequency of participation, the level, and the length of time for which you have participated in the sport(s). Have you suffered any injuries as a result of this activity?

2. Indicate, also, activities, if any, you have previously participated in but no longer continue to do so.

3. If you are currently involved in a formal exercise program please give details as to the nature of the regimen. Indicate type (aerobic, anaerobic), exercises, repetitions, sets, frequency, intensity, duration, and the length of time for which you have been participating in this program.

4. If you currently incorporate a stretching routine into your exercise program please describe in detail the nature of this program. Indicate the specific exercises involved, repetitions, sets and the frequency and duration of the session.

Medical/Orthopaedic History Information

Please answer the following medical/orthopaedic history questionnaire, the responses of which will be kept confidential.

Name: ______________________________ **Date:**__________

1. Are you currently taking any medications for any medical and\or orthpaedic condition (especially non-steroidal anti-inflammatory drugs such as aspirin, acetaminophen, indomethacin) ? If so, indicate drug(s) and condition(s).

2. Do you suffer from any connective tissue disease ? If so, indicate the nature of the condition.

3. Do you have any pathology of the knee, hip, or ankle joints (right or left) ? If so, indicate the nature of the pathology(s).

4. Have you ever injured your knee, hip, or ankle joints (right or left) ? Indicate the nature of the injury(s).

5. Have you ever undergone major or minor surgery of the knee, hip, or ankle joints (right or left) ? If so, indicate the nature of the surgery(s).

APPENDIX B

ANTHROPOMETRIC DATA SHEET AND LABORATORY CONDITIONS

Anthropometric data and laboratory conditions

Name:____

Phone #:____________

I. Standard Measures

- Age (A):_____ Years Date of Birth: \ \

- Height (H):

_______ in _______ in _______ in

_______ m _______ m _______ m

II. Elastic Component

Date:____________ **Time:**____________

Laboratory Conditions:

- Temperature (T):_______ °C

- Humidity Level (HL):_______ %

Flexometer reading (TF):

_______ cm _______ cm

Bodymass (W):

_______ lbs _______ lbs _______ lbs

_______ kg _______ kg _______ kg

Joint Dimensions

Knee Joint

- Knee Breadth (KB):

_______ cm _______ cm _______ cm

- Knee Depth (KD):

________ cm ________ cm ________ cm

- Knee Circumference (KC):

________ cm ________ cm ________ cm

Ankle Joint

- Ankle Breadth (AB):

________ cm ________ cm ________ cm

- Ankle Circumference (AC):

________ cm ________ cm ________ cm

Segment Dimensions

Thigh Segment

- Thigh Length (TL):

________ cm ________ cm ________ cm

- Upper-Thigh Circumference (UTC):

________ cm ________ cm ________ cm

- Gluteal Furrow Depth (GFD):

________ cm ________ cm ________ cm

- Gluteal Furrow Breadth (GFB):

________ cm ________ cm ________ cm

- Midthigh Circumference (MTC):

________ cm ________ cm ________ cm

- Midthigh Depth (MTD):

________ cm ________ cm ________ cm

- Midthigh Breadth (MTB):

________ cm ________ cm ________ cm

- Lower-Thigh Circumference (LTC):

________ cm ________ cm ________ cm

- Lower-Thigh Depth (LTD):

________ cm ________ cm ________ cm

- Lower-Thigh Breadth (LTB):

________ cm ________ cm ________ cm

Calf Segment

- Calf Length (CL):

________ cm ________ cm ________ cm

- Calf Depth (CD):

________ cm ________ cm ________ cm

- Calf Breadth (CB):

________ cm ________ cm ________ cm

- Calf Circumference (CC):

________ cm ________ cm ________ cm

III. Viscous component

Date:________________ Time:________________

Laboratory Conditions:

- Temperature (T):________ °C

- Humidity Level (HL):_________ %

Flexometer reading (TF):

________ cm ________ cm

Suspension Length (d):

$\theta = 10°$

________ cm ________ cm ________ cm

$\theta = 45°$

________ cm ________ cm ________ cm

$\theta = 90°$

________ cm ________ cm ________ cm

$\theta = 110°$

________ cm ________ cm ________ cm

$\theta = 130°$

________ cm ________ cm ________ cm

Bodymass (W):

________ lbs ________ lbs ________ lbs

________ kg ________ kg ________ kg

Joint Dimensions

Knee Joint

- Knee Breadth (KB):

________ cm ________ cm ________ cm

- Knee Depth (KD):

________ cm ________ cm ________ cm

- Knee Circumference (KC):

________ cm ________ cm ________ cm

Ankle Joint

- Ankle Breadth (AB):

________ cm ________ cm ________ cm

- Ankle Circumference (AC):

________ cm ________ cm ________ cm

Segment Dimensions

Thigh Segment

- Thigh Length (TL):

________ cm ________ cm ________ cm

- Upper-Thigh Circumference (UTC):

________ cm ________ cm ________ cm

- Gluteal Furrow Depth (GFD):

________ cm ________ cm ________ cm

- Gluteal Furrow Breadth (GFB):

________ cm ________ cm ________ cm

- Midthigh Circumference (MTC):

________ cm ________ cm ________ cm

- Midthigh Depth (MTD):

________ cm ________ cm ________ cm

- Midthigh Breadth (MTB):

________ cm ________ cm ________ cm

- Lower-Thigh Circumference (LTC):

________ cm ________ cm ________ cm

- Lower-Thigh Depth (LTD):

________ cm ________ cm ________ cm

- Lower-Thigh Breadth (LTB):

________ cm ________ cm ________ cm

Calf Segment

- Calf Length (CL):

________ cm ________ cm ________ cm

- Calf Depth (CD):

________ cm ________ cm ________ cm

- Calf Breadth (CB):

________ cm ________ cm ________ cm

- Calf Circumference (CC):

________ cm ________ cm ________ cm

Notes and Comments:

APPENDIX C

DESCRIPTIONS OF THE ANTHROPOMETRIC PARAMETERS

The following sections describe the anthropometric parameters, and the combinations of them, which were used as independent variables in the statistical analysis.

Circumferences were measured to the nearest millimetre with a flexible tape while lengths, depths, and breadths were measured to the nearest millimetre using an anthropometer (GPM). Parameter descriptions were adapted from the works of Chandler et al., 1975; Heerkins et al., 1985; Webb Associates, 1978; and Yeadon and Morlock (1989).

I. Standard Measures

Body mass (W): Body mass measured on a standard medical scale (Continental) to the nearest one tenth kilogram.

Height (H): Height measured using a standard medical scale (Continental) to the nearest one half centimetre. Subject is barefoot and measurement is taken upon inhalation.

Age (A): The subjects' age in years.

II. Joint Dimensions

a. Knee Joint

Knee Breadth (KB): The subject stands erect with the feet about 10 cm apart. The maximum breadth of the right knee across the femoral epicondyles is measured.

Knee Depth (KD): The subject stands erect with the feet about 10 cm apart. The maximum antero-posterior dimension at the level of the midline of the anterior aspect of the patella of the right knee is measured.

Knee Circumference (KC): The subject stands erect with the feet about 10 cm apart. With the tape perpendicular to the long axis of the leg and passing over the middle of the patella, the circumference of the right knee is measured.

b. Ankle Joint

Ankle Circumference (AC): The subject stands erect with the feet about 10 cm apart. With the tape perpendicular to the long axis of the leg the minimum circumference of the right ankle (above malleoli) is measured.

Ankle Breadth (AB): The subject stands erect with the feet about 10 cm apart. The maximum dimension between the medial and lateral malleoli of the right leg is measured.

III. Segment Dimensions

a. Thigh Segment

Thigh Length (TL): The subject stands erect with the feet together. The distance between the lateral femoral epicondyle and the greater trochanter landmarks of the right thigh is measured.

Upper-Thigh Circumference (UTC): The subject stands erect with the feet 20 to 30 cm apart. With a tape perpendicular to the long axis of the thigh and passing just below the lowest point of the gluteal furrow, the circumference of the right thigh is measured.

Gluteal Furrow Depth (GFD): The subject stands erect with the feet about 10 cm apart. The maximum antero-posterior dimension of the right thigh at the level of the gluteal furrow landmark is measured.

Gluteal Furrow Breadth (GFB): The subject stands erect with the feet 20 to 30 cm apart. The maximum medio-lateral dimension of the right thigh at the level of the gluteal furrow landmark is measured.

Midthigh Circumference (MTC): The subject stands erect with feet about 10 cm apart. With the tape perpendicular to the long axis of the right thigh and at a level midway between the lateral femoral epicondyle and the greater trochanter landmarks (0.5*TL), the circumference of the right thigh is measured.

Midthigh Depth (MTD): The subject stands erect with the feet about 10 cm apart.The maximum antero-posterior dimension of the right thigh at a level midway between the lateral femoral epicondyle and the greater trochanter landmarks (0.5*TL) is measured.

Midthigh Breadth (MTB): The subject stands erect with the feet about 10 cm apart.. The maximum medio-lateral dimension of the right thigh at a level midway between the lateral femoral epicondyle and the greater trochanter landmarks (0.5*TL) is measured.

Lower-Thigh Circumference (LTC): The subject stands erect with feet about 10 cm apart. With the tape perpendicular to the long axis of the thigh and at a level which is 20 percent of the thigh length (0.2*TL) with respect to the lateral femoral epicondyle, the circumference of the right thigh is measured.

Lower-Thigh Depth (LTD): The subject stands erect with the feet about 10 cm apart.

The maximum antero-posterior dimension of the right thigh, at a level which is 20 percent of the thigh length (0.2*TL) with respect to the lateral femoral epicondyle, is measured.

Lower-Thigh Breadth (LTB): The subject stands erect with the feet about 10 cm apart. The maximum medio-lateral dimension of the right thigh, at a level which is 20 percent of the thigh length (0.2*TL) with respect to the lateral femoral epicondyle, is measured.

b. Calf Segment

Calf Length (CL): The subject stands erect with the feet together. The distance between the lateral femoral epicondyle and the lateral fibular malleolus of the right leg is measured.

Calf Circumference (CC): The subject stands erect with the feet about 10 cm apart. With the tape perpendicular to the long axis of the right leg, the maximum circumference of the calf is measured.

Calf Depth (CD): The subject stands erect with the feet about 10 cm apart. The maximum antero-posterior dimension of the right calf at the level of maximum calf circumference is measured.

Calf Breadth (CB): The subject stands erect with the feet about 10 cm apart. The maximum medio-lateral dimension of the right calf at the level of maximum calf circumference is measured.

Suspension distance (*d*): With the subject securely positioned in the small oscillation apparatus (SOA), measure the horizontal distance from the lateral femoral epicondyle of the right knee to the midpoint of the attachment of the distal leg support.

IV. Flexibility Parameter

Trunk Forward Flexion (TF), measured using a modified Wells and Dillon Flexometer, has been used as an indicator of back and hamstring flexibility and to a lesser degree of general flexibility. The following is a summarized protocol adapted from Canadian Standardized Test of Fitness (1987):

i) Subject should warmup sufficiently by performing the hurdlers stretch.

ii) The subject is barefoot, legs fully extended, sitting with the plantar aspect of the feet flat against the horizontal crossboards of the flexometer. The inner edge of the soles of the feet are 2 cm from the edge of the scale.

iii) Keeping the knees fully extended, arms evenly stretched, palms down, the subject slowly, without jerking, bends and reaches forward with head down pushing the sliding marker along the scale with the fingertips as far as possible. The maximum position of flexion is held for two seconds. Trial does not count if the knees flex.

iv) Repeat twice. Record the maximum value to the nearest 0.5 cm.

Normalized trunk forward flexion (TF(NORM)): Since the relative length of the arms and legs will affect the performance on the flexometer, the following parameters were measured in an attempt to normalize the TF value.

Whole arm length (WAL): The subject stands erect with the feet together and the arms and digits fully extended. The distance from the acromion landmark to the bottom of the third digit of the right arm/forearm is measured.

Finger height (FH): The subject stands erect with the feet together and the arms and digits fully extended. The distance from the floor to the bottom of the right third digit is measured.

Whole leg length (WLL): The subject stands erect with the feet together. The distance from the floor to the greater trochanter of the right femur is measured. The following normalized TF was developed:

$$TF(NORM) = \left[\frac{TF}{(WLL - WAL)}\right]^{-1} \tag{C1}$$

V. Derived Parameters

The following parameters were derived from the basic joint and segment dimensions as potential independent variables.

a. Cross sectional areas

Upper-thigh cross sectional area (UTCSA): Based on the assumption that the upper thigh is elliptical in cross section, the following parameter was derived:

$$UTCSA = \pi * GFD * GFB \tag{C2}$$

Midthigh cross sectional area (MTCSA): Based on the assumption that the midthigh is elliptical in cross section, the following parameter was derived:

$$MTCSA = \pi * MTD * MTB \tag{C3}$$

Lower-thigh cross sectional area (LTCSA): Based on the assumption that the lower thigh is elliptical in cross section, the following parameter was derived:

$$LTCSA = \pi * LTD * LTB \tag{C4}$$

b. Overall Circumference

Mean circumference (MC): The mean circumference of the thigh adapted from Yeadon and Morlock (1989) was given by:

$$MC = \frac{UTC + 2 * MTC + KC}{4} \tag{C5}$$

c. Higher order, multiplicative, and combination parameters

The following parameters were also used as potential predictors: KC^2, KC^3, KB^3, KC*KB, and (MTC + CC).

APPENDIX D

ANTHROPOMETRIC DATA OF THE SUBJECT SAMPLE

Table D1. Anthropometric data of the complete subject sample (n=17).

Subject	A (yrs.)	H (cm)	W (kg)	WLL (cm)	WAL (cm)	FH (cm)	KB (cm)	KD (cm)
AR	27.0	172.0	62.8	92.0	80.0	61.0	11.2	11.7
EM	24.0	173.0	98.1	90.0	71.0	69.0	12.9	13.4
BG	27.0	185.0	86.2	97.5	81.0	73.0	12.5	13.6
YF	30.0	176.0	75.3	91.5	80.0	66.5	11.5	12.9
JT	27.0	187.0	79.6	94.5	81.0	70.0	12.1	12.8
RV	24.0	171.0	89.1	89.0	73.0	61.5	12.7	13.1
JC	22.0	174.0	75.1	89.5	88.0	65.0	10.8	12.8
RC	28.0	173.0	59.4	88.0	76.0	66.0	10.1	11.7
JF	29.0	173.0	109.0	84.5	74.0	62.5	14.8	14.9
DS	29.0	175.0	70.6	88.0	88.5	63.0	10.7	11.8
GK	27.0	176.0	84.8	90.0	73.0	69.0	12.5	13.7
FH	22.0	184.0	78.5	94.0	81.0	69.0	11.8	13.2
GW	24.0	170.0	63.0	86.5	73.0	64.0	10.2	11.2
JB	27.0	166.0	64.7	85.0	75.5	59.0	10.1	11.1
BC	23.0	182.0	78.9	91.0	79.0	64.5	10.7	13.4
PP	26.0	174.0	76.6	88.5	73.5	64.0	11.6	13.2
CH	31.0	169.0	73.4	88.0	74.0	63.0	10.7	11.8
Mean	26.3	175.3	77.9	89.9	77.7	65.3	11.6	12.7
S.D.	2.7	5.9	12.9	3.4	5.2	3.7	1.2	1.0
CV(%)	10.4	3.4	16.6	3.8	6.7	5.7	10.7	8.0
Max.	31.0	187.0	109.0	97.5	88.5	73.0	14.8	14.9
Min.	22.0	166.0	59.4	84.5	71.0	59.0	10.1	11.1
Range	9.0	21.0	49.6	13.0	17.5	14.0	4.7	3.8

Table D1. Continued

Sub-ject	KC (cm)	AB (cm)	AC (cm)	TL (cm)	UTC (cm)	GFD (cm)	GFB (cm)	MTC (cm)
AR	36.0	7.1	21.5	40.0	51.0	16.7	15.6	50.0
EM	42.0	6.8	22.0	39.5	74.0	24.3	21.5	68.5
BG	41.5	6.9	25.0	44.4	62.5	19.5	19.0	56.5
YF	38.1	6.6	22.1	39.0	57.5	19.5	17.4	54.0
JT	38.2	7.5	23.5	41.0	59.6	18.5	19.3	54.0
RV	41.0	7.6	24.0	38.3	66.0	21.5	19.7	58.5
JC	36.0	6.4	21.0	38.3	57.0	17.9	17.6	53.0
RC	35.0	6.5	20.5	37.5	50.5	16.6	16.1	47.5
JF	45.0	7.4	24.5	38.1	70.0	25.5	21.0	64.5
DS	35.5	7.2	21.5	37.5	57.0	18.2	18.6	51.5
GK	40.0	6.9	23.0	41.7	66.5	21.5	19.2	61.0
FH	39.0	7.2	23.0	40.1	58.0	18.7	18.6	56.0
GW	34.5	6.4	21.5	37.5	54.5	17.2	16.4	49.0
JB	34.0	6.5	22.0	37.9	55.5	17.8	16.5	50.0
BC	37.0	7.0	22.5	40.9	57.5	18.1	17.7	54.5
PP	39.5	7.0	24.0	40.8	61.0	20.3	17.7	54.5
CH	35.0	6.7	21.5	39.3	57.5	18.8	16.9	55.5
Mean	38.1	6.9	22.5	39.5	59.7	19.4	18.2	55.2
S.D.	3.1	0.4	1.3	1.9	6.3	2.5	1.7	5.5
CV(%)	8.2	5.5	5.8	4.7	10.6	12.9	9.2	10.0
Max.	45.0	7.6	25.0	44.4	74.0	25.5	21.5	68.5
Min.	34.0	6.4	20.5	37.5	50.5	16.6	15.6	47.5
Range	11.0	1.2	4.5	6.9	23.5	8.9	5.9	21.0

Table D1. Continued

Subject	MTD (cm)	MTB (cm)	LTC (cm)	LTD (cm)	LTB (cm)	CL (cm)	CD (cm)	CB (cm)
AR	16.4	14.7	38.5	12.7	10.6	43.2	11.3	10.9
EM	22.4	20.5	54.0	17.1	16.6	42.5	13.0	12.5
BG	18.1	17.2	46.5	14.6	13.9	46.0	13.2	12.3
YF	18.0	16.3	43.0	13.8	12.3	43.6	11.9	11.0
JT	17.0	17.4	42.0	13.5	12.4	46.4	12.0	11.9
RV	19.0	18.3	47.0	15.3	14.2	41.6	13.0	13.1
JC	16.5	15.6	45.0	14.6	13.4	47.5	11.6	11.5
RC	15.6	14.9	37.0	11.6	10.7	42.0	10.5	10.3
JF	20.6	19.9	54.0	17.7	16.6	40.2	13.6	15.0
DS	16.4	15.9	39.8	12.3	11.7	42.7	11.2	10.6
GK	19.9	18.3	50.5	16.0	14.4	43.9	12.5	12.3
FH	18.3	17.3	46.0	15.6	13.5	46.4	12.1	12.3
GW	15.8	15.0	39.0	12.6	11.5	42.4	11.3	10.9
JB	16.8	15.6	38.0	12.3	11.2	40.5	11.3	10.6
BC	17.7	16.6	44.5	14.4	12.9	45.0	11.8	11.1
PP	18.4	15.8	44.5	14.2	12.9	41.8	11.7	12.8
CH	17.6	16.1	43.0	13.1	12.5	42.0	11.8	11.5
Mean	17.9	16.8	44.3	14.2	13.0	43.4	12.0	11.8
S.D.	1.8	1.7	5.2	1.7	1.8	2.2	0.8	1.2
CV(%)	10.0	10.0	11.7	12.2	13.6	5.0	6.9	10.0
Max.	22.4	20.5	54.0	17.7	16.6	47.5	13.6	15.0
Min.	15.6	14.7	37.0	11.6	10.6	40.2	10.5	10.3
Range	6.8	5.8	17.0	6.1	6.0	7.3	3.1	4.7

Table D1. Continued

Sub-ject	CC (cm)	TF(NORM) (Unitless)
AR	35.5	0.40
EM	42.0	0.45
BG	40.0	0.67
YF	37.0	0.25
JT	38.5	0.48
RV	41.0	0.55
JC	36.0	0.05
RC	33.0	0.46
JF	45.5	0.34
DS	35.0	-0.02
GK	40.0	0.51
FH	39.0	0.47
GW	35.5	0.37
JB	35.5	0.28
BC	36.0	0.28
PP	39.5	0.50
CH	37.5	0.40
Mean	38.0	0.40
S.D.	3.1	0.20
CV(%)	8.2	45.80
Max.	45.5	0.67
Min.	33.0	-0.02
Range	12.5	0.69

APPENDIX E

CALIBRATION CURVES FOR THE LOAD CELL, STRAIN GAUGED SENSING MEMPER, AND THE POTENTIOMETER

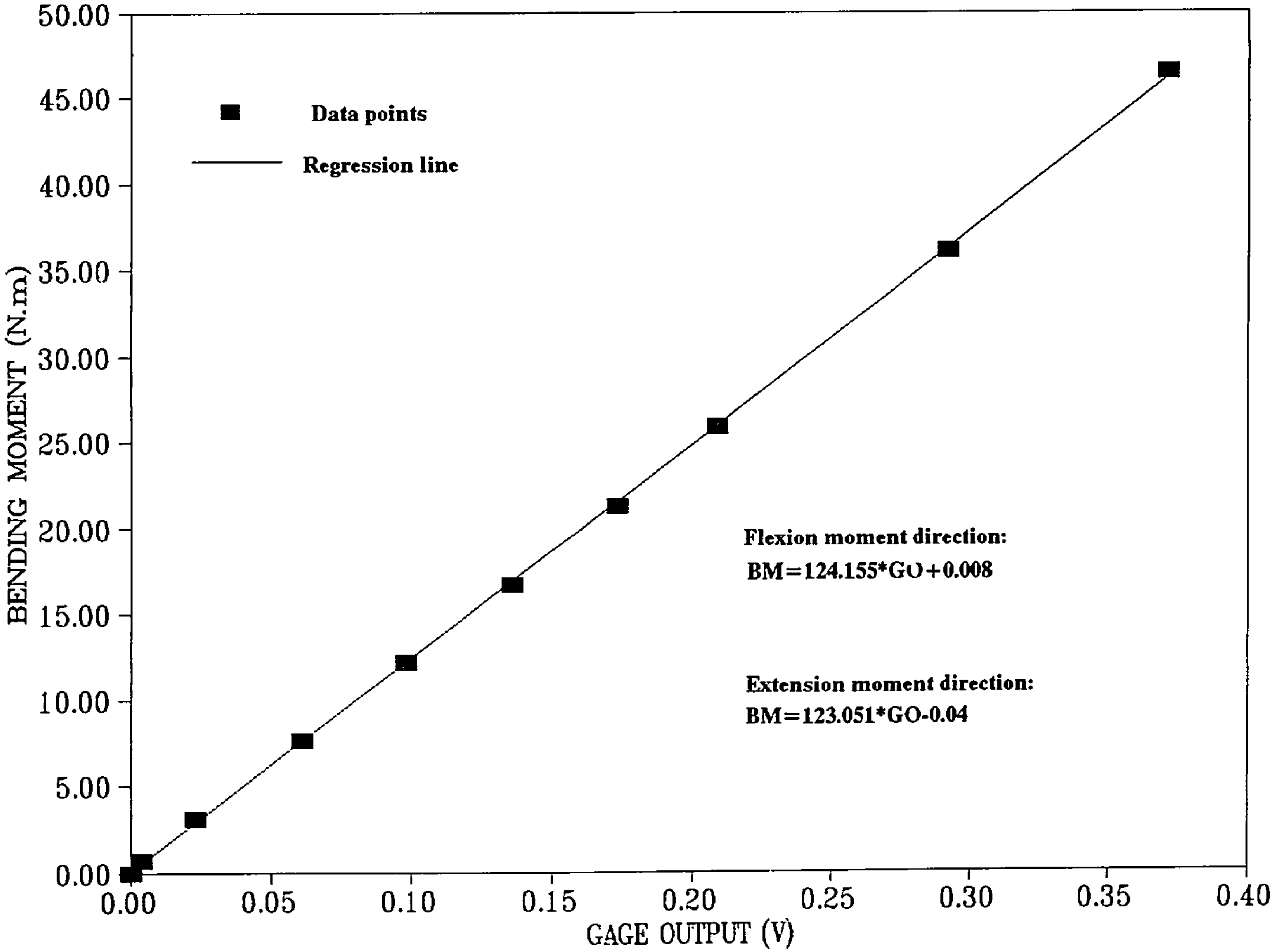

Figure E1. Calibration curve for the strain gauged sensing member of the HKA. Data is for the flexion moment direction. The data for the extension moment direction is slightly different.

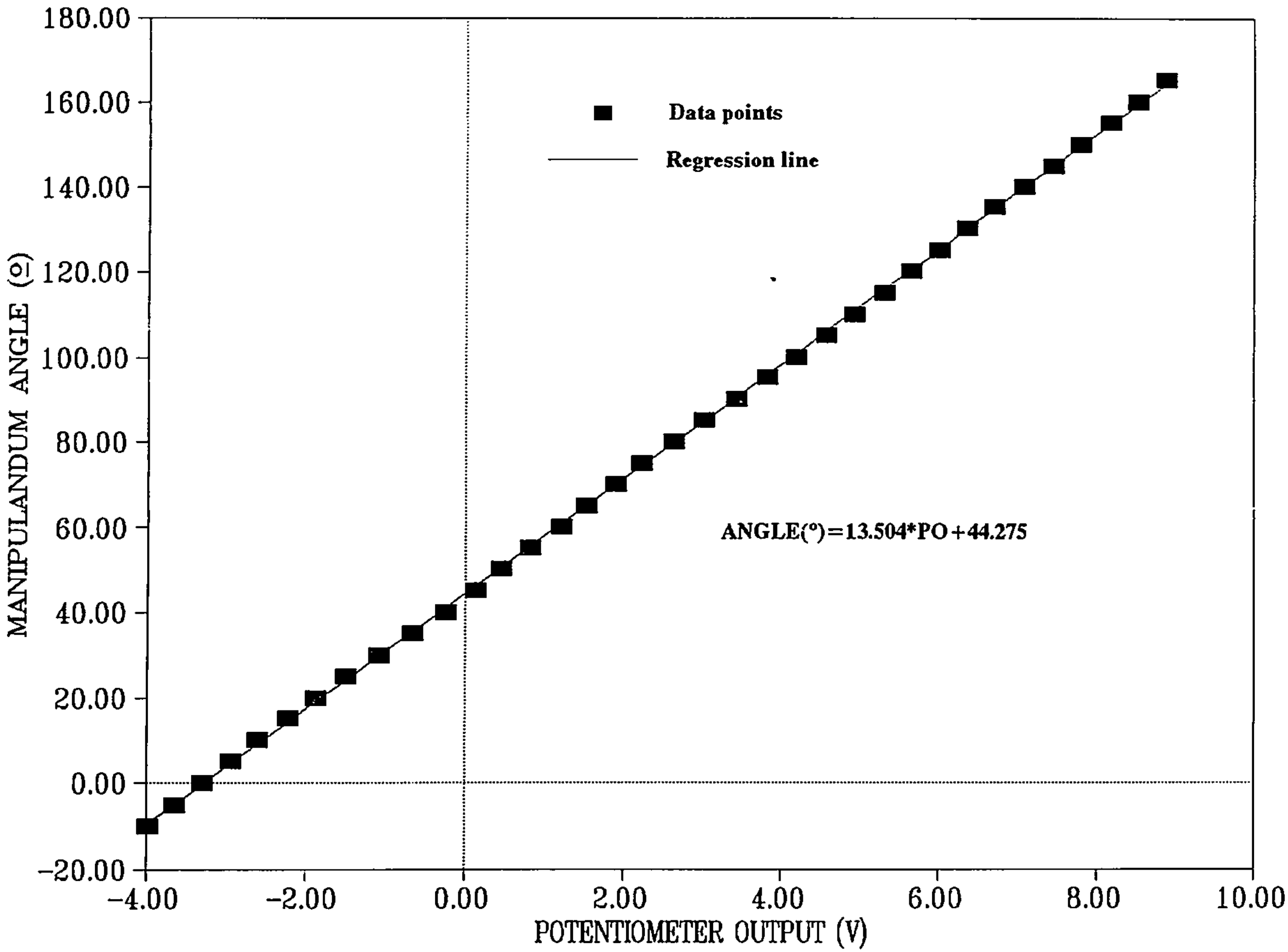

Figure E2. Calibration curve for the potentiometer of the HKA.

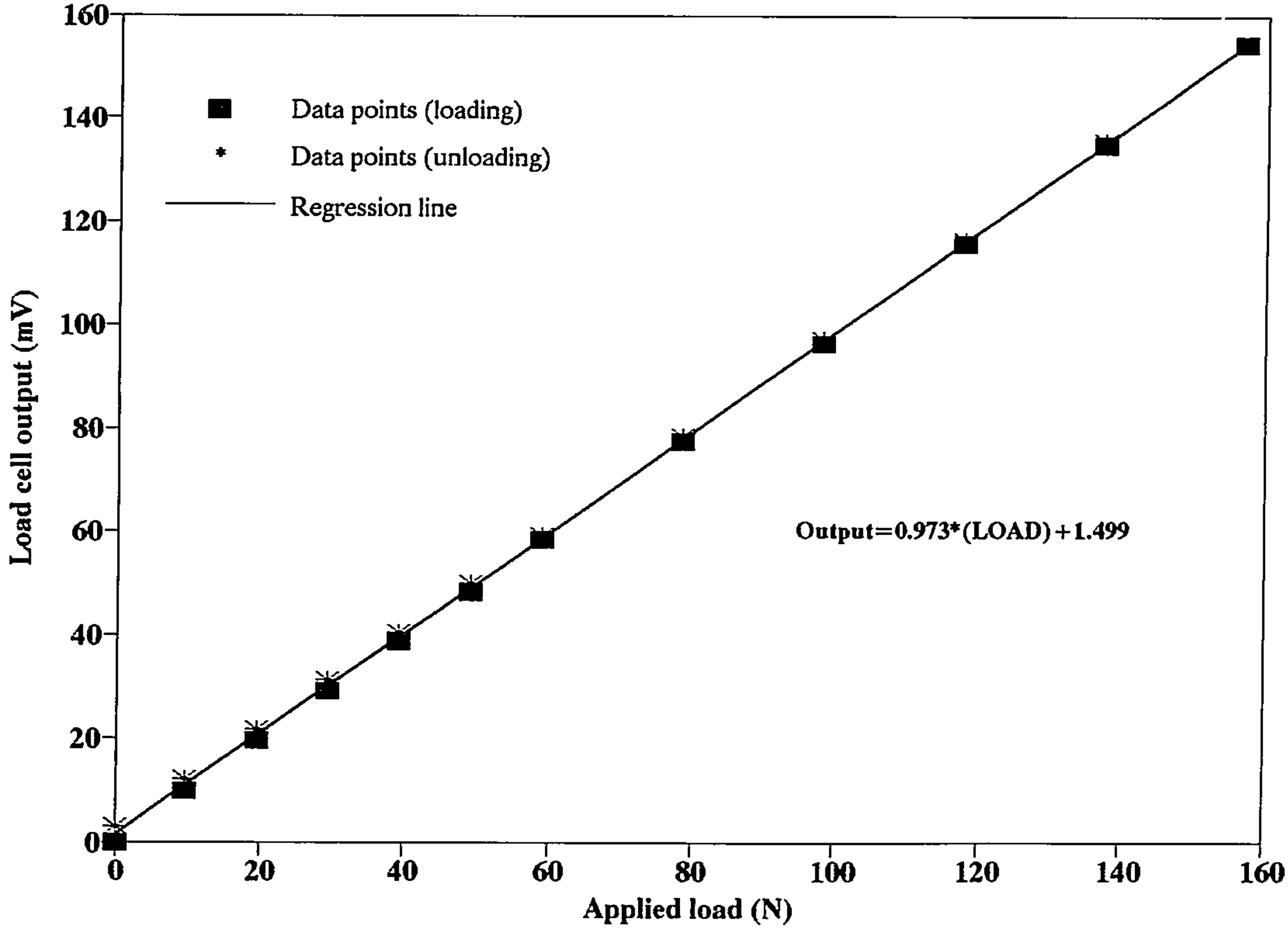

Figure E3. Calibration curve of the loadcell of the SOA.